January 2011

The Functions of Autophagy Genes in Lymphocytes and Osteoclasts

Brian Miller
Washington University in St. Louis

WASHINGTON UNIVERSITY IN ST. LOUIS

Division of Biology and Biomedical Sciences

Immunology

Dissertation Examination Committee:
Herbert W. Virgin, IV, Chair
Emily Cheng
Stuart Kornfeld
John Russell
Wojciech Swat
Steven Teitelbaum

THE FUNCTIONS OF AUTOPHAGY GENES IN LYMPHOCYTES AND OSTEOCLASTS

by

Brian Christopher Miller

A dissertation presented to the
Graduate School of Arts and Sciences
of Washington University in
partial fulfillment of the
requirements for the degree
of Doctor of Philosophy

May 2011

Saint Louis, Missouri

ABSTRACT OF THE DISSERTATION

The Functions of Autophagy Genes in Lymphocytes and Osteoclasts

by

Brian Christopher Miller

Doctor of Philosophy in Biology and Biomedical Sciences

(Immunology)

Washington University in St. Louis, 2011

Professor Herbert W. Virgin, IV, Chairperson

Macroautophagy (herein autophagy) is a process by which cells degrade long-lived proteins and organelles. The autophagy pathway and autophagy genes have been implicated in many functions in the cell such as protecting against metabolic stress, degrading damaged organelles, and regulating vesicular trafficking. To study the role of autophagy in primary cells with important physiologic functions, we generated mice lacking essential autophagy genes in B lymphocytes, T lymphocytes, and osteoclasts. We found that the essential autophagy gene *Atg5* was important for B cell development and for the maintenance of B-1a B cell numbers but not peripheral B-2 B cell numbers. In T cells, deletion of the essential autophagy genes *Atg5* or *Atg7* resulted in decreased thymocyte and peripheral T cell numbers *in vivo* and a decrease in cell proliferation *in vitro*. Autophagy genes play a critical role in T cell homeostasis, but do not appear important for peripheral B-2 B cell homeostasis *in vivo.* Whole-genome transcriptional profiling of *Atg5*-deficient and wild-type thymocytes suggested abnormalities in

mitochondria in the absence of *Atg5*. We confirmed this observation by demonstrating that peripheral *Atg5*-deficient T cells had an increase in mitochondrial mass that correlated with increased Annexin-V staining in these cells. We speculate that autophagy is required in T cells for the removal of damaged or aged mitochondria and that excess mitochondria contribute to increased cell death in autophagy-deficient T cells. In contrast to lymphocytes, deletion of autophagy genes in osteoclasts did not result in dramatic abnormalities in cell development. However, the biochemical pathway necessary for autophagy was critical for directional secretion in osteoclasts. We found that the autophagosome marker LC3 localized to the resorptive microenvironment in osteoclasts. Deleting *Atg5* or *Atg7* or overexpressing a dominant negative mutant of ATG4B to inhibit LC3 conjugation reduced localization of lysosomal markers at the resorptive surface and decreased bone resorption *in vitro*. Furthermore, mice lacking *Atg5* in osteoclasts and other myeloid-lineage cells were protected from ovarectomy-induced bone loss, a mouse model of osteoporosis. Together, these studies demonstrate that autophagy genes are important in cell development, survival, mitochondrial maintenance, and directional secretion in physiologically important, primary mammalian cells.

Acknowledgements

First and foremost I would like to thank my wife, Yamini, for her support. Earning a PhD requires a lot of personal growth, and Yamini was there to encourage and guide me throughout the process. She helped keep me smiling during the rough patches and celebrated with me during the good times. Our relationship is a tremendous source of strength for me.

I also want to thank my parents, Gary and Barbara, and my sister and brother-in-law, Lori and Benjamin, for their encouragement. They help me maintain perspective on what is important in life. My in-laws, Vikas, Priya, and Arti, have also been an incredible source of support throughout this process.

Next I would like to thank my thesis mentor, Skip Virgin. I am constantly impressed by how much he cares about the progress and training of his students. No matter how many additional responsibilities he acquired, he always worked to make time for us. I appreciated his patience as I slowly learned to become a scientist and his infectious enthusiasm about research that helped motivate me during the difficult times. Most of all, I know that Skip will continue to be an excellent mentor and advocate for me throughout my life, no matter where my future may take me.

My thesis committee has been instrumental in helping me to grow and develop as a scientist. Wojciech Swat and Steven Teitelbaum served as important mentors for me

when my research took me into their fields of study. John Russell was also particularly helpful in guiding my scientific progress. I appreciate all of their time and effort.

I have been fortunate to have excellent collaborators within Washington University. I worked closely with Lynn Stephenson and Wojciech Swat on the B and T cell work described in this thesis. I have also collaborated with Carl DeSelm and Steven Teitelbaum to study the function of autophagy genes in osteoclasts. This has been a very productive collaboration on a project that required each of our expertise to progress. I wish Carl the best of luck as he moves forward with this work.

I have also worked with many outstanding scientists outside of Washington University who have generously provided their insights, reagents, technical assistance, and data. Heather Pua, You-Wen He, Heung Kyu Lee, and Akiko Iwasaki were very helpful in collaborating on the functions of *Atg5* in B cells. Aylwin Ng, Jason Eisenberg, and Ramnik Xavier were important contributors to our understanding of the transcriptional abnormalities in *Atg5*-deficient T cells. Noboru Mizushima and Tamotsu Yoshimori have been very generous with their reagents and expertise.

I would also like to thank:

- My fellow autophagy researchers in the Virgin lab, who have struggled with me through the years to develop the tools and expertise necessary to make progress in this difficult field: Zijiang Zhao, Ken Cadwell, and recently Larissa Thackray, Monique Bruinsma, and Nicole Maloney.

- All current and former members of the Virgin lab, who provided guidance, encouragement, and friendship throughout my PhD. Erik Barton, Douglas White, Joy Loh, and Ken Cadwell have been particularly important mentors during my training.

- Bonnie Meltzer, Skip's assistant, for her constant efforts to help in any and every way that she can.

- Darren Kreamalmeyer, who manages our mouse colony. Darren is always able to magically produce a mouse when necessary for that critical experiment.

- My friends in St. Louis and around the world for their encouragement.

I would like to acknowledge the Infectious Disease Pre-Doctoral Training Grant, which funded this research between 2006 and 2008.

Table of Contents

Figures and Tables

CHAPTER 1

Introduction

Overview

To maintain homeostasis, cells must both build new macromolecules and organelles and degrade excess or damaged ones. Macroautophagy (herein autophagy) is a cellular degradative process by which cells recycle both organelles and long-lived proteins. This process is critical for survival, as mice lacking one of the genes required for autophagy die within one day of birth[1,2,3]. This introduction will give a summary of the process of autophagy and the functions of autophagy genes, with an emphasis on their roles in cell survival and vesicle trafficking and secretion. The work presented in this thesis will describe the functions of autophagy genes in lymphocytes and osteoclasts, so the development, survival, and function of these cells will be briefly discussed.

The Autophagy Pathway

While the molecular machinery of autophagy was first characterized in yeast, gene homologues have been discovered in higher eukaryotes, suggesting that the process is evolutionarily conserved. The autophagy pathway can be divided into four stages: vesicle nucleation to form an isolation membrane, expansion and closure of the isolation membrane around cytoplasm to form a double-membrane bound autophagosome, fusion of the autophagosome with the endo-lysosomal pathway, and breakdown of vesicle contents in the lysosome (Fig. 1-1). Autophagy can be induced by a variety of cellular stresses, although many mammalian cell types appear to have some level of constitutive autophagy[4,2]. These stressors include starvation[4], growth factor deprivation[5], ER stress[6,7], microbial infection[8,9,10,11,12], hypoxia[13,14], and accumulation of reactive oxygen species[15].

While the conditions that produce these stress signals are diverse, many of their signaling pathways converge in the inactivation of the serine/threonine kinase mTor, a master regulator in the initiation of the autophagy cascade. Inhibition of mTor activity results in activation of a class III phosphatidylinositol 3-kinase, Vps34, in complex with Beclin-1 and other molecules (reviewed in [16]). Activation of this class III PI3K is necessary for nucleation of the isolation membrane[17] (reviewed in [18]).

Formation of the autophagosome requires the recruitment of two ubiquitin-like pathways necessary for isolation membrane elongation and closure[19]. The E1-like enzyme required for both conjugation systems is ATG7[20,21,1]. The first system conjugates the ubiquitin-like molecule ATG12 to a lysine in ATG5 via the action of the E2-like enzyme ATG10[20,22,23,24]. The majority of ATG5 in mammalian cells is found conjugated to ATG12[24]. ATG5-ATG12 binds to ATG16L1, which is thought to target the complex to the forming autophagosome[25]. The ATG5-ATG12 conjugate has E3 ubiquitin ligase-like activity for the second ubiquitin-like system, the ATG8 conjugation system[26]. There are many species-specific homologues of ATG8 in mammalian cells, including LC3, GATE16, GABARAP, and ATG8L[27,28,29], although LC3 is the best characterized of these molecules in the context of autophagy.

The ubiquitin-like molecule LC3 is first cleaved by ATG4B, a mammalian homologue of yeast ATG4[30,31], exposing a C-terminal glycine residue and forming LC3-I[30]. LC3 is then activated by ATG7, transferred to the E2-like enzyme ATG3, and finally conjugated onto the lipid phosphatidylethanolamine (PE) via an isopeptide bond

with the exposed glycine residue[32,30]. Conjugated LC3 (LC3-II) localizes to the isolation membrane[30,31] where its membrane-fusion activity is thought to mediate proper membrane expansion and/or closure[33,3,34]. ATG4B also functions to deconjugate LC3 from PE after formation of the autophagosome[35]. Interestingly, a recent study has suggested that macroautophagy may exist in mammalian cells by a mechanism that does not require the ATG12/LC3 conjugation cascades[36]. Although the physiologic significance of this alternative pathway is unclear, this finding highlights the complexity of mammalian autophagy.

Much less is known about the molecular mechanisms required for the fusion of the autophagosome with endo-lysosomal vesicles in mammalian cells. This step likely involves machinery important for the endo-lysosomal trafficking pathway such as the Rab small GTPase family. Indeed, Rab7, which is involved in late endosomal transport, phagosome maturation, and lysosome homeostasis[37,38,39], has been shown to be important in the fusion of autophagosomes with late endosomes/lysosomes[40,41,42]. After fusion, lysosomal enzymes degrade the contents of the inner membrane[43] which are subsequently exported back into the cytosol to be recycled as substrates of synthetic pathways.

Measuring Autophagy

The development of reliable and quantifiable assays to measure autophagy over the past two decades has allowed significant advancement in this field. Autophagy was first discovered by electron microscopy, and this technique is still widely used to quantify autophagosomes[44,45,46]. The lipidation of LC3 during autophagosome formation allows

unconjugated (LC3-I) and conjugated (LC3-II) forms to be distinguished by their electrophoretic mobility[30]. Because LC3 is degraded when the autophagosome fuses with the lysosome, inhibiting lysosome degradation is important for measuring the accumulation of LC3-II as a measure of autophagic activity over time (reviewed in [44]). A GFP-LC3 fusion protein has also been generated to allow the localization and quantification of autophagosomes within cells[30] (reviewed in [44]). It is important to note that LC3 can be conjugated in the absence of autophagosome formation (reviewed in [44]) and form punctuate structures independent of autophagy[47]. Finally, levels of the protein p62, which binds LC3 and is degraded by autophagy[48], are used as a indicator of autophagic activity (reviewed in [44]).

Functions of Autophagy Genes

In addition to its role in recycling, autophagy has been implicated in many cellular functions based largely on studies using gene knockdown and gene deletion approaches. However, autophagy genes may have other functions in the cell. For example, the requirement for *Atg5* in autophagy is clear[49,24], but *Atg5* can also induce cell death and inhibit cytokine production independent of its role in the LC3 conjugation pathway[50,51,52,53]. Given this caveat, there is a growing literature suggesting that autophagy or autophagy genes function in many different contexts in the cell (reviewed in [54]).

The function of autophagy genes shows remarkable cell-type specificity. For example, numerous secretory cells have co-opted autophagy genes for their specialized

function[55,56,57,58,59], whereas antigen presenting cells use this pathway to process cytoplasmic antigens for presentation[60,61]. Other functions of autophagy and autophagy genes seem to be conserved in many different cell types – for example, the ability of autophagy to maintain cell viability during starvation and stress[5,62,63] or degrade intracellular pathogens[12,64,65]. Because of the cell-specific and multifunctional roles of autophagy genes, it is important to study their function in physiologically relevant cell types.

Autophagy genes in cell survival

One of the first discovered functions of autophagy is to maintain cell viability during cell stress[5,66,67]. Autophagy genes have been shown to be important for cell survival after removal of growth hormones, conceivably by allowing cells to acquire nutrients from the degradation of cellular constituents[5]. In conditions of hypoxia, increased reactive oxygen species (ROS) production, or mitochondrial damage, autophagy can be targeted to degrade mitochondria to protect cells from the toxic byproducts of mitochondrial respiration[13,14,15,68]. Deletion of autophagy genes in yeast or murine liver, β-islet cells, embryonic fibroblasts, cell lines, or macrophages results in the accumulation of mitochondria[69,57,1,70,71,72].

ROS are one of the major destructive byproducts of mitochondria. ROS can induce DNA damage and oxidize proteins and lipids necessary for cellular function and survival[73,74,75]. Many different cell types have been shown to accumulate ROS when autophagy genes are knocked down or deleted, including yeast[69], mouse embryonic

fibroblasts[15,70], transformed fibroblasts[72], and macrophages[70,76]. In addition to decreasing ROS levels, autophagy may also mitigate the negative effects of ROS by degrading oxidized protein aggregates and damaged organelles[77,78,79,80]. As evidence of the *in vivo* importance of this function of autophagy, inhibiting autophagy genes in Drosophila or Arabidopsis increases the sensitivity of the flies and plants to oxidative stress-induced death[79,80]. As ROS have been shown to induce autophagy in various cell types[15,81,82], this suggests a negative feedback loop whereby increased ROS activate autophagy, which functions to decrease ROS levels and allay the effects of ROS damage.

Paradoxically, a few studies suggest that autophagy can increase ROS, resulting in cell death[83,84]. Many groups have reported that inhibition of autophagy results in decreased cell death[85,86], even in the same cell types where it has been shown to have pro-survival functions[66]. Autophagy can function to induce or accelerate cell death (i.e. autophagy causes an increase of ROS that are toxic to the cell[83]), but it may also be a distinct mechanism by which cells can die (reviewed in [87]). The function of autophagy as cell death mechanism is unclear and will not be further discussed in this thesis (reviewed in [87]). Still, it is clear that autophagy can function to both protect cells and induce cell death. One hypothesis to explain this paradox is that autophagy normally has a cytoprotective role, but can result in cell death when overutilized (reviewed in [88]).

Autophagy genes in vesicle trafficking and secretion

Many of the proteins involved in the induction of the autophagy pathway also have functions in vesicular trafficking. The Vps34 complex, for example, can pair with

different subunits to induce autophagy or function in endosomal vacuolar sorting[89,90] (reviewed in [91]). There is now a growing literature suggesting that autophagy genes downstream of the Vps34 complex can have a role in vesicular trafficking independent of autophagosome formation. *Atg5* is important for the fusion of phagosomes with lysosomes in macrophages[92]. Beclin-1 and LC3 were found to localize on the phagosome, but no double-membrane bound structures associated with the phagosome were observed. *Atg5* is also important for clearance of Toxoplasma from infected macrophages[65]. *Atg5*-deficient macrophages failed to localize a key immunity-related GTPase, Irga6[93], to the vacuole containing the parasite (parasitophorous vacuole) and failed to recruit LAMP1 positive lysosomes to this structure. No double-membrane bound structures were observed associated with the parasitophorous vacuole. Interestingly, both of these papers report a defect in the fusion of lysosomes with intracellular vesicles, raising the possibility that a common mechanism is involved in both processes.

A novel role of autophagy genes in cell secretion has also been recently suggested. Paneth cell secretion of lysozyme is deficient in mice that have deleted or reduced levels of ATG5, ATG7, or ATG16L1 in the gut epithelium[55,56]. Deletion of *Atg7* in pancreatic β-cells disrupts insulin secretion[57,58]. Finally, mice heterozygous for Beclin-1 have a deficiency in melanosome production by melanocytes, resulting in alterations in coat color[59]. These studies provide compelling evidence suggesting a role for autophagy genes in granule secretion, and it will be important to determine if this function is generalized to other secretory cell types. Moreover, the mechanism by which

the autophagy pathway or autophagy genes contribute to vesicle trafficking and secretion is of great interest.

This thesis will explore the functions of autophagy genes in primary mouse B and T lymphocytes and osteoclasts, three cell types with physiologically relevant functions that can be studied *in vivo* and *in vitro*. The life and death of lymphocytes is a tightly regulated process that allows rapid and massive expansion of cells followed by similarly drastic reduction over the course of an immune response, providing a well-studied system to examine the function of autophagy genes in cell survival and development. Osteoclast function is dependent upon temporally and spatially regulated secretion, allowing mechanistic studies of the function of autophagy genes in cell secretion.

B Cell Subsets

B lymphocytes have a variety of functions in the immune response (reviewed in [94]), including the secretion of antibody, presentation of antigen[95,96], and production of cytokines[97,98]. B cells are classified into two subsets, B-1 and B-2, based on cell surface marker expression, developmental origin, and functional properties (reviewed in [99]). B-2 B cells develop from hematopoietic stem cells in the bone marrow, undergoing a series of maturational stages that can be defined by expression of cell surface markers (Hardy fractions A-F)[100]. B-2 B cells exit the bone marrow as immature cells that finish their development in the spleen as transitional B cells[101]. The majority of B-2 B cells develop into follicular B cells, which are found in B cell follicles and respond to infection with

production of high-affinity antibodies (reviewed in [102]). B-2 B cells also develop into marginal zone B cells, which are located in the spleen and rapidly produce antibodies against blood-borne antigens (reviewed in [103]).

B-1 B cells are part of the innate immune system and are located primarily in body cavities. B-1 B cells are further subdivided into B-1a and B-1b subsets based on expression of the cell surface protein CD5. Studies indicate that B-1a cells produce natural antibodies, defined as antibodies present in the serum before exposure to exogenous antigen (reviewed in [104]). Natural antibodies are important for early control of viral and bacterial infection[105,106]. Unlike the spontaneous secretion of antibody by B-1a B cells, B-1b cells are induced to secrete antibody that is important for the clearance of pathogens[107] (reviewed in [99]).

The developmental origin of B-1 B cells is still controversial, with two competing models under study. According to the selection model, B-1 and B-2 B cells are derived from a common progenitor that differentiates into one of the two lineages based on antigen selection at the transitional stage (reviewed in [108]). Alternatively, the lineage model proposes that B-1 and B-2 B cells originate from distinct progenitors. The lineage model is supported by the recent identification of a B-1 B cell progenitor in fetal and adult tissues[109]. It has also been suggested that B-1a and B-1b B cells have distinct progenitors and lineages[110].

The Role of Autophagy Genes in B Cells

There is little known about the functions of autophagy and autophagy genes in B cells. Two papers demonstrate that autophagy is a constitutive process in human B cell lines[61,60], which the authors suggest may be involved in bringing cytosolic antigens to load onto MHC class II. B cell receptor (BCR) signaling stimulates autophagy[111], which is important for synergistic signaling of the BCR and Toll-like receptor 9 (TLR9), an innate immune receptor that recognizes unmethylated DNA [112]. Together these studies suggest that autophagy is a constitutive process that can be upregulated in B cells and that may be important for antigen presentation and B cell signaling.

T Cell Survival

T cells are key regulators and effectors of the immune response responsible for both the clearance of pathogens and, when dysregulated, autoimmune disease. For this reason, T cell homeostasis is a tightly regulated process. T cells differentiate from the pluripotent hematopoietic stem cell in the bone marrow and complete their development in the thymus, where they undergo a series of well-defined stages defined by cell surface marker expression and T cell receptor (TCR) gene rearrangement (reviewed in [113]). Mature, naïve T cells then emigrate from the thymus to the periphery, where their survival is regulated by cytokines and signals through the T[114,115,116,117] (reviewed in [118]). Previously activated T cells can die by a process known as activation-induced cell death (AICD) via signaling through TNF receptor superfamily members such as CD95/Fas and TNFR1[116,119] (reviewed in [120]). Activated cells can also die by neglect when they do not

receive appropriate survival factors, known as activated cell-autonomous death (ACAD), which is thought to be mediated through the balance of pro- and anti-apoptotic Bcl-2 family members[121] (reviewed in [118,120]).

ROS regulate T cell activation and homeostasis by modulating cell signaling, proliferation, and apoptosis[122,123,124] (reviewed in [75,125]). ROS are involved in the upregulation of FasL following T cell activation, a process important for AICD[126,127]. ROS also downregulate expression of the anti-apoptotic molecule Bcl-2 in activated T cells, resulting in ACAD[128,129].

The Role of Autophagy Genes in T cells

Autophagy plays a critical role in the development and survival of T lymphocytes. This process is constitutively active in the thymus[130,4] and upregulated after T cell activation[131,132]. Multiple studies suggest that autophagy and autophagy genes can contribute to T cell death, such as after growth factor withdrawal[131] or in the context of T cells lacking FADD activity, caspase-8, or Irgm-1[133,134]. T cells exposed to the env protein of HIV also undergo cell death that can be blocked by inhibiting autophagy[135]. However, deletion of the autophagy gene *Atg5* in primary T lymphocytes results in decreased survival[132]. In summary, autophagy genes may be important for cell survival in normal T cells, but excessive induction of autophagy or autophagy in the context of certain genetic deletions may serve as a pro-death mechanism.

Osteoclast Function

Osteoclasts are the primary cell responsible for bone degradation. The coordination of the bone resorption activity of osteoclasts with the bone forming activity of osteoblasts is critical for the maintenance of skeletal integrity and calcium homeostasis (reviewed in [136]). Diseases disrupting osteoclast activity result in osteopetrosis, an increase in bone mass. In contrast, increased osteoclast activity reduces bone mass, resulting in osteopenia and osteoporosis (reviewed in [137]).

Osteoclasts differentiate from cells of the monocyte lineage by fusion of precursors into a polykaryon under the influence of M-CSF and RANKL[138] (reviewed in [137]). The osteoclast is activated and polarizes after recognizing the bone substrate via signaling through cell surface molecules such as the αvβ3 integrin[139] (reviewed in [140,137]) (Fig. 1-2). One of the first steps is the formation of a sealing zone, an area of tight adherence of the osteoclast to the bone matrix. The extracellular mediators of this junction are still in question, but intracellularly there is an accumulation of microfilaments that form an actin ring. To degrade bone, osteoclasts deliver vesicles containing lysosomal enzymes to the interior of the actin ring where they fuse with the plasma membrane, forming a region of membrane folds termed the ruffled border (reviewed in [141]). Bone degradation by osteoclasts requires the action of hydrogen ions and lysosomal enzymes. Hydrogen ions are important for the demineralization of bone and are secreted by the action of the vacuolar H+ ATPase[142,143,144]. The hydrogen ions are generated by a carbonic anhydrase enzyme in the cell, which combines water and

carbon dioxide to generate hydrogen ions and biocarbonate[145] (reviewed in [137]). Electrical neutrality of the cell and resorption pit is maintained by a chloride/bicarbonate pump in the basolateral cell surface (away from the bone) and a chloride channel in the apical surface (against the bone)[146] (reviewed in [137]). After demineralization, enzymes such as cathepsin K degrade the organic matrix of bone[147,148]. The degraded collagen fragments are transcytosed across the cell for exocytosis at the basolateral side of the osteoclast opposite the bone[149,150].

A number of lines of evidence suggest that the vesicles fusing with the plasma membrane are lysosomes, often called "secretory lysosomes" (reviewed in [151]). First, lysosomal proteins such as LAMP1, LAMP2, and the vacuolar H+ ATPase are localized to the plasma membrane at the ruffled border[152,153,144]. Second, Rabs associated with late endosomes (Rab7 and Rab9) have also been localized on the ruffled border[152,153,154], and Rab7 has been shown to be important for formation of the ruffled border[155]. Finally, lysosome-associated enzymes such as cathepsin K are found in the extracellular bone resorption pit[156]. It has also been shown that small, coated vesicles from the trans-Gogli network containing lysosomal enzymes traffic to the ruffled border and fuse with the plasma membrane[157], thus the exact nature of the vesicle or vesicles necessary for ruffled border formation and bone degradation is unclear.

The molecular mechanisms responsible for the directional secretion of vesicles in osteoclasts are poorly understood. Rab7 is an important GTPase for vesicular trafficking of late endosomes[39] and maturation of autophagosomes[40,41,42] and is important for

formation of the ruffled border and localization of the vacuolar H+ ATPase in osteoclasts[155]. Rab3D, which localizes to the trans-Golgi network, and Synaptotagmin VII, an accessory molecule of vesicle fusion proteins involved in lysosome exocytosis[158], are two additional molecules important for osteoclast secretion[159,160]. The machinery of vesicle fusion and the signals targeting vesicles to the ruffled border are still unknown.

Experimental Systems

Given our goal to understand the role of autophagy genes in B cells, T cells, and osteoclasts, we generated mice lacking *Atg5* or *Atg7* in these cell types to study the *in vivo* phenotypes and serve a source of primary cells for *in vitro* studies. Knockout mice lacking either *Atg5* or *Atg7* are born in mendelian ratios but die within the first day of life[1,2]. Because of the neonatal lethality, mice containing loxP-flanked *Atg5* and *Atg7* genes have been generated to allow cell-type specific deletion of these essential autophagy genes[1,78]. We bred mice with two copies of a loxP-flanked ("floxed") *Atg5* or *Atg7* gene with mice expressing the Cre recombinase under control of a B cell specific promoter (CD19-*Cre*)[161], T cell specific promoter (Lck-*Cre*)[162], or monocyte/granulocyte specific promoter (LyzM-*Cre*)[163]. These mice should express the Cre recombinase in B cells, T cells, or osteoclasts, resulting in the cell-type specific deletion of the *Atg5* or *Atg7* floxed alleles. We also reconstituted the hematopoietic compartment of irradiated *Rag1*$^{-/-}$ or CD45.1 mice with fetal liver stem cells from *Atg5*$^{-/-}$ pups, giving us a second *in vivo* system to study the effects of *Atg5* deletion in B and T cells.

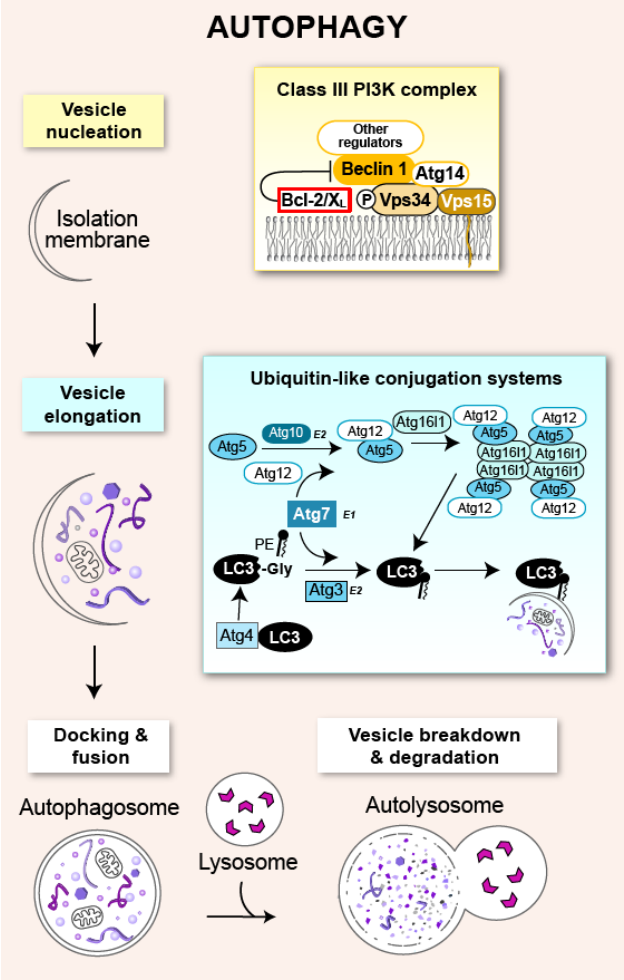

Figure 1-1. Overview of the mammalian autophagy pathway

The autophagy pathway can be divided into four stages. Stage 1 - vesicle nucleation to form an isolation membrane, requires the activity of a class III PI3K complex. Stage 2 - expansion and closure of the isolation membrane around cytoplasm to form a double-membrane bound autophagosome, requires two highly conserved ubiquitin-like conjugation systems that function to conjugate LC3 to phosphatidylethanolamine. Stage 3 - fusion of the autophagosome with the endo-lysosomal pathway. Stage 4 - breakdown of vesicle contents in the lysosome. Figure adapted from Virgin and Levine, 2009[164].

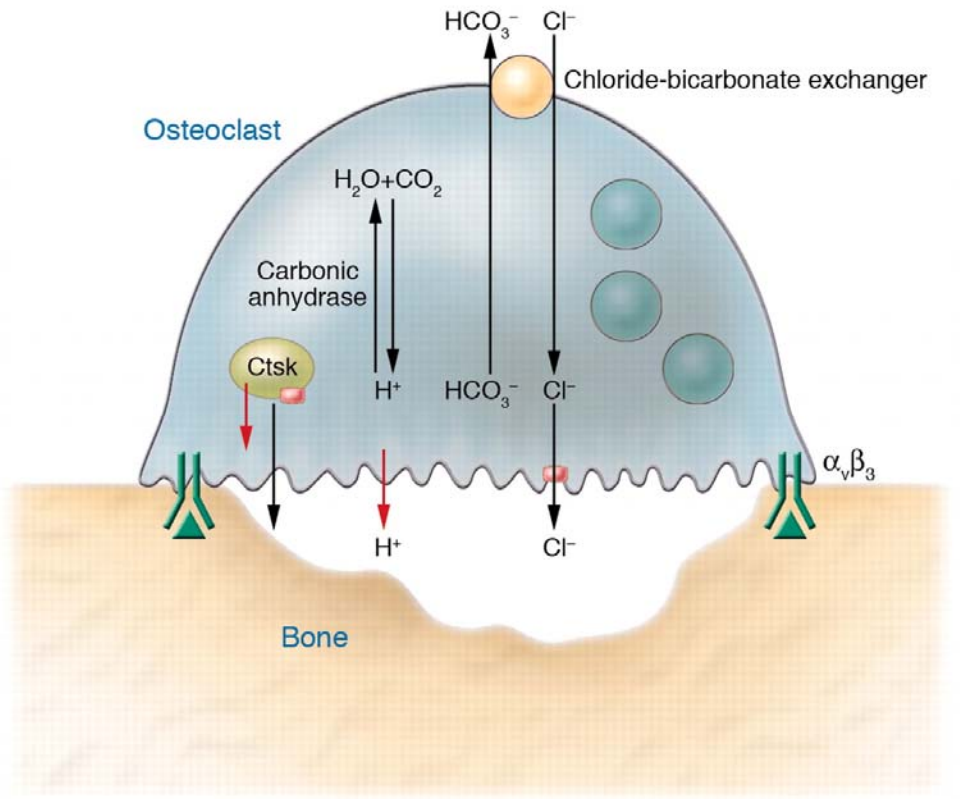

Figure 1-2. Function of the bone-resorbing osteoclast

Osteoclast bone resorption requires activation of the osteoclast by recognition of the bone substrate via receptors such as the αvβ3 integrin. Vesicles containing cathepsin K (Ctsk), vacuolar H+ ATPases (red arrow), and chloride channels (pink box) are inserted into the plasma membrane against the bone, forming a ruffled border. Hydrogen ions are pumped into the resorption pit, generated by the action of carbonic anhydrase in the cell. Electrical neutrality in the cell and resorption pit is maintained by the chloride channel and chloride-bicarbonate exchanger. After demineralization of the bone, the organic matrix is degraded by the action of cathepsin K and other enzymes. Figure adapted from www.biology-online.org.

References

1. Komatsu, M. *et al.* Impairment of starvation-induced and constitutive autophagy in Atg7-deficient mice. *J. Cell Biol.* **169**, 425-434 (2005).

2. Kuma, A. *et al.* The role of autophagy during the early neonatal starvation period. *Nature.* **432**, 1032-1036 (2004).

3. Sou, Y.S. *et al.* The Atg8 conjugation system is indispensable for proper development of autophagic isolation membranes in mice. *Mol. Biol. Cell.* **19**, 4762-4775 (2008).

4. Mizushima, N., Yamamoto, A., Matsui, M., Yoshimori, T. & Ohsumi, Y. In vivo analysis of autophagy in response to nutrient starvation using transgenic mice expressing a fluorescent autophagosome marker. *Mol Biol Cell.* **15**, 1101-1111 (2004).

5. Lum, J.J. *et al.* Growth factor regulation of autophagy and cell survival in the absence of apoptosis. *Cell.* **120**, 237-248 (2005).

6. Yorimitsu, T., Nair, U., Yang, Z. & Klionsky, D.J. Endoplasmic reticulum stress triggers autophagy. *J. Biol. Chem.* **281**, 30299-30304 (2006).

7. Kouroku, Y. *et al.* ER stress (PERK/eIF2alpha phosphorylation) mediates the polyglutamine-induced LC3 conversion, an essential step for autophagy formation. *Cell Death. Differ.* **14**, 230-239 (2007).

8. Talloczy, Z. *et al.* Regulation of starvation- and virus-induced autophagy by the eIF2alpha kinase signaling pathway. *Proc. Natl. Acad. Sci. U. S. A.* **99**, 190-195 (2002).

9. Xu, Y. *et al.* Toll-like receptor 4 is a sensor for autophagy associated with innate immunity. *Immunity.* **27**, 135-144 (2007).

10. Shelly, S., Lukinova, N., Bambina, S., Berman, A. & Cherry, S. Autophagy is an essential component of Drosophila immunity against vesicular stomatitis virus. *Immunity.* **30**, 588-598 (2009).

11. Yano, T. *et al.* Autophagic control of listeria through intracellular innate immune recognition in drosophila. *Nat. Immunol.* **9**, 908-916 (2008).

12. Nakagawa, I. *et al.* Autophagy defends cells against invading group a Streptococcus. *Science.* **306**, 1037-1040 (2004).

13. Zhang, H. *et al.* Mitochondrial autophagy is a HIF-1-dependent adaptive metabolic response to hypoxia. *J. Biol. Chem.* (2008).

14. Papandreou, I., Lim, A.L., Laderoute, K. & Denko, N.C. Hypoxia signals autophagy in tumor cells via AMPK activity, independent of HIF-1, BNIP3, and BNIP3L. *Cell Death Differ.* **15**, 1572-1581 (2008).

15. Scherz-Shouval, R. *et al.* Reactive oxygen species are essential for autophagy and specifically regulate the activity of Atg4. *EMBO J.* **26**, 1749-1760 (2007).

16. Yan, Y. & Backer, J.M. Regulation of class III (Vps34) PI3Ks. *Biochem. Soc. Trans.* **35**, 239-241 (2007).

17. Petiot, A., Ogier-Denis, E., Blommaart, E.F., Meijer, A.J. & Codogno, P. Distinct classes of phosphatidylinositol 3'-kinases are involved in signaling pathways that control macroautophagy in HT-29 cells. *J Biol Chem.* **275**, 992-998 (2000).

18. He, C. & Klionsky, D.J. Regulation Mechanisms and Signaling Pathways of Autophagy. *Annu. Rev. Genet.* (2009).

19. Tanida, I., Ueno, T. & Kominami, E. LC3 conjugation system in mammalian autophagy. *Int. J. Biochem. Cell Biol.* **36**, 2503-2518 (2004).

20. Mizushima, N. *et al.* A protein conjugation system essential for autophagy. *Nature.* **395**, 395-398 (1998).

21. Tanida, I., Tanida-Miyake, E., Ueno, T. & Kominami, E. The human homolog of Saccharomyces cerevisiae Apg7p is a Protein-activating enzyme for multiple substrates including human Apg12p, GATE-16, GABARAP, and MAP-LC3. *J Biol. Chem.* **276**, 1701-1706 (2001).

22. Shintani, T. *et al.* Apg10p, a novel protein-conjugating enzyme essential for autophagy in yeast. *EMBO. J.* **18**, 5234-5241 (1999).

23. Mizushima, N., Sugita, H., Yoshimori, T. & Ohsumi, Y. A new protein conjugation system in human. The counterpart of the yeast Apg12p conjugation system essential for autophagy. *J Biol. Chem.* **273**, 33889-33892 (1998).

24. Mizushima, N. *et al.* Dissection of autophagosome formation using Apg5-deficient mouse embryonic stem cells. *J Cell Biol.* **152**, 657-668 (2001).

25. Fujita, N., Itoh, T., Fukuda, M., Noda, T. & Yoshimori, T. The Atg16L Complex Specifies the Site of LC3 Lipidation for Membrane Biogenesis in Autophagy. *Mol. Biol. Cell.* **19**, 2092-2100 (2008).

26. Hanada, T. *et al.* The ATG12-ATG5 conjugate has a novel e3-like activity for protein lipidation in autophagy. *J. Biol. Chem.* (2007).

27. Hemelaar, J., Lelyveld, V.S., Kessler, B.M. & Ploegh, H.L. A single protease, Apg4B, is specific for the autophagy-related ubiquitin-like proteins GATE-16, MAP1-LC3, GABARAP, and Apg8L. *J Biol Chem.* **278**, 51841-51850 (2003).

28. Tanida, I., Komatsu, M., Ueno, T. & Kominami, E. GATE-16 and GABARAP are authentic modifiers mediated by Apg7 and Apg3. *Biochem. Biophys. Res. Commun.* **300**, 637-644 (2003).

29. Tanida, I., Sou, Y.S., Minematsu-Ikeguchi, N., Ueno, T. & Kominami, E. Atg8L/Apg8L is the fourth mammalian modifier of mammalian Atg8 conjugation mediated by human Atg4B, Atg7 and Atg3. *FEBS. J.* **273**, 2553-2562 (2006).

30. Kabeya, Y. *et al.* LC3, a mammalian homologue of yeast Apg8p, is localized in autophagosome membranes after processing. *EMBO J.* **19**, 5720-5728 (2000).

31. Kabeya, Y. *et al.* LC3, GABARAP and GATE16 localize to autophagosomal membrane depending on form-II formation. *J. Cell Sci.* **117**, 2805-2812 (2004).

32. Ichimura, Y. *et al.* A ubiquitin-like system mediates protein lipidation. *Nature.* **408**, 488-492 (2000).

33. Xie, Z., Nair, U. & Klionsky, D.J. Atg8 controls phagophore expansion during autophagosome formation. *Mol. Biol. Cell.* **19**, 3290-3298 (2008).

34. Nakatogawa, H., Ichimura, Y. & Ohsumi, Y. Atg8, a ubiquitin-like protein required for autophagosome formation, mediates membrane tethering and hemifusion
4. *Cell.* **130**, 165-178 (2007).

35. Kirisako, T. *et al.* The reversible modification regulates the membrane-binding state of Apg8/Aut7 essential for autophagy and the cytoplasm to vacuole targeting pathway. *J Cell Biol.* **151**, 263-276 (2000).

36. Nishida, Y. *et al.* Discovery of Atg5/Atg7-independent alternative macroautophagy. *Nature.* **461**, 654-658 (2009).

37. Harrison, R.E., Bucci, C., Vieira, O.V., Schroer, T.A. & Grinstein, S. Phagosomes fuse with late endosomes and/or lysosomes by extension of membrane protrusions along microtubules: role of Rab7 and RILP. *Mol Cell Biol.* **23**, 6494-6506 (2003).

38. Bucci, C., Thomsen, P., Nicoziani, P., McCarthy, J. & van, D.B. Rab7: a key to lysosome biogenesis. *Mol. Biol. Cell.* **11**, 467-480 (2000).

39. Vitelli, R. *et al.* Role of the small GTPase Rab7 in the late endocytic pathway. *J Biol. Chem.* **272**, 4391-4397 (1997).

40. Jager, S. *et al.* Role for Rab7 in maturation of late autophagic vacuoles. *J. Cell Sci.* **117**, 4837-4848 (2004).

41. Kimura, S., Noda, T. & Yoshimori, T. Dissection of the autophagosome maturation process by a novel reporter protein, tandem fluorescent-tagged LC3. *Autophagy.* **3**, 452-460 (2007).

42. Gutierrez, M.G., Munafo, D.B., Beron, W. & Colombo, M.I. Rab7 is required for the normal progression of the autophagic pathway in mammalian cells. *J Cell Sci.* **117**, 2687-2697 (2004).

43. Tanida, I., Minematsu-Ikeguchi, N., Ueno, T. & Kominami, E. Lysosomal turnover, but not a cellular level, of endogenous LC3 is a marker for autophagy. *Autophagy.* **1**, 84-91 (2005).

44. Klionsky, D.J. *et al.* Guidelines for the use and interpretation of assays for monitoring autophagy in higher eukaryotes. *Autophagy.* **4**, 151-175 (2008).

45. Klionsky, D.J. Autophagy: from phenomenology to molecular understanding in less than a decade. *Nat. Rev. Mol. Cell Biol.* **8**, 931-937 (2007).

46. Takeshige, K., Baba, M., Tsuboi, S., Noda, T. & Ohsumi, Y. Autophagy in yeast demonstrated with proteinase-deficient mutants and conditions for its induction. *J Cell Biol.* **119**, 301-311 (1992).

47. Kuma, A., Matsui, M. & Mizushima, N. LC3, an autophagosome marker, can be incorporated into protein aggregates independent of autophagy: caution in the interpretation of LC3 localization. *Autophagy.* **3**, 323-328 (2007).

48. Pankiv, S. *et al.* p62/SQSTM1 binds directly to Atg8/LC3 to facilitate degradation of Ubiquitinated protein aggregates by autophagy. *J. Biol. Chem.* (2007).

49. Mizushima, N., Ohsumi, Y. & Yoshimori, T. Autophagosome formation in mammalian cells. *Cell Struct. Funct.* **27**, 421-429 (2002).

50. Codogno, P. & Meijer, A.J. Atg5: more than an autophagy factor. *Nat. Cell Biol.* **8**, 1045-1047 (2006).

51. Yousefi, S. *et al.* Calpain-mediated cleavage of Atg5 switches autophagy to apoptosis. *Nat. Cell Biol.* **8**, 1124-1132 (2006).

52. Pyo, J.O. *et al.* Essential roles of Atg5 and FADD in autophagic cell death: dissection of autophagic cell death into vacuole formation and cell death. *J. Biol. Chem.* **280**, 20722-20729 (2005).

53. Jounai, N. *et al.* The Atg5 Atg12 conjugate associates with innate antiviral immune responses. *Proc Natl Acad Sci U. S. A.* **104**, 14050-14055 (2007).

54. Levine, B. & Kroemer, G. Autophagy in the Pathogenesis of Disease. *Cell.* **132**, 27-42 (2008).

55. Cadwell, K., Patel, K.K., Komatsu, M., Virgin, H.W. & Stappenbeck, T.S. A common role for Atg16L1, Atg5, and Atg7 in small intestinal Paneth cells and Crohn's disease. *Autophagy.* **5**, 250-252 (2008).

56. Cadwell, K. *et al.* A key role for autophagy and the autophagy gene Atg16l1 in mouse and human intestinal Paneth cells. *Nature.* **456**, 259-263 (2008).

57. Ebato, C. *et al.* Autophagy is important in islet homeostasis and compensatory increase of Beta cell mass in response to high-fat diet. *Cell Metab.* **8**, 325-332 (2008).

58. Jung, H.S. *et al.* Loss of autophagy diminishes pancreatic Beta cell mass and function with resultant hyperglycemia. *Cell Metab.* **8**, 318-324 (2008).

59. Ganesan, A.K. *et al.* Genome-wide siRNA-based functional genomics of pigmentation identifies novel genes and pathways that impact melanogenesis in human cells. *PLoS Genet.* **4**, e1000298 (2008).

60. Paludan, C. *et al.* Endogenous MHC class II processing of a viral nuclear antigen after autophagy. *Science.* **307**, 593-596 (2005).

61. Schmid, D., Pypaert, M. & Munz, C. Antigen-loading compartments for major histocompatibility complex class II molecules continuously receive input from autophagosomes. *Immunity.* **26**, 79-92 (2007).

62. Bernales, S., McDonald, K.L. & Walter, P. Autophagy counterbalances endoplasmic reticulum expansion during the unfolded protein response. *PLoS. Biol.* **4**, e423 (2006).

63. Ogata, M. *et al.* Autophagy is activated for cell survival after endoplasmic reticulum stress. *Mol. Cell Biol.* **26**, 9220-9231 (2006).

64. Gutierrez, M.G. *et al.* Autophagy is a defense mechanism inhibiting BCG and Mycobacterium tuberculosis survival in infected macrophages. *Cell.* **119**, 753-766 (2004).

65. Zhao, Z. *et al.* Autophagosome-independent essential function for the autophagy protein Atg5 in cellular immunity to intracellular pathogens. *Cell Host Microbe.* **4**, 458-469 (2008).

66. Wang, Y. *et al.* Loss of macroautophagy promotes or prevents fibroblast apoptosis depending on the death stimulus. *J. Biol. Chem.* **283**, 4766-4777 (2008).

67. Boya, P. *et al.* Inhibition of macroautophagy triggers apoptosis. *Mol. Cell Biol.* **25**, 1025-1040 (2005).

68. Elmore, S.P., Qian, T., Grissom, S.F. & Lemasters, J.J. The mitochondrial permeability transition initiates autophagy in rat hepatocytes. *FASEB J.* **15**, 2286-2287 (2001).

69. Zhang, Y. *et al.* The role of autophagy in mitochondria maintenance: characterization of mitochondrial functions in autophagy-deficient S. cerevisiae strains. *Autophagy.* **3**, 337-346 (2007).

70. Tal, M.C. *et al.* Absence of autophagy results in reactive oxygen species-dependent aplification of RLR signaling. *Proc. Natl. Acad. Sci. U. S. A.* **106**, 2770-2775 (2009).

71. Wang, Y. *et al.* Loss of macroautophagy promotes or prevents fibroblast apoptosis depending on the death stimulus. *J Biol. Chem.* **283**, 4766-4777 (2008).

72. Zhang, H. *et al.* Mitochondrial autophagy is an HIF-1-dependent adaptive metabolic response to hypoxia. *J Biol. Chem.* **283**, 10892-10903 (2008).

73. Fruehauf, J.P. & Meyskens, F.L., Jr. Reactive oxygen species: a breath of life or death? *Clin. Cancer Res.* **13**, 789-794 (2007).

74. Yamamura, H. Redox control of protein tyrosine phosphorylation. *Antioxid. Redox. Signal.* **4**, 479-480 (2002).

75. Hildeman, D.A., Mitchell, T., Kappler, J. & Marrack, P. T cell apoptosis and reactive oxygen species. *J. Clin. Invest.* **111**, 575-581 (2003).

76. Saitoh, T. *et al.* Loss of the autophagy protein Atg16L1 enhances endotoxin-induced IL-1beta production. *Nature.* **456**, 264-268 (2008).

77. Komatsu, M. *et al.* Loss of autophagy in the central nervous system causes neurodegeneration in mice. *Nature.* **441**, 880-884 (2006).

78. Hara, T. *et al.* Suppression of basal autophagy in neural cells causes neurodegenerative disease in mice. *Nature.* **441**, 885-889 (2006).

79. Simonsen, A. *et al.* Promoting basal levels of autophagy in the nervous system enhances longevity and oxidant resistance in adult Drosophila. *Autophagy.* **4**, 176-184 (2008).

80. Xiong, Y., Contento, A.L., Nguyen, P.Q. & Bassham, D.C. Degradation of oxidized proteins by autophagy during oxidative stress in Arabidopsis. *Plant. Physiol.* **143**, 291-299 (2007).

81. Kunchithapautham, K. & Rohrer, B. Apoptosis and autophagy in photoreceptors exposed to oxidative stress. *Autophagy.* **3**, 433-441 (2007).

82. Chen, Y., Millan-Ward, E., Kong, J., Israels, S.J. & Gibson, S.B. Oxidative stress induces autophagic cell death independent of apoptosis in transformed and cancer cells. *Cell Death Differ.* **15**, 171-182 (2008).

83. Yu, L. *et al.* Autophagic programmed cell death by selective catalase degradation. *Proc. Natl. Acad. Sci. U. S. A.* **103**, 4952-4957 (2006).

84. Kissova, I. *et al.* Lipid oxidation and autophagy in yeast. *Free. Radic. Biol. Med.* **41**, 1655-1661 (2006).

85. Berry, D.L. & Baehrecke, E.H. Growth arrest and autophagy are required for salivary gland cell degradation in Drosophila. *Cell.* **131**, 1137-1148 (2007).

86. Koike, M. *et al.* Inhibition of autophagy prevents hippocampal pyramidal neuron death after hypoxic-ischemic injury. *Am. J Pathol.* **172**, 454-469 (2008).

87. Kroemer, G. & Levine, B. Autophagic cell death: the story of a misnomer. *Nat Rev. Mol. Cell Biol.* **9**, 1004-1010 (2008).

88. Gozuacik, D. & Kimchi, A. Autophagy as a cell death and tumor suppressor mechanism. *Oncogene.* **23**, 2891-2906 (2004).

89. Matsunaga, K. *et al.* Two Beclin 1-binding proteins, Atg14L and Rubicon, reciprocally regulate autophagy at different stages. *Nature Cell Biology.* Epub ahead of print (2009).

90. Zhong, Y. *et al.* Distinct regulation of autophagic activity by Atg14L and Rubicon associated with Beclin 1-phosphatidylinositol-3-kinase complex. *Nat. Cell Biol.* **11**, 468-476 (2009).

91. Longatti, A. & Tooze, S.A. Vesicular trafficking and autophagosome formation. *Cell Death. Differ.* **16**, 956-965 (2009).

92. Sanjuan, M.A. *et al.* Toll-like receptor signaling in macrophages links the autophagy pathway to phagocytosis. *Nature.* **450**, 1253-1257 (2007).

93. Taylor, G.A., Feng, C.G. & Sher, A. Control of IFN-gamma-mediated host resistance to intracellular pathogens by immunity-related GTPases (p47 GTPases). *Microbes. Infect.* **9**, 1644-1651 (2007).

94. Dalakas, M.C. Invited article: inhibition of B cell functions: implications for neurology. *Neurology.* **70**, 2252-2260 (2008).

95. Serreze, D.V. & Silveira, P.A. The role of B lymphocytes as key antigen-presenting cells in the development of T cell-mediated autoimmune type 1 diabetes. *Curr Dir. Autoimmun.* **6**, 212-227 (2003).

96. Silveira, P.A. *et al.* The preferential ability of B lymphocytes to act as diabetogenic APC in NOD mice depends on expression of self-antigen-specific immunoglobulin receptors. *Eur J Immunol.* **32**, 3657-3666 (2002).

97. Krzysiek, R. *et al.* Antigen receptor engagement selectively induces macrophage inflammatory protein-1 alpha (MIP-1 alpha) and MIP-1 beta chemokine production in human B cells. *J Immunol.* **162**, 4455-4463 (1999).

98. Kaser, A. *et al.* B lymphocyte-derived IL-16 attracts dendritic cells and Th cells. *J Immunol.* **165**, 2474-2480 (2000).

99. Montecino-Rodriguez, E. & Dorshkind, K. New perspectives in B-1 B cell development and function. *Trends Immunol.* **27**, 428-433 (2006).

100. Hardy, R.R., Carmack, C.E., Shinton, S.A., Kemp, J.D. & Hayakawa, K. Resolution and characterization of pro-B and pre-pro-B cell stages in normal mouse bone marrow. *J. Exp. Med.* **173**, 1213-1225 (1991).

101. Loder, F. *et al.* B cell development in the spleen takes place in discrete steps and is determined by the quality of B cell receptor-derived signals. *J. Exp. Med.* **190**, 75-89 (1999).

102. Casola, S. Control of peripheral B-cell development. *Curr. Opin. Immunol.* **19**, 143-149 (2007).

103. Lopes-Carvalho, T. & Kearney, J.F. Development and selection of marginal zone B cells. *Immunol. Rev.* **197**, 192-205 (2004).

104. Baumgarth, N., Tung, J.W. & Herzenberg, L.A. Inherent specificities in natural antibodies: a key to immune defense against pathogen invasion. *Springer Semin. Immunopathol.* **26**, 347-362 (2005).

105. Ochsenbein, A.F. *et al.* Control of early viral and bacterial distribution and disease by natural antibodies. *Science.* **286**, 2156-2159 (1999).

106. Briles, D.E. *et al.* Antiphosphocholine antibodies found in normal mouse serum are protective against intravenous infection with type 3 streptococcus pneumoniae. *J Exp. Med.* **153**, 694-705 (1981).

107. Haas, K.M., Poe, J.C., Steeber, D.A. & Tedder, T.F. B-1a and B-1b cells exhibit distinct developmental requirements and have unique functional roles in innate and adaptive immunity to S. pneumoniae. *Immunity.* **23**, 7-18 (2005).

108. Dorshkind, K. & Montecino-Rodriguez, E. Fetal B-cell lymphopoiesis and the emergence of B-1-cell potential. *Nat. Rev. Immunol.* **7**, 213-219 (2007).

109. Montecino-Rodriguez, E., Leathers, H. & Dorshkind, K. Identification of a B-1 B cell-specified progenitor. *Nat. Immunol.* **7**, 293-301 (2006).

110. Tung, J.W., Mrazek, M.D., Yang, Y., Herzenberg, L.A. & Herzenberg, L.A. Phenotypically distinct B cell development pathways map to the three B cell lineages in the mouse. *Proc. Natl. Acad. Sci. U. S. A.* **103**, 6293-6298 (2006).

111. Watanabe, K., Ichinose, S., Hayashizaki, K. & Tsubata, T. Induction of autophagy by B cell antigen receptor stimulation and its inhibition by costimulation. *Biochem. Biophys. Res. Commun.* **374**, 274-281 (2008).

112. Chaturvedi, A., Dorward, D. & Pierce, S.K. The B cell receptor governs the subcellular location of Toll-like receptor 9 leading to hyperresponses to DNA-containing antigens. *Immunity.* **28**, 799-809 (2008).

113. Bommhardt, U., Beyer, M., Hunig, T. & Reichardt, H.M. Molecular and cellular mechanisms of T cell development. *Cell Mol. Life. Sci.* **61**, 263-280 (2004).

114. Rathmell, J.C., Vander Heiden, M.G., Harris, M.H., Frauwirth, K.A. & Thompson, C.B. In the absence of extrinsic signals, nutrient utilization by lymphocytes is insufficient to maintain either cell size or viability. *Mol. Cell.* **6**, 683-692 (2000).

115. Rathmell, J.C., Farkash, E.A., Gao, W. & Thompson, C.B. IL-7 enhances the survival and maintains the size of naive T cells. *J Immunol.* **167**, 6869-6876 (2001).

116. Van, P.L., Ibraghimov, A. & Abbas, A.K. The roles of costimulation and Fas in T cell apoptosis and peripheral tolerance. *Immunity.* **4**, 321-328 (1996).

117. Clarke, S.R. & Rudensky, A.Y. Survival and homeostatic proliferation of naive peripheral CD4+ T cells in the absence of self peptide:MHC complexes. *J Immunol.* **165**, 2458-2464 (2000).

118. Marrack, P. & Kappler, J. Control of T cell viability. *Annu. Rev. Immunol.* **22**, 765-787 (2004).

119. Ashwell, J.D., Cunningham, R.E., Noguchi, P.D. & Hernandez, D. Cell growth cycle block of T cell hybridomas upon activation with antigen. *J Exp. Med.* **165**, 173-194 (1987).

120. Hildeman, D.A., Zhu, Y., Mitchell, T.C., Kappler, J. & Marrack, P. Molecular mechanisms of activated T cell death in vivo. *Curr. Opin. Immunol.* **14**, 354-359 (2002).

121. Hildeman, D.A. *et al.* Activated T cell death in vivo mediated by proapoptotic bcl-2 family member bim. *Immunity.* **16**, 759-767 (2002).

122. Perl, A., Gergely, P., Jr., Nagy, G., Koncz, A. & Banki, K. Mitochondrial hyperpolarization: a checkpoint of T-cell life, death and autoimmunity. *Trends Immunol.* **25**, 360-367 (2004).

123. Jackson, S.H., Devadas, S., Kwon, J., Pinto, L.A. & Williams, M.S. T cells express a phagocyte-type NADPH oxidase that is activated after T cell receptor stimulation. *Nat. Immunol.* **5**, 818-827 (2004).

124. Jones, R.G. *et al.* The proapoptotic factors Bax and Bak regulate T Cell proliferation through control of endoplasmic reticulum Ca(2+) homeostasis. *Immunity.* **27**, 268-280 (2007).

125. Williams, M.S. & Kwon, J. T cell receptor stimulation, reactive oxygen species, and cell signaling. *Free Radic. Biol. Med.* **37**, 1144-1151 (2004).

126. Bauer, M.K. *et al.* Role of reactive oxygen intermediates in activation-induced CD95 (APO-1/Fas) ligand expression. *J. Biol. Chem.* **273**, 8048-8055 (1998).

127. Devadas, S., Zaritskaya, L., Rhee, S.G., Oberley, L. & Williams, M.S. Discrete generation of superoxide and hydrogen peroxide by T cell receptor stimulation: selective regulation of mitogen-activated protein kinase activation and fas ligand expression. *J. Exp. Med.* **195**, 59-70 (2002).

128. Hildeman, D.A. *et al.* Reactive oxygen species regulate activation-induced T cell apoptosis. *Immunity.* **10**, 735-744 (1999).

129. Hildeman, D.A. *et al.* Control of Bcl-2 expression by reactive oxygen species. *Proc Natl Acad Sci U. S. A.* **100**, 15035-15040 (2003).

130. Nedjic, J., Aichinger, M., Emmerich, J., Mizushima, N. & Klein, L. Autophagy in thymic epithelium shapes the T-cell repertoire and is essential for tolerance. *Nature.* **455**, 396-400 (2008).

131. Li, C. *et al.* Autophagy is induced in CD4+ T cells and important for the growth factor-withdrawal cell death. *J. Immunol.* **177**, 5163-5168 (2006).

132. Pua, H.H., Dzhagalov, I., Chuck, M., Mizushima, N. & He, Y.W. A critical role for the autophagy gene Atg5 in T cell survival and proliferation. *J. Exp. Med.* **204**, 25-31 (2007).

133. Bell, B.D. *et al.* FADD and caspase-8 control the outcome of autophagic signaling in proliferating T cells. *Proc Natl Acad Sci U. S. A.* **105**, 16677-16682 (2008).

134. Feng, C.G. *et al.* The immunity-related GTPase Irgm1 promotes the expansion of activated CD4+ T cell populations by preventing interferon-gamma-induced cell death. *Nat Immunol.* **9**, 1279-1287 (2008).

135. Espert, L. *et al.* Autophagy is involved in T cell death after binding of HIV-1 envelope proteins to CXCR4. *J. Clin. Invest.* **116**, 2161-2172 (2006).

136. Zaidi, M. Skeletal remodeling in health and disease. *Nat. Med.* **13**, 791-801 (2007).

137. Teitelbaum, S.L. & Ross, F.P. Genetic regulation of osteoclast development and function. *Nat. Rev. Genet.* **4**, 638-649 (2003).

138. Yasuda, H. *et al.* Osteoclast differentiation factor is a ligand for osteoprotegerin/osteoclastogenesis-inhibitory factor and is identical to TRANCE/RANKL. *Proc. Natl. Acad. Sci. U. S. A.* **95**, 3597-3602 (1998).

139. McHugh, K.P. *et al.* Mice lacking beta3 integrins are osteosclerotic because of dysfunctional osteoclasts. *J Clin Invest.* **105**, 433-440 (2000).

140. Everts, V. & Beertsen, W. External Lysosomes: The Osteoclast and Its Unique Capacities to Degrade Mineralised Tissues. Lysosomes. 144-155 (2005).

141. Coxon, F.P. & Taylor, A. Vesicular trafficking in osteoclasts. *Semin. Cell Dev. Biol.* **19**, 424-433 (2008).

142. Baron, R., Neff, L., Louvard, D. & Courtoy, P.J. Cell-mediated extracellular acidification and bone resorption: evidence for a low pH in resorbing lacunae and localization of a 100-kD lysosomal membrane protein at the osteoclast ruffled border. *J Cell Biol.* **101**, 2210-2222 (1985).

143. Mattsson, J.P. *et al.* Isolation and reconstitution of a vacuolar-type proton pump of osteoclast membranes. *J Biol. Chem.* **269**, 24979-24982 (1994).

144. Blair, H.C., Teitelbaum, S.L., Ghiselli, R. & Gluck, S. Osteoclastic bone resorption by a polarized vacuolar proton pump. *Science.* **245**, 855-857 (1989).

145. Sly, W.S., Hewett-Emmett, D., Whyte, M.P., Yu, Y.S. & Tashian, R.E. Carbonic anhydrase II deficiency identified as the primary defect in the autosomal recessive syndrome of osteopetrosis with renal tubular acidosis and cerebral calcification. *Proc. Natl. Acad. Sci. U. S. A.* **80**, 2752-2756 (1983).

146. Kornak, U. *et al.* Loss of the ClC-7 chloride channel leads to osteopetrosis in mice and man. *Cell.* **104**, 205-215 (2001).

147. Gowen, M. *et al.* Cathepsin K knockout mice develop osteopetrosis due to a deficit in matrix degradation but not demineralization. *J Bone. Miner. Res.* **14**, 1654-1663 (1999).

148. Saftig, P. *et al.* Impaired osteoclastic bone resorption leads to osteopetrosis in cathepsin-K-deficient mice. *Proc. Natl. Acad. Sci. U. S. A.* **95**, 13453-13458 (1998).

149. Nesbitt, S.A. & Horton, M.A. Trafficking of matrix collagens through bone-resorbing osteoclasts. *Science.* **276**, 266-269 (1997).

150. Salo, J., Lehenkari, P., Mulari, M., Metsikko, K. & Vaananen, H.K. Removal of osteoclast bone resorption products by transcytosis. *Science.* **276**, 270-273 (1997).

151. Blott, E.J. & Griffiths, G.M. Secretory lysosomes. *Nat. Rev. Mol. Cell Biol.* **3**, 122-131 (2002).

152. Akamine, A. *et al.* Increased synthesis and specific localization of a major lysosomal membrane sialoglycoprotein (LGP107) at the ruffled border membrane of active osteoclasts. *Histochemistry.* **100**, 101-108 (1993).

153. Maeda, H., Akasaki, K., Yoshimine, Y., Akamine, A. & Yamamoto, K. Limited and selective localization of the lysosomal membrane glycoproteins LGP85 and LGP96 in rat osteoclasts. *Histochem. Cell Biol.* **111**, 245-251 (1999).

154. Zhao, H., Ettala, O. & Vaananen, H.K. Intracellular membrane trafficking pathways in bone-resorbing osteoclasts revealed by cloning and subcellular localization studies of small GTP-binding rab proteins. *Biochem. Biophys. Res. Commun.* **293**, 1060-1065 (2002).

155. Zhao, H., Laitala-Leinonen, T., Parikka, V. & Vaananen, H.K. Downregulation of small GTPase Rab7 impairs osteoclast polarization and bone resorption. *J Biol. Chem.* **276**, 39295-39302 (2001).

156. Yamaza, T. *et al.* Study of immunoelectron microscopic localization of cathepsin K in osteoclasts and other bone cells in the mouse femur. *Bone.* **23**, 499-509 (1998).

157. Baron, R. *et al.* Polarized secretion of lysosomal enzymes: co-distribution of cation-independent mannose-6-phosphate receptors and lysosomal enzymes along the osteoclast exocytic pathway. *J Cell Biol.* **106**, 1863-1872 (1988).

158. Martinez, I. *et al.* Synaptotagmin VII regulates Ca(2+)-dependent exocytosis of lysosomes in fibroblasts. *J Cell Biol.* **148**, 1141-1149 (2000).

159. Zhao, H. *et al.* Synaptotagmin VII regulates bone remodeling by modulating osteoclast and osteoblast secretion. *Dev. Cell.* **14**, 914-925 (2008).

160. Pavlos, N.J. *et al.* Rab3D regulates a novel vesicular trafficking pathway that is required for osteoclastic bone resorption. *Mol. Cell Biol.* **25**, 5253-5269 (2005).

161. Rickert, R.C., Roes, J. & Rajewsky, K. B lymphocyte-specific, Cre-mediated mutagenesis in mice. *Nucleic Acids Res.* **25**, 1317-1318 (1997).

162. Lee, P.P. *et al.* A critical role for Dnmt1 and DNA methylation in T cell development, function, and survival. *Immunity.* **15**, 763-774 (2001).

163. Clausen, B.E., Burkhardt, C., Reith, W., Renkawitz, R. & Forster, I. Conditional gene targeting in macrophages and granulocytes using LysMcre mice. *Transgenic Research.* **8**, 265-277 (1999).

164. Virgin, H.W. & Levine, B. Autophagy genes in immunity. *Nat. Immunol.* **10**, 461-470 (2009).

CHAPTER 2

The Autophagy Gene *Atg5* Plays an Important Role in B Cell Development and B-1a B Cell Maintenance

Portions of this chapter are excerpted from:

Miller BC, Zhao Z, Stephenson LM, Cadwell K, Pua HH, Lee HK, Mizushima NN, Iwasaki A, He YW, Swat W, Virgin HW 4th. The autophagy gene ATG5 plays an essential role in B lymphocyte development. *Autophagy*. 2008 Apr 1;4(3):309-14.

Abstract

Macroautophagy (herein autophagy) is an evolutionarily conserved process, requiring the gene *Atg5*, by which cells recycle organelles and long-lived proteins. Here we show that *Atg5* is required for B cell development in the bone marrow and the homeostasis of B-1a B cells. Deletion of *Atg5* in B lymphocytes using Cre-LoxP technology or repopulation of irradiated mice with $Atg5^{-/-}$ fetal liver progenitors resulted in a dramatic reduction in B-1a B cells in the peritoneum. $Atg5^{-/-}$ progenitors exhibited a significant defect in B cell development at the pro- to pre-B cell transition, although a proportion of pre-B cells survived to populate the periphery. Once in the periphery, *Atg5*-deficient peripheral B-2 B cells have no increase in markers of cell death and proliferate normally *in vitro.* In contrast, inefficient B cell development in the bone marrow was associated with increased cell death, indicating that *Atg5* is important for B cell survival during development. We conclude that *Atg5* is differentially required at discrete stages of development in distinct, but closely related, cell lineages.

Introduction

Autophagy has been reported to be a constitutive process in B cells that is important for antigen presentation and signaling[1,2,3,4], but the function of autophagy genes in B cell survival and development are unknown. To address these questions we deleted the essential autophagy gene *Atg5* in primary B lymphocytes *in vivo.*

Developing B cells subsets can be identified in the mouse by expression of cell surface markers that correspond to gene rearrangements in the immunoglobulin locus (reviewed in [5]). One convenient method to distinguish developing B cells is by the Hardy classification system[6]. The early fractions of developing B cells (fractions A-C, also known as pre-pro-B cells and pro-B cells) express CD43 and undergo rearrangement of the heavy chain locus. The final CD43+ fraction, fraction C', expresses the heavy chain on the cell surface with the surrogate light chain. Cells that have successfully rearranged the heavy chain divide and lose expression of CD43. These cells make up the final developing B cell fractions in the bone marrow (fractions D and E). Fraction D, also known as late pre-B cells (fraction C' are considered early pre-B cells), rearranges the light chain locus such that fraction E is the first developing B cell to express the complete immunoglobulin on the cell surface[6]. Fraction E cells leave the bone marrow to finish their development in the spleen, but can return as mature B cells (fraction F). In the spleen, immature B cells go through at least two transitional stages before finishing their maturation (reviewed in [7]). These stages can be defined by cell surface expression of IgM and IgD[8].

Mature B cells are divided into two major classifications: B-1 and B-2 B cells. B-1 B cells are further subdivided into B-1a and B-1b cells based on expression of the marker CD5 and functional properties (reviewed in [9]). B-2 B cells are subdivided into marginal zone and follicular B cells, two functionally distinct classes that differ in their expression of CD21 and CD23 (reviewed in [10]). Together, these B cells produce antibodies important from initial infection to long-lived memory responses.

In this chapter we evaluated the role of *Atg5* in B cell development and homeostasis. While B-2 B cells can be generated from *Atg5*$^{-/-}$ precursor cells and populate peripheral lymphoid organs, *Atg5* was required for efficient development from pro- to pre-B cells in the bone marrow. The absence of *Atg5* was associated with a significant increase in the death of Hardy fraction D-F B cells. In addition to its function during development, *Atg5* is important for the maintenance of mature B-1a B cells.

Results

Atg5 is required to maintain normal numbers of peripheral B-1 B cells

To study the role of the autophagy gene *Atg5* in B cells, we generated *Atg5*$^{-/-}$ chimeric mice. *Atg5*$^{-/-}$ or wild-type fetal liver cells were used to reconstitute irradiated *Rag1*$^{-/-}$ hosts[11]. In the peritoneum, *Atg5*$^{-/-}$ reconstituted mice had decreased numbers of B-1a B cells (16 fold), B-1b B cells (4 fold), and B-2 B cells (6 fold) (Fig. 2-1). Lymph node B-2 B cell repopulation was equivalent between wild type and *Atg5*$^{-/-}$ chimeras, while both B-1 and B-2 B cell numbers were decreased in the spleen approximately 50% (B-2 B cells: $p = 0.017$; B-1 B cells: $p = 0.035$). The proportion of transitional, mature follicular, and marginal zone B-2 B cells in the spleen were normal, however (Fig. 2-2). This data indicates that *Atg5* has a role in maintaining both B-1 and B-2 B cell numbers in the periphery, with a more dramatic role in B-1a B cells.

Atg5 is required for the survival of pre-B cells

The observed decrease in peripheral B cells in *Atg5*$^{-/-}$ chimeras could be due to a decrease in B cell production in the bone marrow or an increase in cell death in the periphery. To test the first hypothesis, we evaluated the stages of bone marrow B cell development in *Atg5*$^{-/-}$ versus wild-type fetal-liver reconstituted irradiated CD45.1[12] and *Rag1*$^{-/-}$ hosts (Fig. 2-3 and 2-4). FACS analysis of donor pro-B cells from CD45.1 chimeras revealed no significant differences in cell numbers of fraction A-C' developing B cells (Fig. 2-3). In contrast, analysis of *Atg5*$^{-/-}$ *Rag1*$^{-/-}$ chimeric mice revealed a

decrease in Hardy fractions D (3.7 fold reduction), E (8.3 fold reduction), and F (11.8 fold reduction) (Fig. 2-4). CD45.1 chimeras had a similar deficiency of fractions D, E, and F (data not shown). This data indicates that *Atg5* has a critical role in the final stages of bone marrow B cell development. We hypothesized that *Atg5* may be required for B cell survival after the pro-B cell stage of development. FACS analysis of freshly isolated bone marrow cells revealed a greater percentage of fraction D-F cells were dead or dying in $Atg5^{-/-}$ $Rag1^{-/-}$ chimeric mice compared with control mice as measured by Annexin-V and 7-AAD (Fig. 2-5; $Atg5^{+/+}$: 3.2 ± 0.8%; $Atg5^{-/-}$: 22.2 ± 5.3%; p = 0.0056). We conclude that *Atg5* is required as a survival factor for developing B cells after the pro-B to pre-B cell transition in the bone marrow.

B-2 B cells survive normally in the periphery without *Atg5*

Although the role of *Atg5* in B cell development could explain the deficiency in peripheral $Atg5^{-/-}$ B cells, we could not rule out that *Atg5* is also required for B cell survival in the periphery. To determine if *Atg5* is required for B cell homeostasis without the confounding role of *Atg5* in B cell development, we expressed Cre recombinase in the B cells of mice containing two copies of a knock-in *Atg5* gene in which LoxP sites were inserted flanking the third exon [$Atg5^{flox/flox}$][13]. B cell specific expression of Cre was obtained using the B cell specific CD19 promoter [CD19-*Cre*][14]. Although the expression of Cre from the CD19 promoter effectively deletes loxP-flanked DNA in more than 90-95% of mature B cells, it results in incomplete DNA rearrangement in pre-B

cells[14]. Given that the CD19-*Cre* construct replaces the wild-type *CD19* gene and could therefore have an effect on B cells independent of the deletion of *Atg5*[15], all mice were bred to have only one copy of CD19-*Cre*. Furthermore, we used *Atg5* wild-type CD19-*Cre*+ mice (herein CD19-*Cre* mice) as a control in subsequent experiments.

We confirmed rearrangement of the $Atg5^{flox}$ alleles specifically in CD19+ B cells from $Atg5^{flox/flox}$-CD19-*Cre*+ mice using PCR (data not shown). In addition, B cells from $Atg5^{flox/flox}$-CD19-*Cre*+ mice did not express detectable ATG5-ATG12 conjugate and failed to convert LC3-I to LC3-II (Fig. 2-6). Splenic B cells from control $Atg5^{flox/flox}$-CD19-*Cre*- mice expressed ATG5-ATG12 conjugate and converted LC3-I to LC3-II (Fig. 2-6). We conclude that *Atg5* is specifically deleted from peripheral CD19+ B lymphocytes in our mice and that, as expected[16], loss of *Atg5* inhibits classical macroautophagy as shown by loss of the capacity to generate LC3-II from LC3-I.

We next determined whether *Atg5* is required to maintain normal numbers of B cells in peripheral tissues of adult mice. Importantly, we observed no difference in B cell development in fractions A through E in $Atg5^{flox/flox}$-CD19-*Cre*+ mice (data not shown). There was a twofold decrease in fraction F cells in $Atg5^{flox/flox}$-CD19-*Cre*+ mice compared with $Atg5^{flox/flox}$-CD19-*Cre*- controls ($Atg5^{flox/flox}$-CD19-*Cre*-: $1.6 \pm 0.27 \times 10^6$; $Atg5^{flox/flox}$-CD19-*Cre*+: $0.81 \pm 0.16 \times 10^6$; $p = 0.0243$). This was consistent with, although less severe than, the decrease in fraction F cells observed in chimeric mice. There was no decrease in fraction F cells in CD19-*Cre* mice (data not shown). In the periphery, $Atg5^{flox/flox}$-CD19-*Cre*+ mice had normal numbers of B220+ B lymphocytes in

the spleen and lymph nodes, and IgM and IgD were expressed normally on these cells. The percentage and number of splenic and lymph node mature recirculating B cells and transitional B cells was comparable between *Atg5*$^{flox/flox}$-CD19-*Cre*-, CD19-*Cre*, and *Atg5*$^{flox/flox}$-CD19-*Cre*+ mice (Fig. 2-7). As expected, there were no differences in the numbers of T cell subsets in the thymus or periphery in these mice (data not shown). As more than 95% of splenic and nearly 100% of lymph node B cells are B-2 B cells[9], it follows that B-2 B cell numbers are normal in the spleen and lymph node in the absence of *Atg5*.

We next asked if *Atg5* is required for B-2 B cell survival or proliferation. To determine if *Atg5* is required for B cell survival, we evaluated Annexin-V and 7-AAD staining of freshly isolated splenic and lymph node B220+ cells and observed no differences in the numbers of dead or dying B cells (data not shown). We assessed proliferation by stimulating total splenocytes *in vitro* with LPS and measuring CFSE dye dilution. Flow cytometry of the splenocytes after 72 hours revealed no difference in the ability of the *Atg5*-deficient B cells to divide in response to LPS (Fig. 2-8). Together, this data suggests that *Atg5* is not essential for the maintenance of B-2 B cell populations in the periphery and is not important for B-2 B cell survival or proliferation. We hypothesize that the decrease in splenic B-2 B cells in *Atg5*$^{-/-}$ chimeric animals is due to the important role of *Atg5* in pre-B cells during development.

Atg5 is required in a cell-intrinsic manner to maintain normal numbers of B-1a B cells

In contrast to these findings for B-2 B cells, *Atg5*$^{flox/flox}$-CD19-*Cre*+ mice showed a 5-fold decrease in the number of B-1a B cells in the peritoneum (Fig. 2-9; *Atg5*$^{flox/flox}$-CD19-*Cre*-: 4.5 ± 1.2 x 10^5; *Atg5*$^{flox/flox}$-CD19-*Cre*+: 0.76 ± 0.19 x 10^5; p = 0.0079). There was no statistically significant difference in the number of B-1b or B-2 B cells in the peritoneum of *Atg5*$^{flox/flox}$-CD19-*Cre*+ mice. There was also no decrease in B-1a B cell numbers in CD19-*Cre* mice (Fig. 2-9). One explanation for this finding would be that *Atg5* is required for expression of CD5, a marker of B-1a B cells. In the peritoneum, both B-1a and B-1b B cells are B220^{lo}, IgM^{hi}, IgD^{lo}, and CD23-[9]. We therefore analyzed expression of these additional markers on peritoneal B cells (Fig. 2-9B and 2-9C). We found that *Atg5*$^{flox/flox}$-CD19-*Cre*+ mice contained fewer B-1 B cells in the peritoneum than *Atg5*$^{flox/flox}$-CD19-*Cre*- or CD19-*Cre* mice, confirming that the deficiency of B-1a B cells shown using CD5/B220 staining was not an artifact due to lack of CD5 expression in *Atg5*-deficient cells. In addition, we confirmed that this deficiency is specific for B-1a B cells but not B-1b B cells (Fig. 2-9C). We conclude that the requirement for *Atg5* to maintain B-1a B cell numbers is cell-intrinsic since only B cells lack *Atg5* in *Atg5*$^{flox/flox}$-CD19-*Cre*+ mice. This suggests that the observed results in *Atg5*$^{-/-}$ chimeric mice may also be due to cell-intrinsic effects of *Atg5* deficiency.

As B-1a B cells are responsible for the production of natural antibodies (reviewed in [9]), we next measured natural antibody titers in these mice. Anti-

phosphocholine antibodies have been shown to be an important natural antibody for protection against *Streptococcus pneumonia*[17]. Interestingly, there was no dramatic decrease in the levels of anti-phosphocholine IgM antibodies in the serum of *Atg5*$^{flox/flox}$-CD19-*Cre*+ mice (Fig. 2-10), despite the reduction in B-1a B cells in these animals. We hypothesize that the remaining B-1a B cells in *Atg5*$^{flox/flox}$-CD19-*Cre*+ mice produce sufficient quantities of natural antibody to compensate for the reduction in cell numbers.

Discussion

In this chapter we demonstrate a critical role for the autophagy gene *Atg5* in specific B cell developmental stages and lineages. *Atg5* is required for the efficient development and survival of pre-B cells in the bone marrow. A few B-2 B cells survive this transition and are able to populate peripheral lymphoid tissues, where *Atg5* does not seem to be required for their survival or proliferation. In the absence of *Atg5* there is also a dramatic reduction in peripheral B-1a B cells.

The requirement for *Atg5* in autophagy is clear[16,18]. Therefore, we can safely conclude from our studies in *Atg5*$^{flox/flox}$-CD19-*Cre*+ mice that autophagy is not required for the maintenance of peripheral B-2 B cell numbers. However, *Atg5* may have other roles in addition to its primary role in autophagy[19]. ATG5 can be cleaved by calpain and gain pro-death activity[20]. The protein can also interact with Fas-associated protein with death domain (FADD) to trigger autophagic cell death[21]. We believe it unlikely that these pro-death roles of *Atg5* are related to our findings in which *Atg5* is required for the survival of B cells.

Our results, in conjunction with the *Atg5*$^{-/-}$ T cell characterization by Pua *et al.*[12] and our work in Chapter 3 of this thesis, demonstrate that *Atg5* is differentially required in T cells versus B cells, two cell types from a common developmental lineage. Recently it has been suggested that B-1a, B-1b, and B-2 B cells may develop from distinct cell lineages[22,23]. Our results suggest that these distinct lineages have differential

requirements for *Atg5* or *Atg5*-dependent autophagy. In addition, our data suggests that *Atg5* or autophagy is required at very specific stages in lymphocyte development.

We were surprised to find no decrease in anti-phosphocholine natural antibody titers in *Atg5*$^{flox/flox}$-CD19-C*re*+ mice. We speculate that the reduction in B-1a B cell numbers is compensated by an increase in antibody production by the remaining cells. To test the ability of these mice to increase production of B-1a B cell derived antibodies, it would be interesting to stimulate these cells via immunization with *Streptococcus pneumonia* polysaccharides[24]. We predict that *Atg5*$^{flox/flox}$-CD19-C*re*+ mice would have decreased anti-pneumococcal titers after stimulation compared with control mice due to the reduced numbers of B-1a B cells.

It is intriguing to speculate that the critical role for *Atg5* in the maintenance of B-1a B cells in the periphery and for efficient pro-B cell to pre-B cell transition during B-2 B cell development in the bone marrow are related phenomena. B-1a B cells maintain their numbers in the adult by self-renewal[25]. We speculate that B-1a B cells lacking *Atg5* may not be able to self-renew efficiently resulting in decreased peripheral numbers. In this case the effects of *Atg5* on B-2 and B-1a B cells may reflect a critical role for *Atg5* in survival during specific stages of cellular differentiation. Given the importance of cytokines and growth factors in B cell development, this might be due to a role for *Atg5* in cytokine-driven differentiation or cell survival after growth factor withdrawal[26].

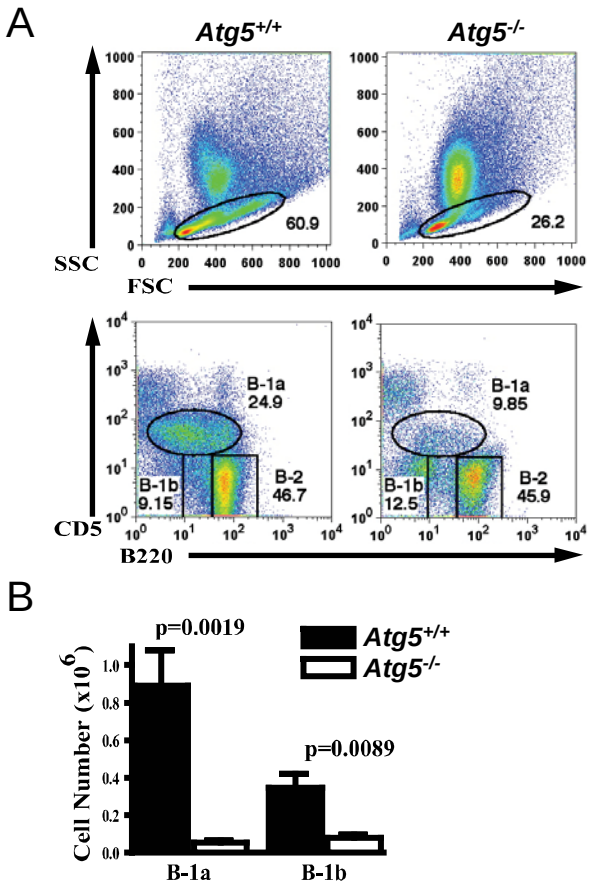

Figure 2-1. B-1 B cells are deficient in *Atg5*$^{-/-}$ chimeric mice

(A) Staining of peritoneal cells from *Atg5*$^{+/+}$ and *Atg5*$^{-/-}$ *Rag1*$^{-/-}$ chimeric mice to identify B cell subsets: B-1a (CD5+, B220^{lo}); B-1b (CD5-, B220^{lo}); B-2 (CD5-, B220^{hi}). Numbers indicate percentage of cells in each gate. Data representative of at least seven mice from four independent experiments. (B) Quantification of B-1 B cells from the peritoneum of *Atg5*$^{+/+}$ and *Atg5*$^{-/-}$ *Rag1*$^{-/-}$ chimeric mice (*Atg5*$^{+/+}$: n = 7; *Atg5*$^{-/-}$: n = 6).

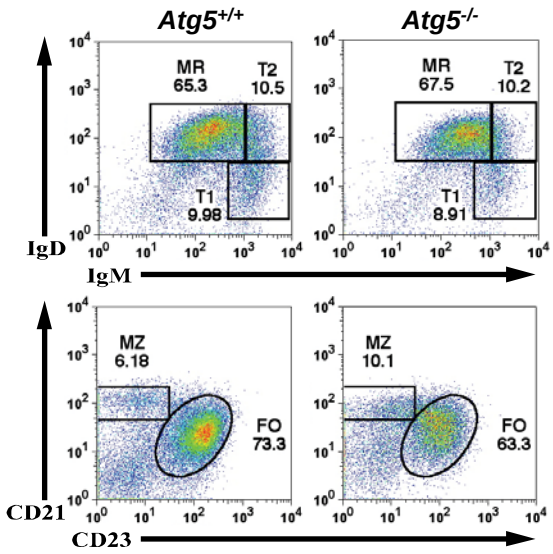

Figure 2-2. No dramatic differences in the percentages of B-2 B cell splenic subsets in *Atg5*$^{-/-}$ chimeric mice

IgM/IgD and CD21/CD23 staining of B220+ lymphocytes from the spleens of *Atg5*$^{+/+}$ and *Atg5*$^{-/-}$ *Rag1*$^{-/-}$ chimeric mice to identify B cell subsets: MR, mature recirculating B cells (IgM^{lo}, IgD^{hi}); T1, transitional type 1 (IgM^{hi}, IgD^{lo}); T2, transitional type 2 (IgM^{hi}, IgD^{hi}) ; MZ, marginal zone B cells (CD21^{hi}, CD23^{lo}); FO, follicular B cells (CD21^{lo}, CD23^{hi}). T1 gating includes marginal zone and splenic B-1 B cells. Data representative of at least eight mice from four independent experiments.

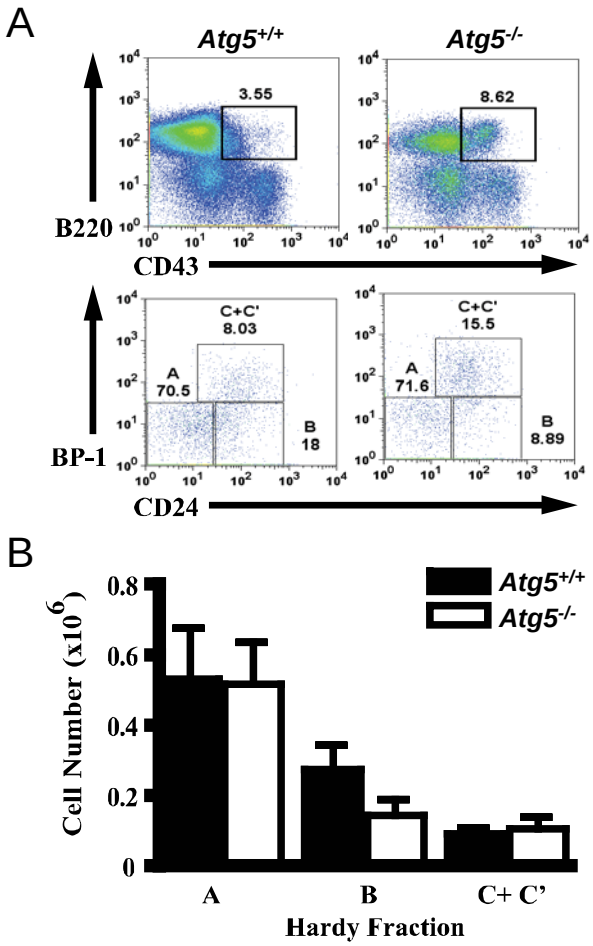

Figure 2-3. *Atg5* is not required for the normal development of pro-B cells in the bone marrow

(A) Flow cytometry of bone marrow cells from *Atg5*$^{+/+}$ and *Atg5*$^{-/-}$ CD45.1 chimeric mice. Cells were gated on CD45.2+, GR1-, Mac1-, and 7-AAD-. B220+, CD43+ cells were further analyzed for expression of BP-1 and CD24. Fraction A (B220+, CD43+, CD24-, BP-1-); Fraction B (B220+, CD43+, CD24+, BP-1-); Fraction C-C' (B220+, CD43+, CD24+, BP-1+). Data representative of at least four mice from four independent

experiments. (B) Quantification of Hardy fractions A-C' in *Atg5*$^{+/+}$ and *Atg5*$^{-/-}$ CD45.1 chimeric mice (n = 4 for each group).

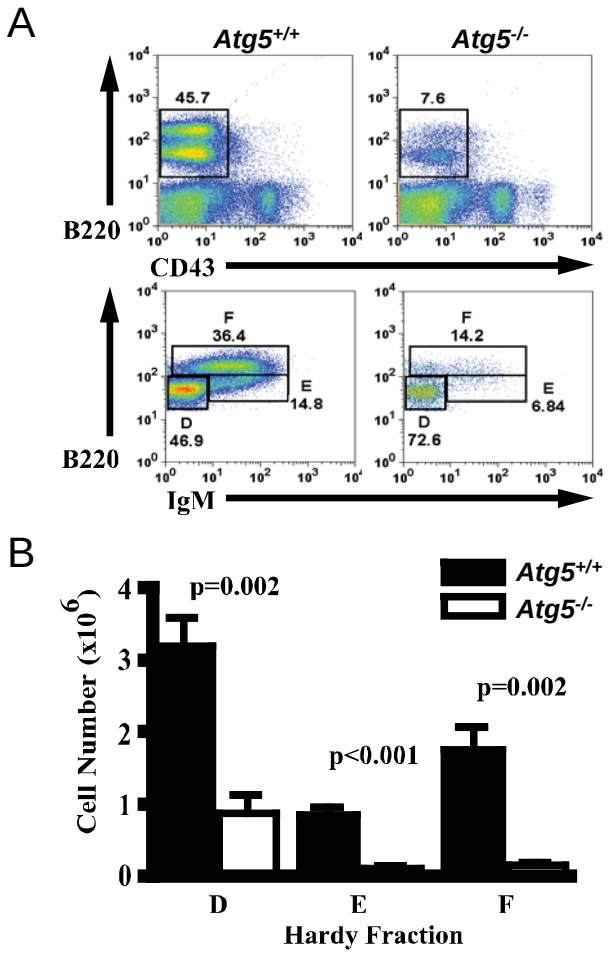

Figure 2-4. *Atg5* is required for normal development of pre-B cells in the bone marrow

(A) Flow cytometry of bone marrow cells from *Atg5*$^{+/+}$ and *Atg5*$^{-/-}$ *Rag1*$^{-/-}$ chimeric mice. Cells were gated on B220+, CD43- and analyzed for expression of IgM. Fraction D (B220+, CD43-, IgM-); Fraction E (B220+, CD43-, IgM^{hi}); Fraction F (B220^{hi}, CD43-, IgM^{lo}). Data representative of at least eight mice from four independent experiments.

(B)) Quantification of Hardy fractions D-F in *Atg5*$^{+/+}$ and *Atg5*$^{-/-}$ *Rag1*$^{-/-}$ chimeric mice (n = 8 for each group).

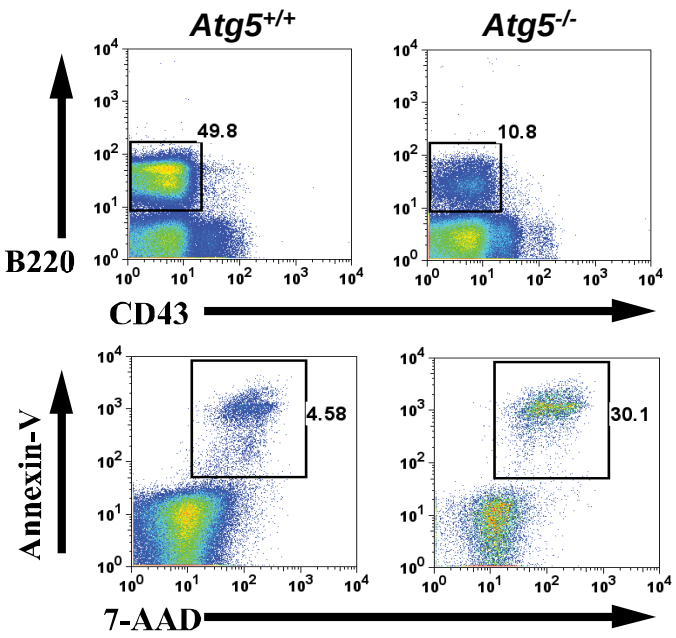

Figure 2-5. A greater percentage of *Atg5*-deficient developing pre-B cells are Annexin-V+ and 7-AAD+ compared with control cells

Flow cytometry of freshly isolated bone marrow cells from *Atg5*$^{+/+}$ and *Atg5*$^{-/-}$ *Rag1*$^{-/-}$ chimeric mice. Cells were gated on B220+, CD43- and analyzed for cell death by Annexin-V and 7-AAD. Data representative of at least six mice from three independent experiments.

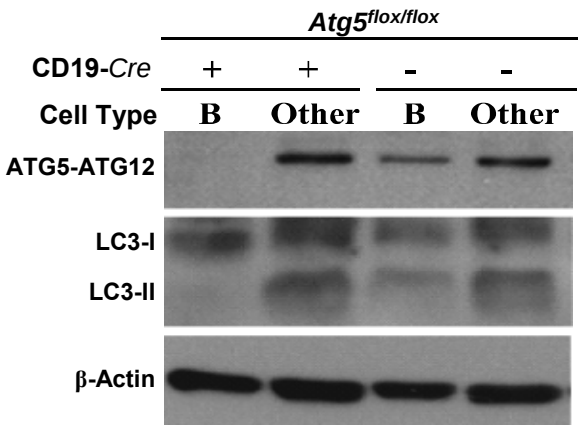

Figure 2-6. B-2 B cells from *Atg5*$^{flox/flox}$-CD19-*Cre*+ mice do not express detectable levels of ATG5

Immunoblotting with antibodies against ATG5 and LC3 from CD19+ (B) and CD19- (Other) bead-purified splenocytes. Representative blot of three independent experiments shown.

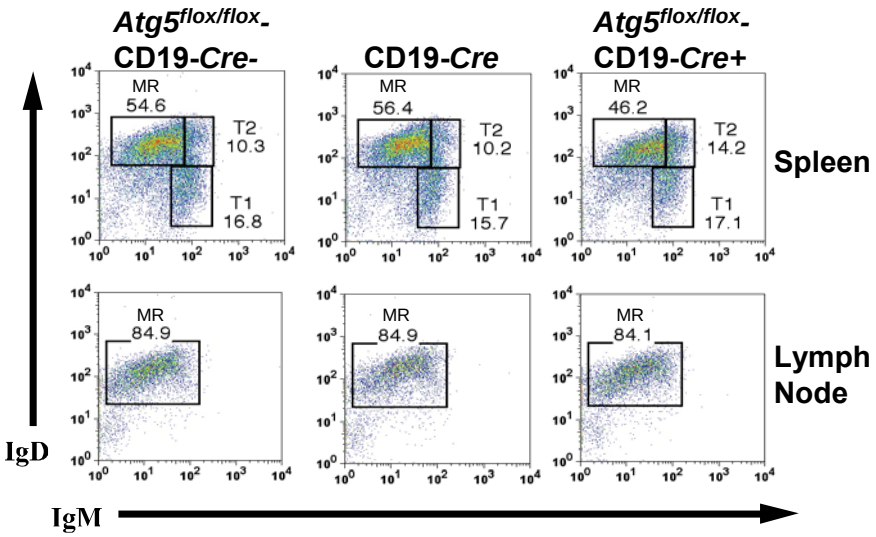

Figure 2-7. No dramatic differences in the percentages of spleen or lymph node B-2 B cells subsets in *Atg5*$^{flox/flox}$-CD19-*Cre*+ mice

IgM and IgD staining of B220+ lymphocytes from the spleen and lymph nodes. MR, mature recirculating B cells (IgM^{lo}, IgD^{hi}); T1, transitional type 1 (IgM^{hi}, IgD^{lo}); T2, transitional type 2 (IgM^{hi}, IgD^{hi}). T1 gating includes marginal zone and splenic B-1 B cells. Data representative of at least ten mice from five independent experiments.

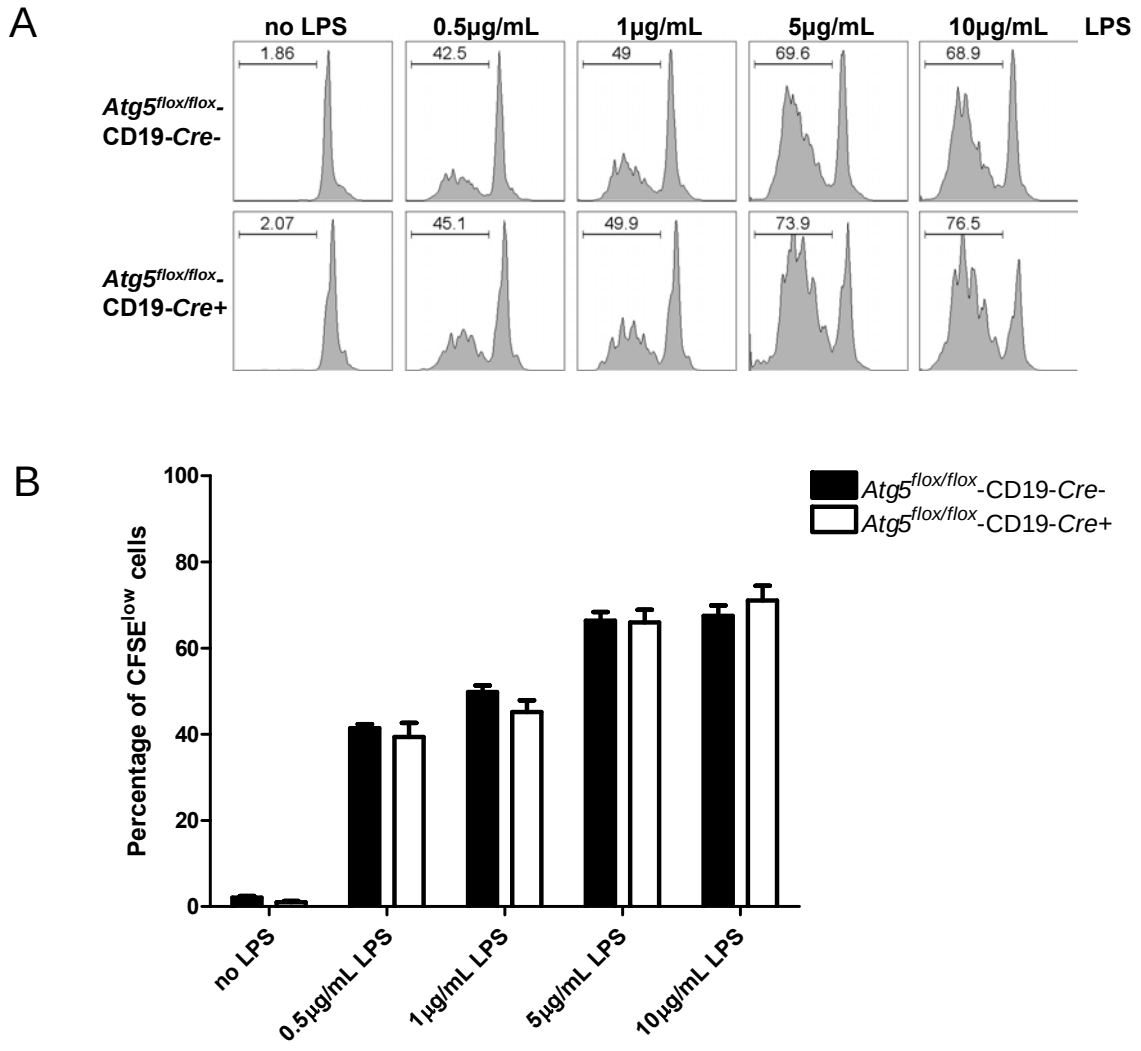

Figure 2-8. *Atg5*-deficient B-2 B cells do not have a defect in proliferation to LPS

(A) Total splenocytes from *Atg5*$^{flox/flox}$-CD19-*Cre*+ and *Atg5*$^{flox/flox}$-CD19-*Cre*- mice were labeled with CFSE and plated with different concentrations of LPS for 72 hours. B cells were gated by forward and side scatter and B220 staining. Representative FACS plots from one of three independent experiments, 6 mice of each genotype. (B) Quantification

of the percentage of $CFSE^{low}$ cells, representing cells that had divided at least once, from 2-3 independent experiments, representing 4-6 mice of each genotype.

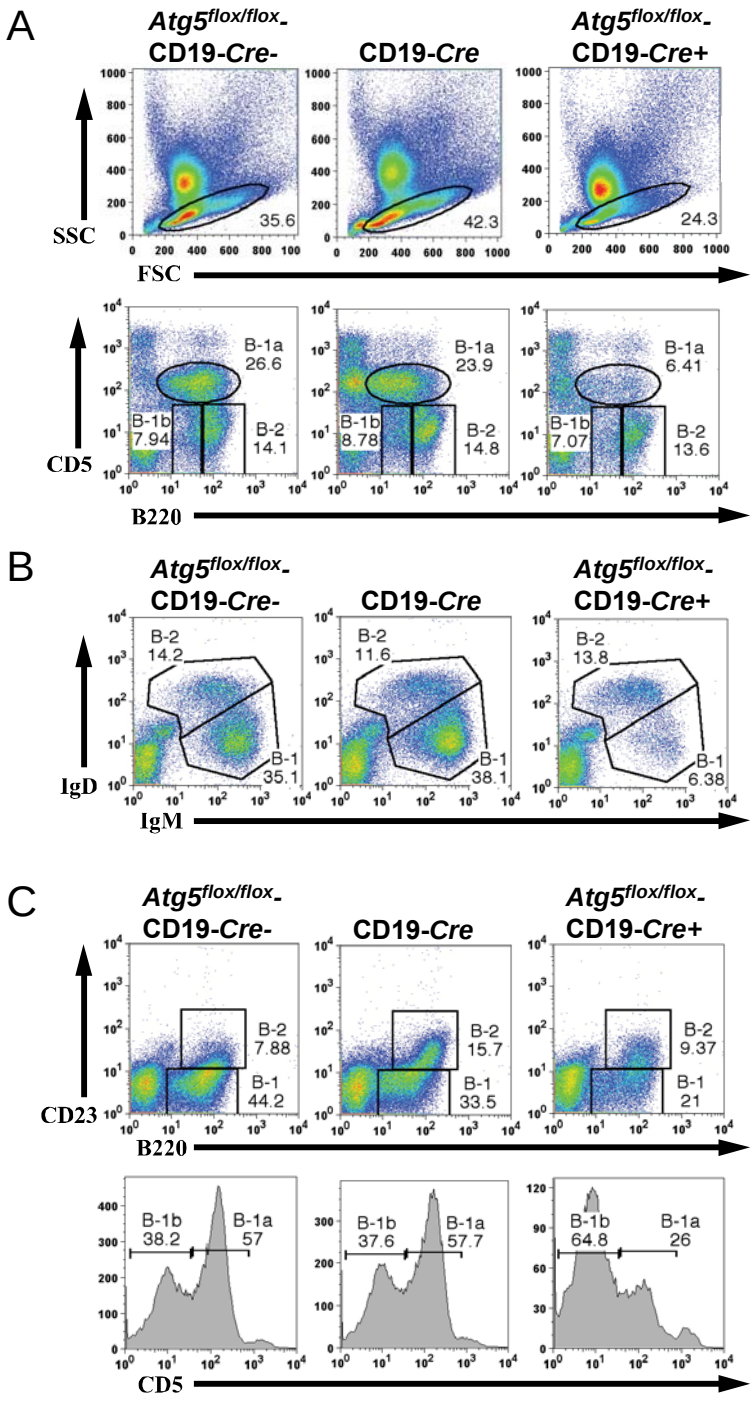

Figure 2-9. B-1a B cells are deficient in the peritoneum of *Atg5*$^{flox/flox}$-CD19-*Cre*+ mice

(A-B) Staining of peritoneal cells to identify B cell subsets: B-1a (CD5+, $B220^{lo}$, CD23-, IgM^{hi}, IgD^{lo}); B-1b (CD5-, $B220^{lo}$, CD23-, IgM^{hi}, IgD^{lo}); B-2 (CD5-, $B220^{hi}$, $CD23^{lo}$, IgM^{lo}, IgD^{hi}). All data is representative of at least five mice from three independent experiments. (C) B-1 B cells are gated by $B220^{lo}$, CD23- and separated into B-1a and B-1b B cells by expression of CD5.

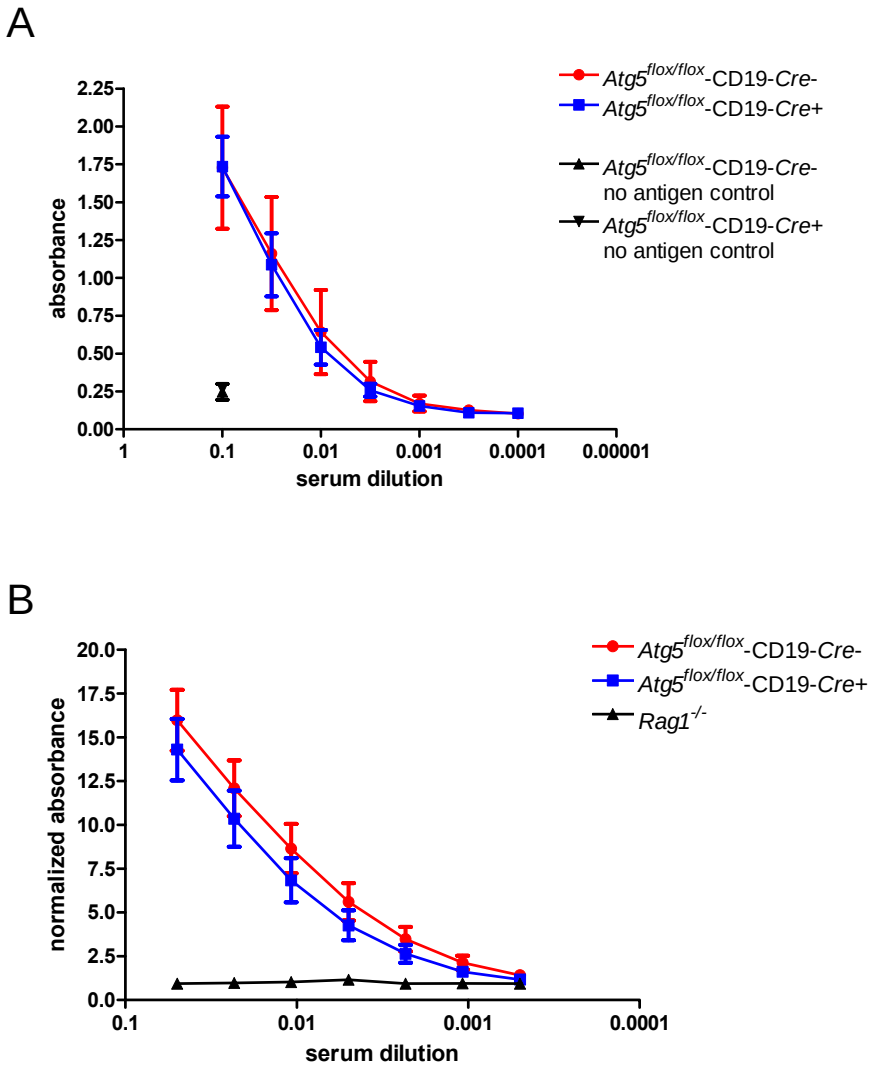

Figure 2-10. No significant decrease in anti-phosphocholine natural antibody titers in *Atg5*$^{flox/flox}$-CD19-*Cre*+ mice

Enzyme-linked immunosorbent assay (ELISA) to detect anti-phosphocholine IgM antibodies in serum from *Atg5*$^{flox/flox}$-CD19-*Cre*+, *Atg5*$^{flox/flox}$-CD19-*Cre*-, and *Rag1*$^{-/-}$ mice. Figure 2-10A shows one representative experiment. There was little absorbance in the no antigen control wells plated with the highest dilution of serum, indicating little

non-specific binding of antibody. Figure 2-10B shows data pooled from 2-3 experiments. To pool the data across experiments, the average absorbance readings for each serum dilution were normalized to the average of the no antigen negative control reading for that mouse. There are no statistically significant differences between *Atg5*$^{flox/flox}$-CD19-*Cre*+ and *Atg5*$^{flox/flox}$-CD19-*Cre*- samples in the linear range of the dilution series (1/200 – 1/20 dilution). n = 9 for *Atg5*$^{flox/flox}$-CD19-*Cre* mice, n = 4 for *Rag1*$^{-/-}$ mice.

Materials and Methods

Mice *ATG5*$^{-/-}$ and *ATG5*$^{flox/flox}$ mice have been previously described[27,13]. C.129P2-Cd19tm1(cre)Cgn/J (CD19-*Cre*) mice, B6.129S7-Rag1tm1Mom/J (*Rag1*$^{-/-}$) mice, and B6.SJL-Ptprca Pepcb/BoyJ (CD45.1) mice were obtained from The Jackson Laboratory (Bar Harbor, ME). In most experiments we compared *ATG5*$^{flox/flox}$-CD19-*Cre*+ to CD19-*Cre* mice and littermate *ATG5*$^{flox/flox}$-CD19-*Cre*- mice. Mice were genotyped as described[13], with the *Atg5* gene detected with the primers exon3-1 (GAATATGAAGGCACACCCCTGAAATG), short2 (GTACTGCATAATGGTTTAAC TCTTGC), and check2 (ACAACGTCGAGCACAGCTGCGCAAGG) using PCR [94°C (4 min); 30 cycles of 94°C (30sec), 60°C (30sec), 72°C (1 min); 72°C (5min)]. The *Cre* gene was detected with primers cre1 (AGGTTCGTTCACTCATGGA) and cre2 (TCGACCAGTTTAGTTACCC) using PCR [94°C (4 min); 25 cycles of 94°C (30sec), 60°C (30sec), 72°C (1 min); 72°C (5min)]. CD45.1 chimeric mice were generated as described[12]. For the generation of *Rag1*$^{-/-}$ chimeric mice, day 15.5-18.5 *Atg5*$^{+/-}$ x *Atg5*$^{+/-}$ fetuses were harvested and genotyped with the REDExtract-N-AmpTM Tissue PCR Kit (Sigma-Aldrich, St. Louis, MO). Sublethally irradiated (600 rad) *Rag1*$^{-/-}$ hosts were injected with cells from one-fourth of a fetal liver. Chimeric mice were analyzed at least 6 weeks after reconstitution. All animal studies were performed in accordance with institutional policies for animal care and usage at the Washington University School of Medicine.

Flow cytometry Single-cell suspensions were prepared from the bone marrow, lymph nodes, spleens, and thymi while peritoneal cells were harvested by lavage[28]. Cells were stained and data collected on a FACSCalibur cytometer (BD Biosciences, San Jose, CA) for analysis using FlowJo software (TreeStar, Ashland, OR). Antibodies against IgM, IgD, TCRβ, B220, BP-1, CD4, CD5, CD8, CD19, CD21, CD23, CD24, and CD43 were from BD Biosciences (San Jose, CA), eBioscience (San Diego, CA), or Southern Biotech (Birmingham, AL). Biotinylated antibodies were detected with streptavidin-PE-Cy7 or streptavidin-APC (BD Biosciences, San Jose, CA). Annexin-V and 7-AAD staining (BD Biosciences, San Jose, CA) was performed as per the manufacturer's instructions except that DMEM was used in place of 1x Binding Buffer. All samples were gated by forward and side scatter on lymphocyte populations for analysis.

Immunoblots B cells were purified using CD19-conjugated microbeads (Miltenyi, Auburn, CA). CD19+ purified B cells and CD19- cells that did not bind to CD19-conjugated magnetic beads were lysed in 2x Laemmli buffer and subjected to immunoblotting using antibodies specific for ATG5[18] (gift of N. Mizushima, Toyko Medical and Dental University, Tokyo, Japan) (1:1000 dilution), LC3 (Novus Biologicals, Littleton, CO) (1:3000 dilution), and β-actin (Sigma-Aldrich, St. Louis, MO) (1:5000 dilution). Immunoblots were developed with HRP-conjugated secondary antibodies (Jackson Immunoreseach Laboratories, West Grove, PA) (1:10,000 dilution) and visualized by chemiluminescence (Amersham Biosciences, Pittsburgh, PA).

Enzyme-linked immunosorbent assay (ELISA) *Atg5*$^{flox/flox}$-CD19-*Cre*+, *Atg5*$^{flox/flox}$-CD19-*Cre*-, and *Rag1*$^{-/-}$ mice were bled by cardiac puncture. 96-well Immulon 2HB flat-bottom plates (Fisher Scientific, Pittsburgh, PA) were coated with 10ug/mL of phosphocholine-BSA (Biosearch Technologies, Novato, CA) or 3% bovine serum albumin (BSA) overnight at 4°C. Wells were blocked with 3% BSA (Sigma, St. Louis, MO) for at least 1 hour at room temperature then washed. Serum was plated in triplicate at dilutions starting at 1:10 or 1:20 and left for 1 hour at room temperature. Plates were washed and 1:1000 anti-IgM antibody conjugated to HRP (Southern Biotech, Birmingham, AL) was added for 1 hour at room temperature. After a final wash, ABTS (2,2'-azino-bis(3-ethylbenzthiazoline-6-sulphonic acid) substrate with 1:1000 dilution of hydrogen peroxide was added to each well for 15 minutes before the reaction was stopped by 0.2N phosphoric acid. Plates were read at 405nm.

B cell proliferation Single cell suspensions of red blood cell-lysed splenocytes were made from *Atg5*$^{flox/flox}$-CD19-*Cre*+ and *Atg5*$^{flox/flox}$-CD19-*Cre*- mice. Cells were incubated with 1μM CFSE (Invitrogen, Carlsbad, CA) for 15 minutes and washed. 10^6 cells were plated in 24-well plates with the indicated concentrations of LPS (Sigma, St. Louis, MO). After 72-84 hours the cells were stained with anti-B220 antibody (BD Biosciences, San Jose, CA) and analyzed by flow cytometry.

Statistical analyses All data were analyzed with Prism software (GraphPad, San Diego, CA) using two-tailed unpaired t tests. Error bars represent SEM.

References

1. Schmid, D., Pypaert, M. & Munz, C. Antigen-loading compartments for major histocompatibility complex class II molecules continuously receive input from autophagosomes. *Immunity.* **26**, 79-92 (2007).

2. Paludan, C. *et al.* Endogenous MHC class II processing of a viral nuclear antigen after autophagy. *Science.* **307**, 593-596 (2005).

3. Watanabe, K., Ichinose, S., Hayashizaki, K. & Tsubata, T. Induction of autophagy by B cell antigen receptor stimulation and its inhibition by costimulation. *Biochem. Biophys. Res. Commun.* **374**, 274-281 (2008).

4. Chaturvedi, A., Dorward, D. & Pierce, S.K. The B cell receptor governs the subcellular location of Toll-like receptor 9 leading to hyperresponses to DNA-containing antigens. *Immunity.* **28**, 799-809 (2008).

5. Hardy, R.R. & Hayakawa, K. B cell development pathways. *Annu. Rev. Immunol.* **19**, 595-621 (2001).

6. Hardy, R.R., Carmack, C.E., Shinton, S.A., Kemp, J.D. & Hayakawa, K. Resolution and characterization of pro-B and pre-pro-B cell stages in normal mouse bone marrow. *J. Exp. Med.* **173**, 1213-1225 (1991).

7. Srivastava, B., Lindsley, R.C., Nikbakht, N. & Allman, D. Models for peripheral B cell development and homeostasis. *Semin. Immunol.* **17**, 175-182 (2005).

8. Loder, F. *et al.* B cell development in the spleen takes place in discrete steps and is determined by the quality of B cell receptor-derived signals. *J. Exp. Med.* **190**, 75-89 (1999).

9. Berland, R. & Wortis, H.H. Origins and functions of B-1 cells with notes on the role of CD5. *Annu. Rev. Immunol.* **20**, 253-300 (2002).

10. Pillai, S., Cariappa, A. & Moran, S.T. Positive selection and lineage commitment during peripheral B-lymphocyte development. *Immunol. Rev.* **197**, 206-218 (2004).

11. Mombaerts, P. *et al.* RAG-1-deficient mice have no mature B and T lymphocytes. *Cell.* **68**, 869-877 (1992).

12. Pua, H.H., Dzhagalov, I., Chuck, M., Mizushima, N. & He, Y.W. A critical role for the autophagy gene Atg5 in T cell survival and proliferation. *J. Exp. Med.* **204**, 25-31 (2007).

13. Hara, T. *et al.* Suppression of basal autophagy in neural cells causes neurodegenerative disease in mice. *Nature.* **441**, 885-889 (2006).

14. Rickert, R.C., Roes, J. & Rajewsky, K. B lymphocyte-specific, Cre-mediated mutagenesis in mice. *Nucleic Acids Res.* **25**, 1317-1318 (1997).

15. Rickert, R.C., Rajewsky, K. & Roes, J. Impairment of T-cell-dependent B-cell responses and B-1 cell development in CD19-deficient mice. *Nature.* **376**, 352-355 (1995).

16. Mizushima, N., Ohsumi, Y. & Yoshimori, T. Autophagosome formation in mammalian cells. *Cell Struct. Funct.* **27**, 421-429 (2002).

17. Briles, D.E. *et al.* Antiphosphocholine antibodies found in normal mouse serum are protective against intravenous infection with type 3 streptococcus pneumoniae. *J Exp. Med.* **153**, 694-705 (1981).

18. Mizushima, N. *et al.* Dissection of autophagosome formation using Apg5-deficient mouse embryonic stem cells. *J Cell Biol.* **152**, 657-668 (2001).

19. Codogno, P. & Meijer, A.J. Atg5: more than an autophagy factor. *Nat. Cell Biol.* **8**, 1045-1047 (2006).

20. Yousefi, S. *et al.* Calpain-mediated cleavage of Atg5 switches autophagy to apoptosis. *Nat. Cell Biol.* **8**, 1124-1132 (2006).

21. Pyo, J.O. *et al.* Essential roles of Atg5 and FADD in autophagic cell death: dissection of autophagic cell death into vacuole formation and cell death. *J. Biol. Chem.* **280**, 20722-20729 (2005).

22. Tung, J.W., Mrazek, M.D., Yang, Y., Herzenberg, L.A. & Herzenberg, L.A. Phenotypically distinct B cell development pathways map to the three B cell lineages in the mouse. *Proc. Natl. Acad. Sci. U. S. A.* **103**, 6293-6298 (2006).

23. Montecino-Rodriguez, E., Leathers, H. & Dorshkind, K. Identification of a B-1 B cell-specified progenitor. *Nat. Immunol.* **7**, 293-301 (2006).

24. Wardemann, H., Boehm, T., Dear, N. & Carsetti, R. B-1a B cells that link the innate and adaptive immune responses are lacking in the absence of the spleen. *J Exp. Med.* **195**, 771-780 (2002).

25. Herzenberg, L.A. & Tung, J.W. B cell lineages: documented at last! *Nat. Immunol.* **7**, 225-226 (2006).

26. Lum, J.J. *et al.* Growth factor regulation of autophagy and cell survival in the absence of apoptosis. *Cell.* **120**, 237-248 (2005).

27. Kuma, A. *et al.* The role of autophagy during the early neonatal starvation period. *Nature.* **432**, 1032-1036 (2004).

28. Steed, A., Buch, T., Waisman, A. & Virgin, H.W. Interferon gamma blocks {gamma}-herpesvirus reactivation from latency in a cell type specific manner. *J. Virol.* **81**, 6134-6140 (2007).

CHAPTER 3

Autophagy Genes are Critical for Homeostasis and Mitochondrial Maintenance in Primary T Lymphocytes

Portions of this chapter are excerpted from:

Stephenson LM, Miller BC, Ng A, Eisenberg J, Zhao Z, Cadwell K, Graham DB, Mizushima NN, Xavier R, Virgin HW, Swat W. Identification of Atg5-dependent transcriptional changes and increases in mitochondrial mass in Atg5-deficient T lymphocytes. *Autophagy*. 2009 Jul;5(5):625-35.

Abstract

Autophagy is implicated in many functions of mammalian cells such as organelle recycling, cell survival, and differentiation, and is essential for the maintenance of T and B lymphocytes. Here, we demonstrate that autophagy is a constitutive process during T cell development. Deletion of the essential autophagy genes *Atg5* or *Atg7* in T cells resulted in decreased thymocyte and peripheral T cell numbers, and *Atg5*-deficient peripheral T cells had an increase in a marker of cell death. We employed functional-genetic and integrative computational analyses to elucidate specific functions of *Atg5* in developing T-lineage lymphocytes. Our whole-genome transcriptional profiling identified a set of 699 genes differentially expressed in *Atg5*-deficient and *Atg5*-sufficient thymocytes (*Atg5*-dependent gene set). Strikingly, the *Atg5*-dependent gene set was dramatically enriched in genes encoding proteins associated with the mitochondrion. In support of a role for autophagy in mitochondrial maintenance in T lineage cells, the deletion of *Atg5* led to increased mitochondrial mass in peripheral T cells. We also observed a correlation between mitochondrial mass and Annexin-V staining in peripheral T cells. We propose that autophagy is critical for mitochondrial maintenance and T cell survival. We speculate that, similar to its role in yeast or mammalian liver cells, autophagy is required in T cells for the removal of damaged or aging mitochondria which contribute to cell death in autophagy-deficient T cells.

Introduction

In Chapter 2 we described the roles of *Atg5* in B lymphocyte development and homeostasis. Given our interest in the cell-type specificity of autophagy genes, we next chose to study these genes in T lymphocytes, a closely related cell lineage. The functions of autophagy and autophagy genes are not well understand in T lymphocytes, with studies reporting both a pro-survival and pro-death role for autophagy[1,2,3,4,5].

Soon after we initiated these studies, Pua *et al.* published the first report of the role of the essential autophagy gene *Atg5* in primary T lymphocytes[5]. They demonstrate that *Atg5* is essential for T cell survival and proliferation using reconstitution of irradiated hosts with *Atg5*$^{-/-}$ fetal liver-derived stem cells. Total thymocyte numbers are reduced in these chimeras. There are striking decreases in CD4+ and CD8+ T cell numbers in peripheral lymphoid tissues, with an increase in the percentage of Annexin-V+ cells. Finally, *Atg5*$^{-/-}$ T lymphocytes have a dramatically reduced ability to proliferate after TCR stimulation[5]. We decided to confirm their findings and explore some of the mechanistic questions raised by the phenotype that they reported. First, is the observed phenotype due to a non-autophagy function of *Atg5*? Second, are there abnormalities in *Atg5*-deficient T cells that might suggest a reason why there are fewer cells *in vivo*?

Autophagy is important for the degradation of damaged and excess mitochondria[6,7,8,9]. Mitochondria have a critical role in T cell survival and activation, functioning in activation-induced signaling pathways and providing ATP and metabolites important for growth of the cell[10] (reviewed in [11]). Mitochondria also contribute to T cell

death. Mitochondria are an important source of reactive oxygen species (ROS), which sensitize T cells to AICD and ACAD[12,13,14,15,16]. In addition, the balance of pro- and anti-apoptotic Bcl-2 family members regulates release of the pro-apoptotic factor cytochrome c from mitochondria, initiating cell death (reviewed in [17]). Interestingly, an increase in mitochondrial mass in T cells has been associated with increased sensitivity to apoptosis in HIV-specific CD8+ T cells[18]. Because of the function of autophagy in the regulation of mitochondria and the importance of mitochondria in T cell survival and death, we hypothesized that mitochondria may accumulate in *Atg5*-deficient T lymphocytes and contribute to T cell death.

Here we demonstrate that autophagy is a constitutive process in developing and mature T cells and that the essential autophagy genes *Atg5* and *Atg7* are required for thymocyte and peripheral T cell homeostasis. In collaboration with Dr. Ramnik Xavier's group, we identify a thymocyte-specific transcriptional signature associated with deficiency of *Atg5* in T cells and provide evidence that *Atg5* is required for regulating mitochondrial mass in peripheral T cells. Finally, we find a correlation between increased mitochondrial mass and increased Annexin-V staining in T cells, suggesting that abnormal mitochondria contribute to cell death in *Atg5*-deficient T cells.

Results

Atg5 and *Atg7* are required for the maintenance of developing and mature T lymphocytes

As a first step to understand the role of autophagy in T cells, we measured the levels of LC3-II as one marker of autophagic activity in developing and mature T lineage cells. We sorted thymic and peripheral T lineage subsets and probed the lysates with anti-LC3 antibodies. We observed robust LC3-II bands in all T cell subsets, indicating that autophagy is an active process in all stages of T cell development (Fig. 3-1A). To confirm that autophagy is an ongoing process in T cells, we cultured thymoyctes for 4 hours in the presence of increasing concentrations of chloroquine. Chloroquine results in an accumulation of LC3-II in actively autophagic cells[19,20]. As expected, LC3-II levels increased in a chloroquine dose-dependent manner (Fig. 3-1B), indicating that autophagy was ongoing in these cells.

Pua *et al.* reported that the essential autophagy gene *Atg5* is essential for normal T cell homeostasis[5], however the mechanism by which *Atg5* controls T cell survival and/or proliferation remains unknown. To address these issues, we generated two different mouse models to delete *Atg5* in T cells. First, we used recombination activating gene (*Rag*)-1-deficient complementation[21,5,22] with E15.5-18.5 fetal liver cells from $Atg5^{-/-}$ or $Atg5^{+/+}$ embryos[23]. As an alternative approach, we generated *Atg5*-deficient T cells by breeding mice with conditionally targeted (floxed) *Atg5*[24] alleles to Lck-*Cre* transgenics

(*Atg5*$^{flox/flox}$-Lck-*Cre*+). In these experiments, *Atg5*$^{flox/flox}$-Lck-*Cre*- mice were used as controls.

We first confirmed that T cells from these two mouse systems lack the ATG5 protein. Thymocyte lysates from *Atg5*$^{-/-}$ chimeras showed no detectable ATG5 protein expression (Fig. 3-2A). We also were unable to detect LC3-II (Fig. 3-2A), indicating that classical macroautophagy is abrogated in the absence of ATG5 in T cells. ATG5 levels were also reduced in *Atg5*$^{flox/flox}$-Lck-*Cre*+ thymocytes (Fig. 3-2B); however residual levels of the protein were still detectable upon overexposure of the membrane, in spite of efficient recombination of the *Atg5*^{flox} locus in thymocytes from *Atg5*$^{flox/flox}$-Lck-*Cre*+ mice (data not shown).

We next analyzed the *in vivo* phenotype of *Atg5*-deficient T cells. In agreement with the previously published report[5], thymus cellularity of *Atg5*-deficient chimeric mice analyzed between 6 and 13 weeks post-fetal liver transfer was decreased approximately 2.4-fold compared to controls (Table 3-1), although there were no discernable alterations in the percentages of CD4- CD8- double negative, CD4+ CD8+ double positive, CD4+ single positive, and CD8+ single positive cells (Fig. 3-3). Moreover, both the percentages and total numbers of CD4+ and CD8+ T cells in the lymph nodes and spleens of *Atg5*$^{-/-}$ chimeric mice were decreased compared to *Atg5*$^{+/+}$ chimeras (Fig. 3-3 and Table 3-1). A similar reduction in total numbers of thymocytes and peripheral T cells was observed in *Atg5*$^{flox/flox}$-Lck-*Cre*+ mice compared to littermate controls (Fig. 3-3

and Table 3-1). We conclude that the decrease in T cell numbers is a result of T cell-intrinsic effects of the loss of *Atg5*.

It is possible that other functions of *Atg5* apart from its role in autophagy may contribute to the phenotypic abnormalities of *Atg5*-deficient T cells[25,26,27]. To address this issue, we deleted *Atg7*, another essential autophagy gene, from T cells using a conditional knockout approach similar to the one described above. We bred mice with conditionally targeted (floxed) *Atg7*[28] alleles to Lck-*Cre* transgenics (*Atg7*$^{flox/flox}$-Lck-*Cre*+). We observed reduced expression of ATG7 in *Atg7*$^{flox/flox}$-Lck-*Cre*+ thymocytes by immunoblot analysis (Fig. 3-2C). Similar to *Atg5*$^{-/-}$ chimeras and *Atg5*$^{flox/flox}$-Lck-*Cre*+ mice, total thymocyte and peripheral CD4+ and CD8+ T cell numbers were also reduced in *Atg7*$^{flox/flox}$-Lck-*Cre*+ mice (Fig. 3-3 and Table 3-1). Together these data suggest that autophagy is required for the maintenance of both developing and peripheral T lymphocytes.

A role for *Atg5* in mitochondrial maintenance and cell survival revealed by integrative computational analysis of whole-genome datasets

To obtain further insights into the functional pathways and networks through which *Atg5* maintains the T cell compartment, we developed an analytical framework that integrates gene expression analyses of wild-type and *Atg5*$^{-/-}$ thymocytes from chimeric mice with diverse information extracted from various genomic screens and

databases including Gene Ontology (GO)[29] for functional classification, HPRD[30] for molecular interactions, HomoloGene[31] for homology mapping of genes, and NCBI PubMed and MILANO for literature co-citation analyses[31,32]. Whole-genome transcriptional profiling of *Atg5*$^{-/-}$ and *Atg5*$^{+/+}$ thymocytes identified a set of 699 differentially expressed genes (of which 259 genes were up-regulated and 440 down-regulated in *Atg5*$^{-/-}$ thymocytes, as compared to wild-type thymocytes) (Fig. 3-4), permitting us to explore functional clusters within the set of differentially expressed genes and identify putative pathways and networks relevant to *Atg5* function in the T lymphoid lineage.

To ascertain whether the *Atg5*-dependent gene set was statistically enriched for genes implicated in subcellular compartment-associated processes, we first analyzed their annotations in Gene Ontology (GO) cellular component categories. Strikingly, the *Atg5*-dependent gene set was dramatically enriched in genes encoding proteins associated with the mitochondrion ($p=3.7x10^{-4}$) and nucleus ($p=1.6x10^{-4}$) (Fig. 3-5). The mitochondrion GO signature was particularly interesting given the suggested association between autophagy and mitochondrial maintenance. We identified 64 mitochondrial-associated genes in the *Atg5*-dependent gene set (Fig. 3-5) from GO annotation and a recent comprehensive genome-wide survey of genes participating in mitochondrial-associated processes[33]. This *Atg5*-dependent gene set GO signature strongly suggests a role for *Atg5* in mitochondrial function and/or maintenance.

As an additional computational strategy to elucidate potential connections of *Atg5* with mitochondrial function, we projected the *Atg5*-dependent gene set onto human

orthologs and generated a human protein-protein interaction network (Fig. 3-6). The network was built by interrogating data from the HPRD database which contains protein-protein interactions from the literature and from multiple large-scale interactome datasets. We next intersected this network analysis with GO cellular compartment annotations. This approach yielded mitochondrion-anchored subnetworks which we then extended by an additional degree of separation, thereby including non-*Atg5*-dependent gene set proteins that interacted with mitochondrion-associated *Atg5*-dependent gene set-encoded products. We observed that many of these interacting partners are also annotated as mitochondrial related, further supporting the involvement of an enriched subset of *Atg5*-dependent gene set in mitochondrial processes.

We next performed a literature (PubMed) co-citation analysis incorporating search terms such as 'mitochondrial biogenesis', 'mitochondrial permeability' and 'electron transport' to gain additional insights into various mitochondrial processes or events in which the *Atg5*-dependent gene set might be involved (Fig. 3-7A). We extended this analysis to include other terms associated with various general cellular processes (e.g. endocytosis) and also events specific to T lineage cells and immune function (Fig. 3-7B). Notably, this analysis revealed described associations in the generation of ROS, lymphocyte activation, and lymphocyte proliferation (Fig. 3-7B) in the context of potential function of *Atg5* in T lineage cells. Our analyses also revealed a connection of *Atg5* with cellular processes in which autophagy genes have been shown to function, such as phagocytosis, endocytosis, and lysosome formation/function[26,34,35] (Fig. 3-7B). Finally, we present a diagrammatic summary of the key mitochondrial-associated

Atg5-dependent genes in Fig. 3-8, assembled from our literature co-citation analysis, gene ontology annotations, network data, and pathway information. Taken together, these transcriptional profiling and computational analyses of orthogonal data, ranging from gene co-regulation to protein-protein interaction network with pathway analysis, suggest a role for *Atg5* in mitochondrial maintenance and function.

Atg5-deficient T cells have a defect in proliferation and increased Annexin-V staining

Given these transcriptional alterations in *Atg5*-deficient T cells, we further characterized the T cells that develop in the absence of *Atg5*. The expression of the maturation marker CD24 (HSA) was similar between wild-type and *Atg5*-deficient T cells, indicating that peripheral *Atg5*-deficient T cells were phenotypically mature. Strikingly, however, we observed an alteration in the expression of markers associated with activation/memory/homeostatic expansion, CD44 and CD62L (Fig. 3-9A and 3-9B). While the majority of wild-type lymph node and splenic T cells were $CD62L^{high}$ $CD44^{low}$, *Atg5*-deficient T cells were predominantly $CD44^{high}$ and $CD62L^{low}$. Peripheral T cells from $Atg7^{flox/flox}$-Lck-*Cre*+ mice had a similar expression profile for CD44 and CD62L (data not shown). Increased cell surface expression of CD44 and decreased expression of CD62L have been reported in T cells undergoing homeostatic expansion[36,37,38,39,40]. Importantly, expression levels of T cell antigen receptor did not appear altered in the *Atg5*-deficient T cells, nor were there significant differences in the expression of the early

activation markers CD25 and CD69 (Fig. 3-9A), consistent with the hypothesis that *Atg5*-deficient T cells may be responding to homeostatic rather than antigen-induced expansion signals[41].

T cells in lymphopenic mice undergo multiple rounds of proliferation in order to reach peripheral homeostasis[42]. The decreased number of peripheral T cells together with a surface phenotype indicative of homeostatic expansion suggest that *Atg5*-deficient T cells may be unable to populate the peripheral lymphoid organs, possibly due to survival defects, resulting in a compensatory proliferative response. Consistent with this view, we found that a higher percentage of freshly isolated T cells from $Atg5^{-/-}$ chimeras stained with Annexin-V compared with T cells from $Atg5^{+/+}$ chimeras. The proportion of Annexin-V+ cells was 1.5- to 2-fold higher in $CD62L^{low}$ *Atg5*-deficient T cells, and 3- to 7-fold higher in $CD62L^{high}$ *Atg5*-deficient T cells (Fig. 3-9C). Annexin-V staining was also elevated in $CD62L^{high}$ populations of $Atg5^{flox/flox}$-Lck-*Cre*+ T cells (Fig. 3-9D). These data suggest that *Atg5* is required for the survival of T lymphocytes.

Consistent with the results of Pua *et al.*[5], *Atg5*-deficient T cells exhibited a severe defect in TCR-induced proliferation (Fig. 3-10). We purified $CD62L^{high}$ T lymphocytes from control and $Atg5^{-/-}$ chimeras, labeled them with CFSE, stimulated them with anti-CD3 and anti-CD28 antibodies, and analyzed proliferation at 72 hours. We also measured blast formation using T cells stimulated with anti-CD3 and anti-CD28 antibodies for 40 hours. We observed a severe reduction in proliferation and the ability

to form blasts in *Atg5*-deficient T cell cultures compared to controls (Fig. 3-10). We conclude that *Atg5* is important for T cell proliferation after antigen receptor stimulation.

Increased mitochondrial mass in *Atg5*-deficient T lymphocytes

Our transcriptional profiling analyses of *Atg5*-deficient T cells raised the possibility that the defects in T cell homeostasis observed in the absence of *Atg5* are due to impaired mitochondrial function. To determine if mitochondria were normal in the absence of *Atg5*, we analyzed mitochondrial mass/volume in single cells using the vital dye Mitotracker green, a mitochondrial specific dye. We observed an increase in Mitotracker staining in *Atg5*-deficient splenic CD4+ and CD8+ T cells from both $Atg5^{-/-}$ chimeric and $Atg5^{flox/flox}$-Lck-*Cre*+ mice relative to controls (Fig. 3-11A and data not shown). The Mitotracker staining of thymocytes from $Atg5^{-/-}$ chimeras was similar to wild-type cells, suggesting that the increase in mitochondrial mass occurred as the T cells aged (data not shown).

We next asked if alterations in mitochondrial mass correlated with the decrease in cell survival in *Atg5*-deficient T cells. We costained splenocytes from $Atg5^{flox/flox}$-Lck-*Cre*+ and $Atg5^{flox/flox}$-Lck-*Cre*- mice with Mitotracker green and Annexin-V. CD4+ and CD8+ T cells that were Mitotracker^{high} had a significantly higher percentage of cells that were Annexin-V+ compared with Mitotracker^{low} T cells (Fig. 3-11B). Although this trend was apparent in both $Atg5^{flox/flox}$-Lck-*Cre*+ and $Atg5^{flox/flox}$-Lck-*Cre*- mice, there was an increase of approximately 15% in the percentage of Annexin-V+ cells within the

Mitotracker^{high} population in *Atg5*$^{flox/flox}$-Lck-*Cre*+ mice (Fig 3-11B). This data shows that mitochondrial mass correlates with Annexin-V staining in CD4+ and CD8+ T cells, suggesting that the increase in mitochondrial mass in *Atg5*-deficient T cells correlates with increased death in these cells.

Discussion

The data presented here indicates that autophagy is an active process during all stages of T lymphocyte development and that deletion of the essential autophagy genes *Atg5* and *Atg7* results in profound abnormalities in T cell maintenance. In addition, we showed that *Atg5* is important for T cell proliferation *in vitro*. Transcriptional profiling of *Atg5*-deficient thymocytes suggests abnormalities in mitochondria in the absence of this autophagy gene. This hypothesis is supported by studies demonstrating that peripheral *Atg5*-deficient T cells have an increase in mitochondrial mass. Mitochondrial mass is correlated with Annexin-V staining in these cells, suggesting a link between mitochondrial abnormalities and *Atg5*-deficient T cell death. Given our gene chip and mitochondrial mass results, we propose that autophagy is required in T lymphocytes for normal mitochondrial maintenance.

Although dramatic mitochondria-related transcriptional changes were observed in thymocytes, we did not observe an increase in mitochondrial mass in *Atg5*-deficient thymocytes, but only in peripheral *Atg5*-deficient T cells. Despite the two-fold decrease in thymus cellularity in *Atg5*$^{-/-}$ chimeras, we also did not observe an increase in Annexin-V staining in the thymus, consistent with previously published results[5]. We hypothesize that we are unable to detect mitochondrial abnormalities because the cells have not yet accumulated sufficient damaged mitochondria to die. Alternatively, the actively phagocytic cells of the thymus responsible for the normal elimination of thymocytes that

have failed the selection process[43] may be quickly removing those *Atg5*-deficient thymocytes that have accumulated damaged mitochondria.

Another group has also recently reported that autophagy genes are important for mitochondrial maintenance in T cells[47]. Pua *et al*. studied *Atg7*-deficient T cells and found that, similar to *Atg5*-deficient cells, these cells have a reduction in peripheral T cell numbers with an increase in markers of apoptosis. Both *Atg7* and *Atg5*-deficient peripheral T cells have an increase in mitochondrial mass, which the authors suggest is due to an inability of the cells to degrade mitochondria as they mature and leave the thymus. *Atg7*-deficient cells also have an abnormal accumulation of ROS and upregulated expression of Bcl-2 and Bak[47]. This report confirms our mitochondrial results in *Atg5*-deficient T cells using *Atg7*-deficient T cells, suggesting that this phenotype is not due to a non-autophagy function of *Atg5*. They also extend our findings to show that the accumulation of mitochondria is associated with alterations in ROS and Bcl-2 family member protein expression, both of which could contribute to increased T cell death[48,12,13,14,15] (reviewed in [49,50]).

We utilized three different approaches in this study to address the importance of autophagy genes in T lineage cells. In the first approach, *Rag*1$^{-/-}$ complementation, analysis of *Atg5*$^{-/-}$ T cells is potentially complicated due to the decrease in viability of *Atg5*$^{-/-}$ chimeras (data not shown) and the deletion of *Atg5* in other hematopoietic cell types in addition to T cells, resulting in defects in other cell lineages[21]. By using a conditional knockout approach we ascertained that *Atg5* is required within T cells for

their maintenance *in vivo*. Our immunoblot results suggest that deletion of the *Atg5*^{flox} alleles may be incomplete in some cells or that the ATG5 protein may be retained for a significant time after gene deletion. Despite these caveats, given that the *in vivo* phenotypes of *Atg5*$^{-/-}$, *Atg5*$^{flox/flox}$-Lck-*Cre*+, and *Atg7*$^{flox/flox}$-Lck-*Cre*+ T cells are similar, it is likely that these phenotypes are due to the lack of autophagy in T cells, and not due to non-autophagy functions of *Atg5*[25] or *Atg7*. However, since ATG7 is essential for the conjugation of ATG5 to ATG12[45,46], it is possible that a non-autophagy role of the ATG5-12 conjugate is responsible. Further studies would be necessary to distinguish between these possibilities.

It is interesting that the transcriptional signature observed here for *Atg5*-deficient thymocytes is quite distinct from the signature observed in Paneth cells that express lower than normal levels of ATG16L1[44]. This suggests that the transcriptional response to autophagy gene-deficiency may differ depending on the primary cell type involved or the specific gene affected. These differences may help to explain the different functions of autophagy genes in closely related cell lineages[21].

.

	ATG5 $^{+/+}$	*ATG5* $^{-/-}$	p value		*Atg5*$^{flox/flox}$-Lck-*Cre*-	*Atg5*$^{flox/flox}$-Lck-*Cre*+	p value		*Atg7*$^{flox/flox}$-Lck-*Cre*-	*Atg7*$^{flox/flox}$-Lck-*Cre*+	p value
Thymus	160.9 ±9.9 (n= 41)	66.8 ±8.0 (n = 44)	p<0.0001		165.0 ±12.2 (n = 25)	108.7 ±9.1 (n = 29)	p=0.0004		155.1 ±19.8 (n=8)	89.8 ±11.6 (n=9)	p=0.0104
Lymph Nodes											
CD4+	13.6 ±0.9 (n=34)	1.3 ±0.3 (n = 37)	p<0.0001		9.1 ±0.9 (n = 16)	4.3 ±1.0 (n = 20)	p=0.0011		7.5 ±1.5 (n=7)	2.3 ±0.4 (n=7)	p=0.0056
CD8+	7.5 ±0.6 (n=34)	0.9 ±0.6 (n = 37)	p<0.0001		5.6 ±0.6 (n = 16)	2.1 ±0.6 (n = 20)	p=0.0005		5.1 ±1.1 (n=7)	0.6 ±0.1 (n=7)	p=0.0020
Spleen											
CD4+	8.1 ±0.6 (n=37)	1.7 ±0.2 (n = 41)	p<0.0001		10.4 ±4.3 (n = 20)	4.3 ±0.6 (n = 24)	p<0.0001		6.2 ±0.9 (n=7)	3.6 ±0.7 (n=7)	p=0.0366
CD8+	4.0 ±0.3 (n=37)	2.5 ±0.4 (n = 41)	p=0.0031		6.2 ±0.6 (n = 20)	3.6 ±0.4 (n = 24)	p=0.0012		4.7 ±0.8 (n=7)	1.0 ±0.3 (n=7)	p=0.0012

Table 3-1. Loss of T cells in *Atg5*$^{-/-}$, *Atg5*$^{flox/flox}$-Lck-*Cre*+, and *Atg7*$^{flox/flox}$-Lck-*Cre*+ mice

Data are mean ± SEM and represent multiples of 10^6 cells. The number of mice per group is indicated in parentheses. Chimera mice were analyzed between 6 and 13 weeks post-reconstitution. *Atg5*$^{flox/flox}$-Lck-*Cre*+ and *Atg5*$^{flox/flox}$-Lck-*Cre*- mice were analyzed between 6 and 13 weeks of age. *Atg7*$^{flox/flox}$-Lck-*Cre*+ and *Atg7*$^{flox/flox}$-Lck-*Cre*- mice were analyzed between 8 and 14 weeks of age.

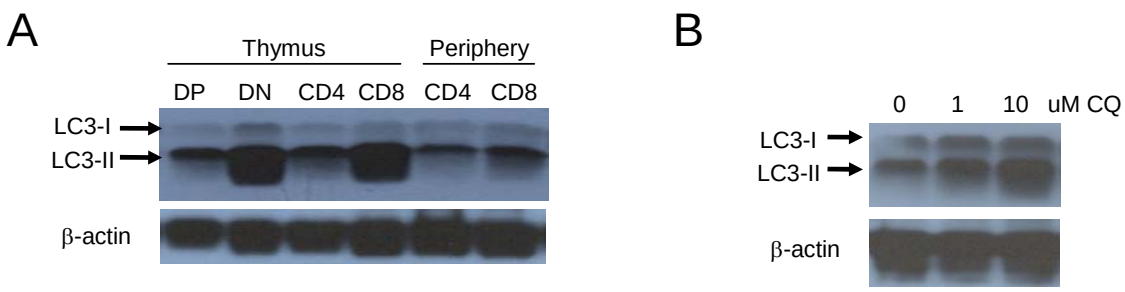

Figure 3-1. Constitutive autophagy in all subsets of wild-type T cells

(A) Lysates from FACS-sorted C57BL/6 thymocytes and MACS-bead sorted peripheral T cells were probed with antibodies against LC3 and β-actin. Representative blot from 4 independent experiments shown. **(**B) Lysates from C57BL/6 thymocytes cultured for 4 hours with the indicated concentrations of chloroquine were probed with antibodies against LC3 and β-actin. Representative blot from 3 independent experiments shown.

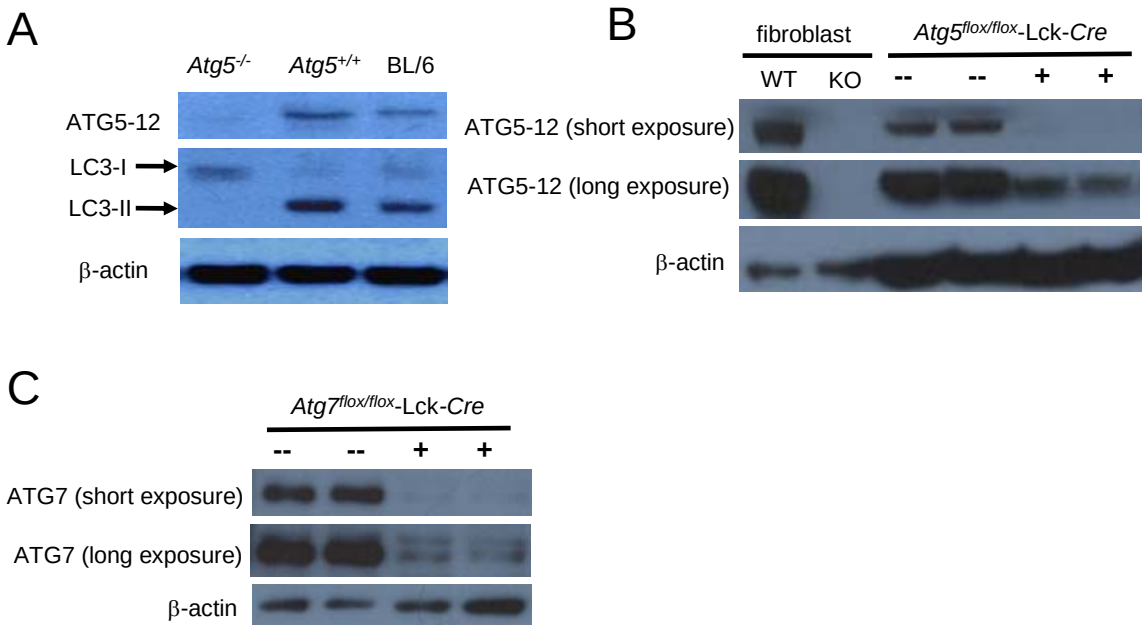

Figure 3-2. Deletion of ATG5 in *Atg5*$^{-/-}$ and *Atg5*$^{flox/flox}$-Lck-*Cre*+ thymocytes and ATG7 in *Atg7*$^{flox/flox}$-Lck-*Cre*+ thymocytes

(A) Lysates from *Atg5*$^{+/+}$ or *Atg5*$^{-/-}$ chimeras or C57BL/6 control thymocytes were probed with antibodies against ATG5, LC3, or β-actin. Representative blot from 2 independent experiments shown. (B) Lysates from *Atg5*$^{+/+}$ and *Atg5*$^{-/-}$ SV40-transformed murine embryonic fibroblasts and from *Atg5*$^{flox/flox}$-Lck-*Cre*+ and *Atg5*$^{flox/flox}$-Lck-*Cre*- thymocytes were probed with antibodies against ATG5 and β-actin. Representative blot from 3 independent experiments shown. (C) Lysates from *Atg7*$^{flox/flox}$-Lck-*Cre*+ and *Atg7*$^{flox/flox}$-Lck-*Cre*- thymocytes were probed with antibodies against ATG7 and β-actin. Representative blot from 2 independent experiments shown.

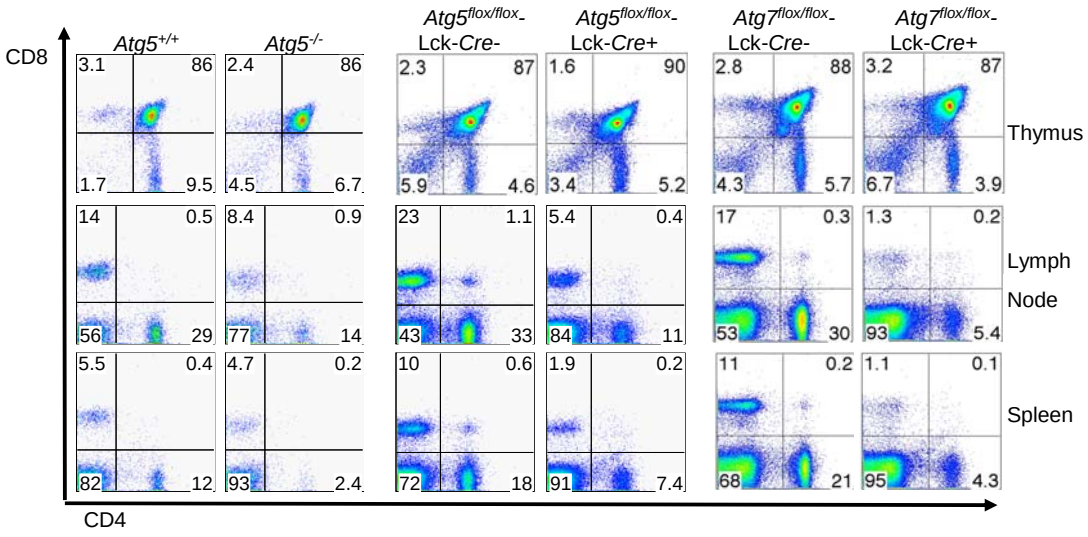

Figure 3-3. Loss of T cells in *Atg5*$^{-/-}$, *Atg5*$^{flox/flox}$-Lck-*Cre*+, and *Atg7*$^{flox/flox}$-Lck-*Cre*+ mice

Single-cell suspensions of thymocytes, splenocytes, and lymph node cells were analyzed by flow cytometry as described in Materials and Methods. Cells were gated by forward and side scatter on lymphocyte populations. Shown is one representative experiment from n ≥ 3 experiments, with at least 7 mice of each genotype analyzed.

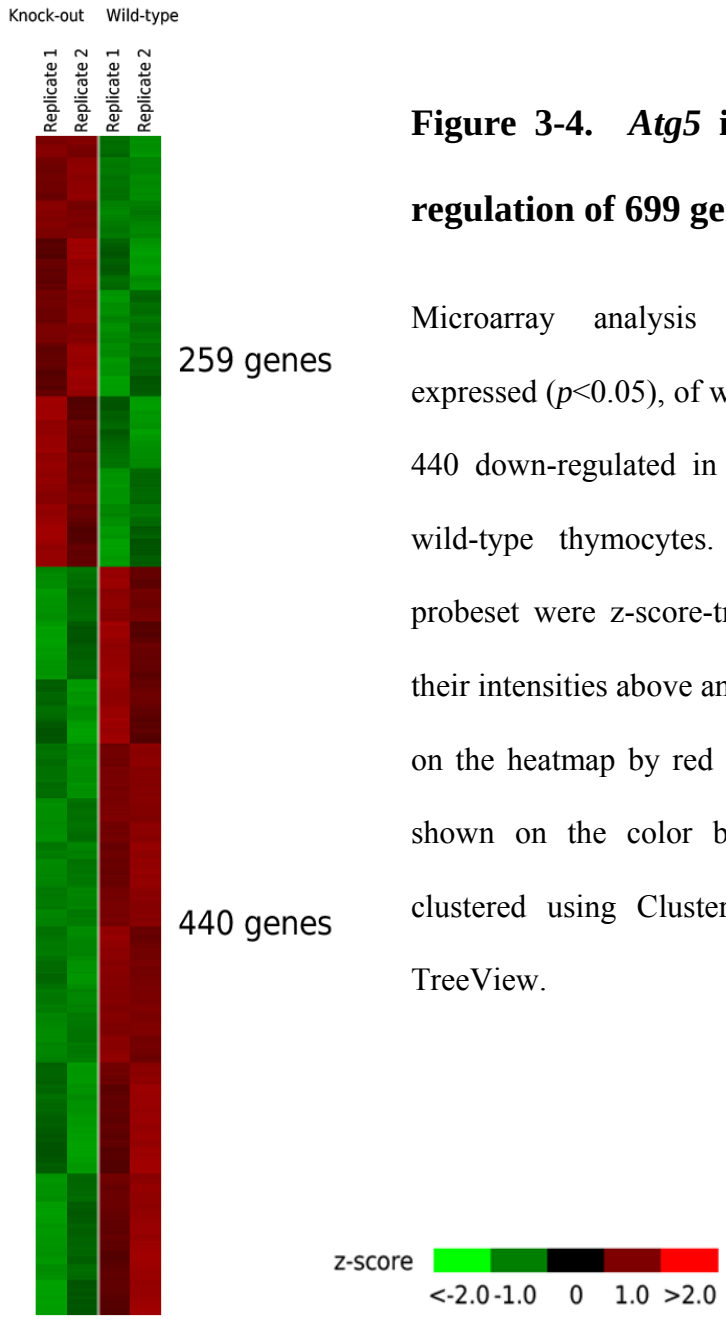

Figure 3-4. *Atg5* is required for the proper regulation of 699 genes in thymocytes

Microarray analysis showing genes differentially expressed ($p<0.05$), of which 259 genes were induced and 440 down-regulated in *Atg5*$^{-/-}$ thymocytes compared to wild-type thymocytes. Expression values for each probeset were z-score-transformed across all arrays and their intensities above and below the mean are represented on the heatmap by red and green colors respectively, as shown on the color bar. Genes were hierarchically clustered using Cluster 3.0 and visualized with Java TreeView.

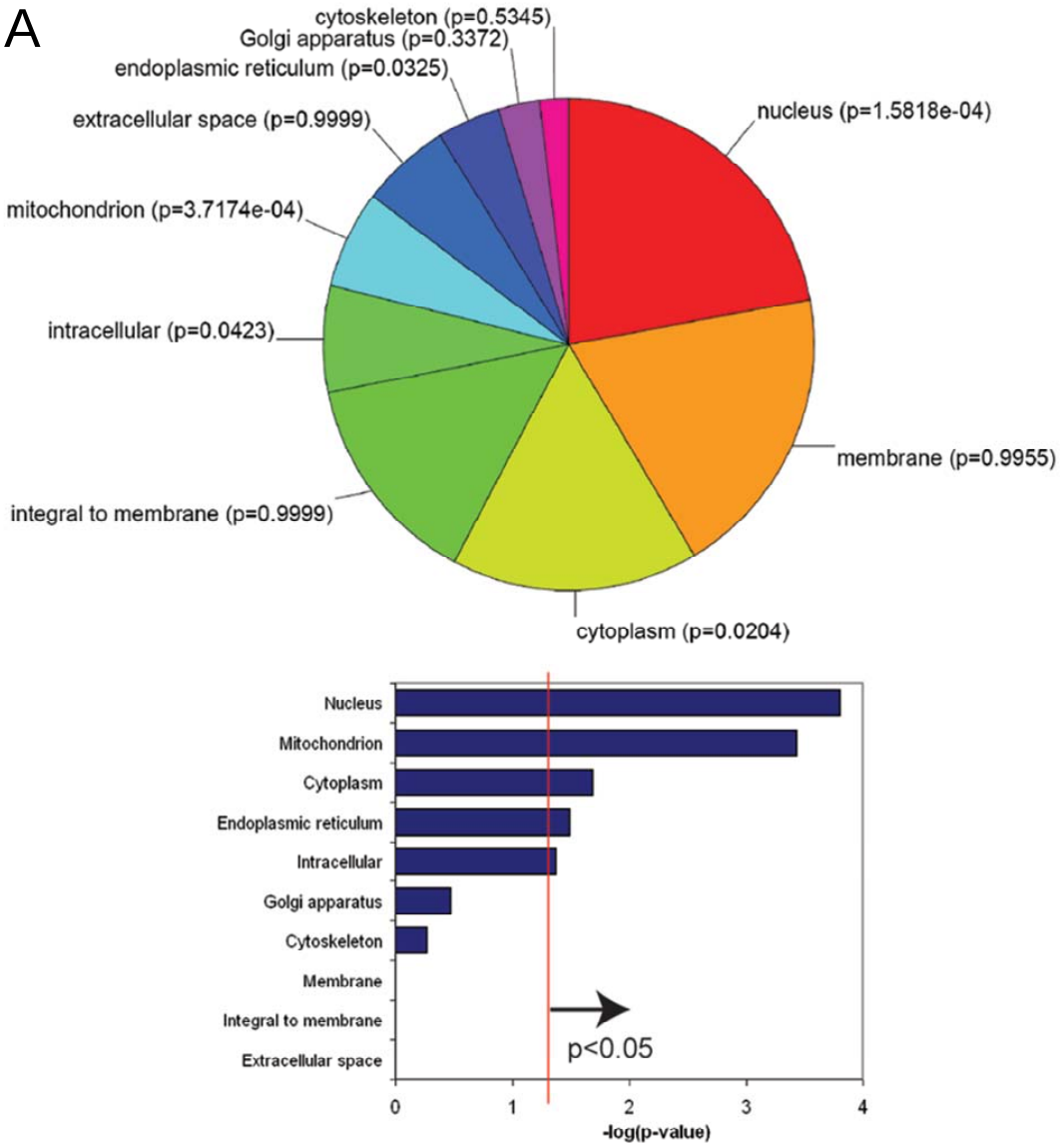

Figure 3-5. *Atg5* is required for the proper regulation of mitochondrial-associated genes

(A) Differentially expressed genes were classified into gene ontology (GO) cellular component categories. Categories assigned with at least 3 genes are displayed in the pie

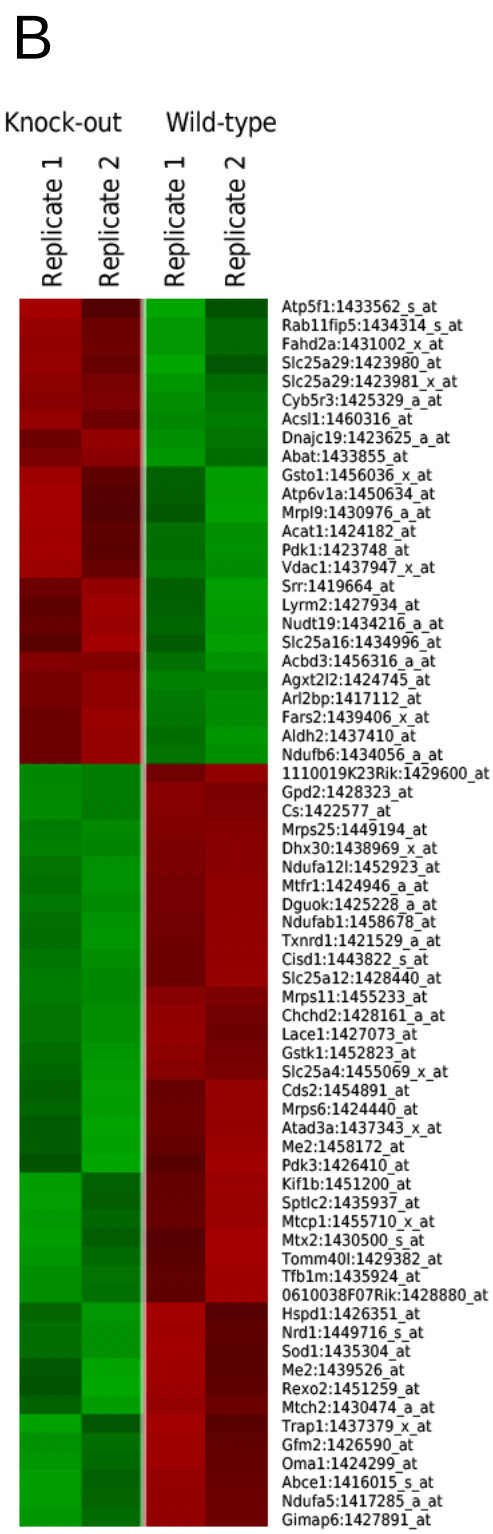

chart, with enrichment *p*-values shown in brackets alongside each category. The bar chart displays enrichment *p*-values as negative log-transformed values, which reveals a dramatic enrichment of mitochondria- and the nucleus-associated genes. (B) 64 differentially expressed genes that fall into the mitochondrion GO category are displayed by heatmap, prepared as described in Fig 3-4.

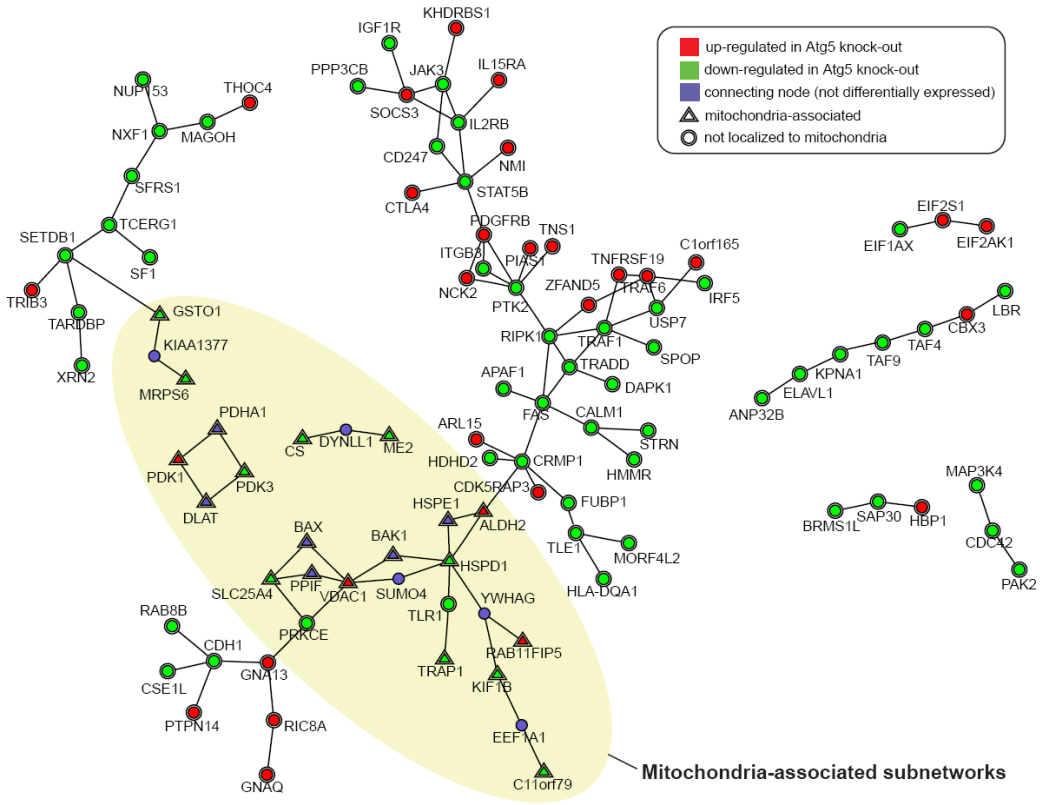

Figure 3-6. Construction of a human protein-protein interaction network

Differentially expressed genes were mapped onto human orthologs for which interaction data was available. Circles representing up-regulated components are colored red and down-regulated components green. Solid lines denote protein-protein interactions. Mitochondrion-anchored subnetworks (highlighted by the grey region) emerged when extending connections by an additional degree of separation, capturing components of interest (blue circles) in the functional neighborhood of mitochondrial-related genes that were found to be differentially expressed. Network clusters containing connections between at least 3 components are displayed.

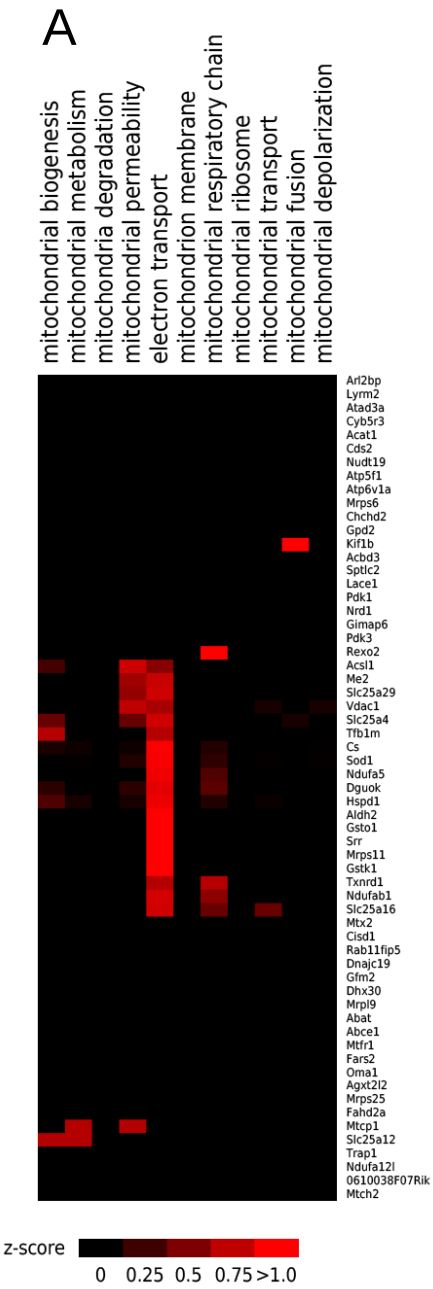

Figure 3-7. Matrices generated from literature co-citation analysis of differentially expressed genes and citation terms associated with mitochondrial and cellular functions

(A) Mitochondrial functions and (B) general cellular processes or specific T-lineage immune functions displayed as a heatmap. The intensity of red on the heatmap denotes the extent to which each gene is co-cited with each specific term in the PubMed database.

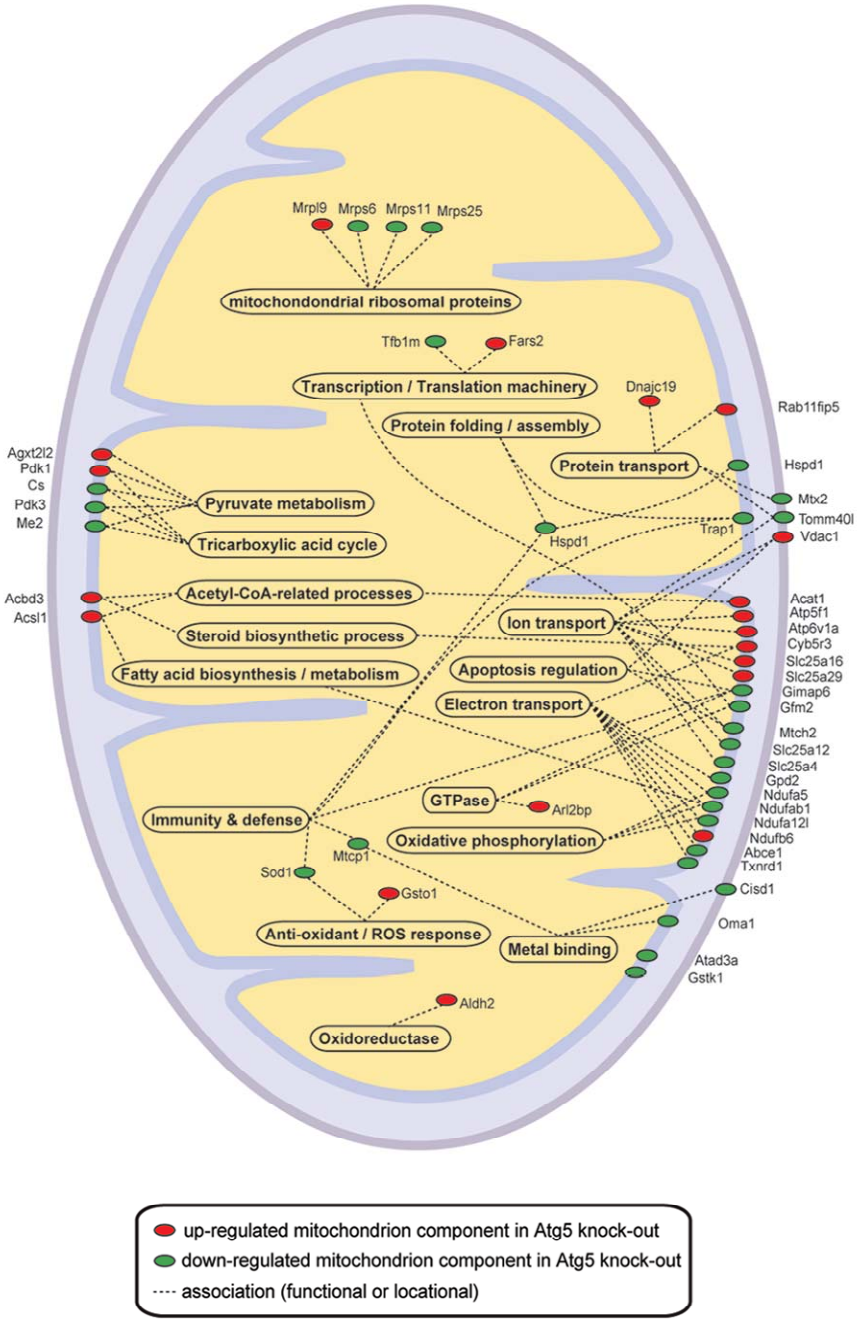

Figure 3-8. Diagrammatic mitochondrion representation showing important differentially-expressed gene products participating in mitochondria-associated processes

Red and green ovals denote up- and down-regulated components in *Atg5*$^{-/-}$ thymocytes, respectively. Functional associations with biological processes are represented by dashed lines.

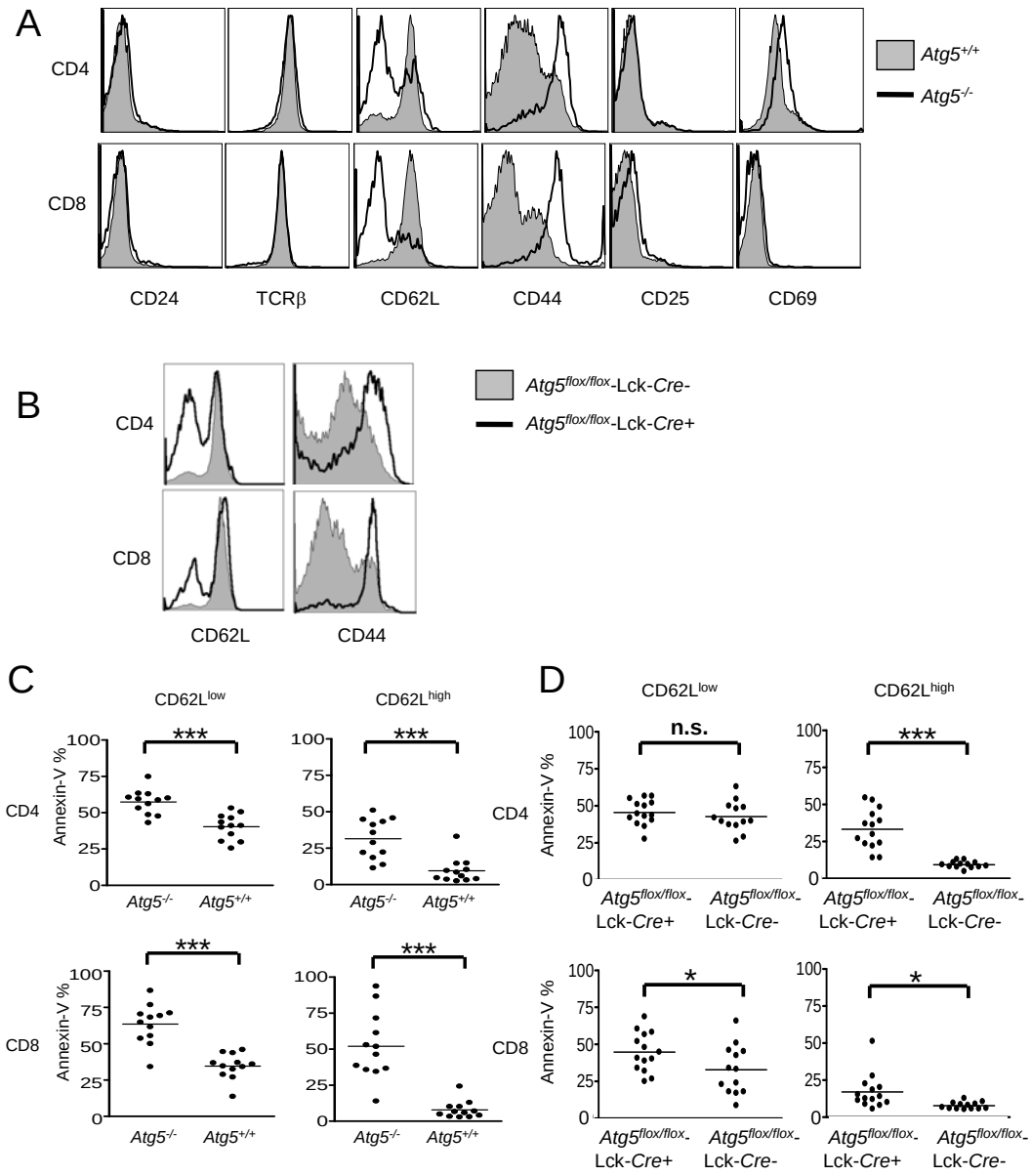

Figure 3-9. A higher percentage of T cells are CD44^{high}, CD62L^{low}, and Annexin-V+ in *Atg5*$^{-/-}$ chimeras and *Atg5*$^{flox/flox}$-Lck-*Cre*+ mice compared with controls

(A-B) Flow cytometric analysis of lymph node T cells from *Atg5*$^{+/+}$ or *Atg5*$^{-/-}$ chimeric mice (A) or *Atg5*$^{flox/flox}$-Lck-*Cre*- and *Atg5*$^{flox/flox}$-Lck-*Cre*+ mice (B). Cells were gated by forward and side scatter for lymphocytes, then gated on CD4+ or CD8+ cells. One representative experiment shown of at least five independent experiments. (C-D) Lymph node T cells from *Atg5*$^{+/+}$ or *Atg5*$^{-/-}$ chimeric mice (C) or *Atg5*$^{flox/flox}$-Lck-*Cre*- and *Atg5*$^{flox/flox}$-Lck-*Cre*+ mice (D) were stained with Annexin-V and antibodies against CD4, CD8, and CD62L. Cells were gated by forward and side scatter for lymphocytes, then gated on CD4+ or CD8+ cells. Data pooled from at least four independent experiments. (* $p < 0.05$, ** $p < 0.005$, *** $p < 0.0005$, n.s. = not statistically significant)

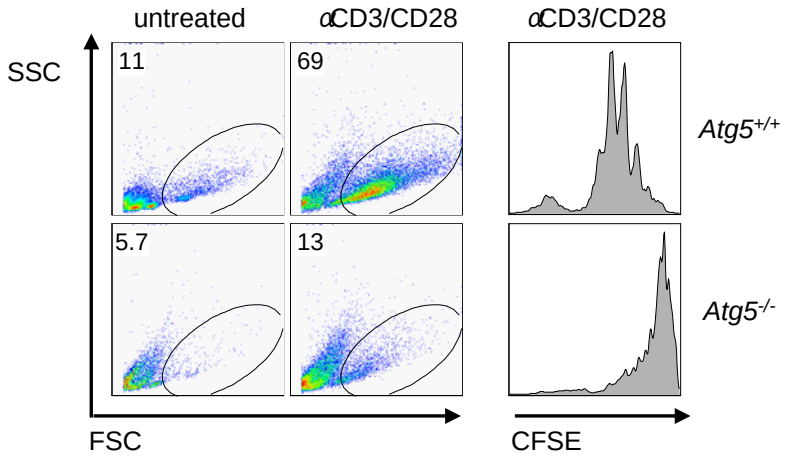

Figure 3-10. *Atg5*-deficient T lymphocytes have a defect in proliferation

Purified CD62L^{high} T cells from *Atg5*$^{+/+}$ or *Atg5*$^{-/-}$ chimeric mice were either untreated or stimulated with anti-CD3 (1μg/mL) and anti-CD28 (1μg/mL) and analyzed 40 hours later for T cell blasts (left panels) or loaded with CFSE, stimulated as above, and analyzed 72 hours later (right panel). Shown is one representative experiment of three.

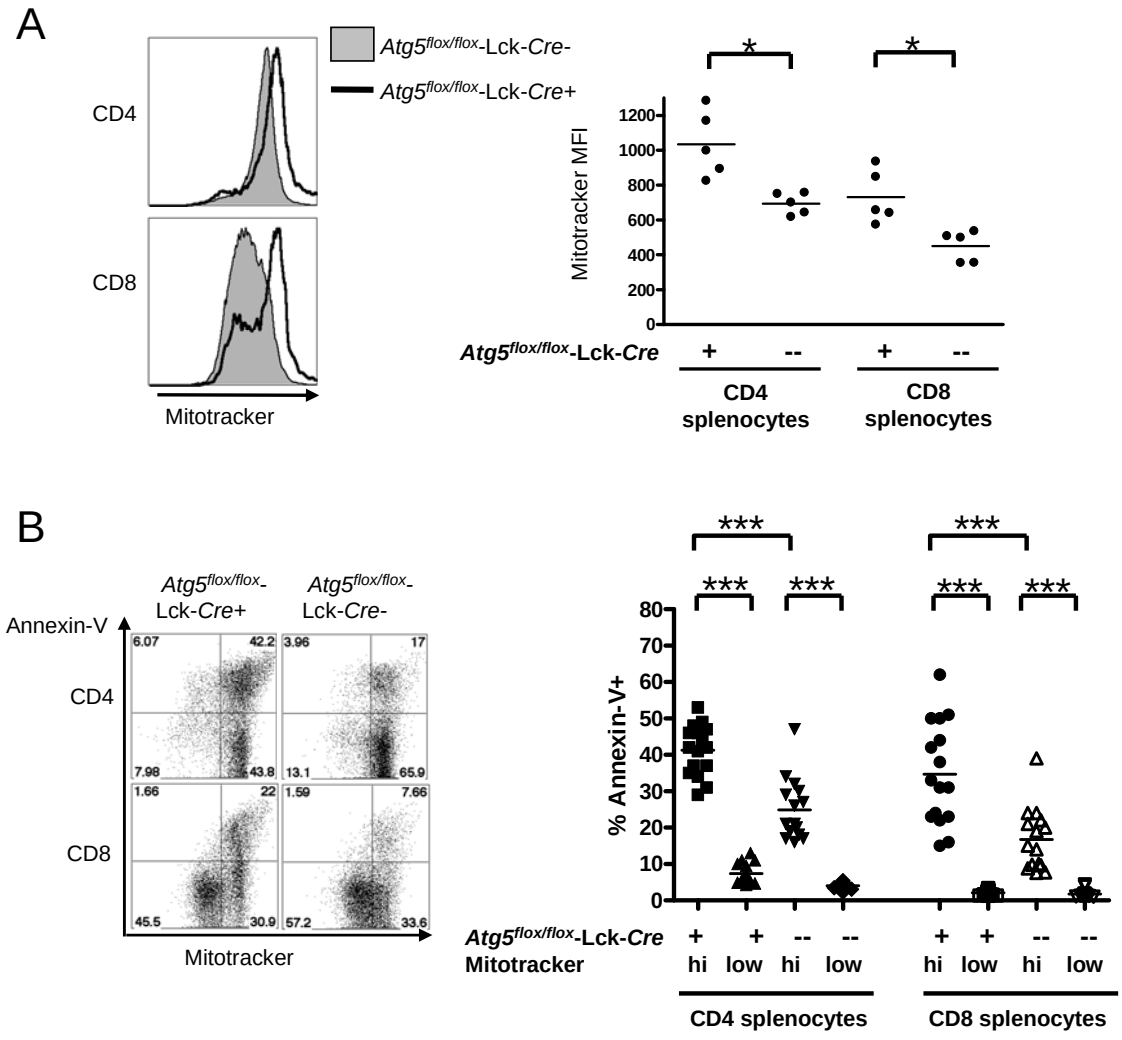

Figure 3-11. *Atg5*-deficient T lymphocytes have an increase in mitochondrial mass

(A) Splenocytes from *Atg5*$^{flox/flox}$-Lck-*Cre*- and *Atg5*$^{flox/flox}$-Lck-*Cre*+ mice were loaded with MitoTracker green, stained with antibodies against CD4 or CD8, and analyzed by flow cytometry. Analysis was performed on CD4+ or CD8+ splenocytes without gating by forward and side scatter. Shown are representative FACS plots of at least fifteen mice

of each genotype and the quantification of the mean fluorescence intensity (MFI) of Mitotracker staining from one of three independent experiments. (B) Splenocytes from *Atg5*$^{flox/flox}$-Lck-*Cre*- and *Atg5*$^{flox/flox}$-Lck-*Cre*+ mice were stained with CD4, CD8, Mitotracker green, and Annexin-V. Representative FACS plots and quantification of the percentage of Annexin-V+ cells from the Mitotracker^{high} and Mitotracker^{low} gates are shown. Analysis was performed on CD4+ or CD8+ splenocytes without gating by forward and side scatter. Data pooled from three independent experiments. (* $p < 0.05$, ** $p < 0.005$, *** $p < 0.0005$, n.s. = not statistically significant)

Materials and Methods

Mice and cells The generation of *Atg5*$^{-/-}$, *Atg5*$^{flox/flox}$, and *Atg7*$^{flox/flox}$ mice has been previously described[24,23,28]. Chimeric mice were generated by reconstituting sublethally irradiated B6.129S7-*Rag1*$^{tm1Mom/}$J (*Rag1*$^{-/-}$, The Jackson Laboratory, #002216) mice with *Atg5*$^{+/+}$ or *Atg5*$^{-/-}$ fetal liver cells, as previously described[21]. *Atg5*$^{flox/flox}$ and *Atg7*$^{flox/flox}$ were bred to Lck-*Cre* (C57BL/6NTac-TgN(Lck-Cre)) transgenic mice (Taconic, #004197, Hudson, NY). Mice were maintained at Washington University School of Medicine in accordance with institutional policies for animal care and usage. *Atg5*$^{-/-}$ and *Atg5*$^{+/+}$ embryonic fibroblasts were generated from day 13.5 embryos. To establish immortalized cell lines, 10^6 cells were transformed with 1μg of pEF321-T, an SV40 large T antigen expression vector (a gift from T. Hansen), by the FuGENE HD transfection reagent (Roche, Basel, Switzerland) according to the manufacturer's instructions.

Genotyping Genotyping of the mice was performed as described[24,28], with the *Cre* gene detected with primers cre1 (AGGTTCGTTCACTCATGGA) and cre2 (TCGACCAGTTTAGTTACCC) using PCR [94°C(4 min); 25 cycles of 94°C (30 sec), 60°C (30 sec), 72°C (1 min); 72°C (5 min)]. The *Atg5* gene was detected with the primers exon3-1 (GAATATGAAGGCACACCCCTGAAATG), short2 (GTACTGCATAATGGTTTAACTCTTGC), and check2 (ACAACGTCGAGCA CAGCTGCGCAAGG) using PCR [94°C (4 min); 30 cycles of 94°C (30 sec), 60°C (30 sec), 72°C (1 min); 72°C (5 min)]. The same PCR program was used with the primers

short2, check2, and 5L2 (CAGGGAATGGTGTCTCCCAC) to check for the *Atg5*^{flox} and deleted *Atg5*^{flox} alleles in thymocytes from *Atg5*$^{flox/flox}$ Lck-*Cre*+ and *Atg5*$^{flox/flox}$ Lck-*Cre*- mice. The *Atg7*^{flox} allele was detected with primers Hind-Fw (TGGCTGCTACTTCTGCAATGATGT) and Pst-Rv (CAGGACAGAGACCATCAGCTCCAC) using PCR [94°C (5min); 30 cycles of 94°C (20 sec), 68°C (30 sec), 72°C (90 sec); 72°C (10 min)]. Confirmation of the wild type *Atg7* locus was done with primers Ex14 F (TCTCCCAAGACAAGACAGGGTGAA) and Ex14 R (AAGCCAAAGGAAACCAAGGGAGTG) using PCR [94°C (5min); 35 cycles of 94°C (20 sec), 60°C (15 sec), 72°C (60 sec); 72°C (10 min)].

Stimulation and proliferation assays Single cell suspensions from the spleens and lymph nodes of chimeric mice were first B cell depleted using negative selection with anti-B220-Dynal beads (Invitrogen, Carlsbad, CA), followed by positive selection for CD62L^{high} lymphocytes. Briefly, cells were incubated with biotin-conjugated anti-CD62L antibody (Caltag, Carlsbad, CA) followed by anti-biotin MACs beads (Miltenyi Biotec, Auburn, CA) and isolated according to the manufacturer's instructions. CD62L^{high} purities were greater than 90%. Lymph node T cells were plated at 1x10^6/mL in complete media (DMEM (Gibco, Carlsbad, CA) plus 10% fetal calf serum (FCS), 100Units/mL penicillin, 100ug/mL streptomycin, 1mM sodium pyruvate, 2mM L-glutamine, 1x non-essential amino acids (Gibco, Carlsbad, CA) and 57uM β-mercaptoethanol). Cells were stimulated with 1.0 μg/mL anti-CD3 and 1.0 μg/mL anti-

CD28 (BD Biosciences, San Jose, CA). To label cells with CFSE, cells were incubated with 1μM CFSE (Invitrogen, Carlsbad, CA) for 30 minutes at 37° and then washed in complete media. Labeled cells were cultured with the indicated stimuli for 72 hours and then analyzed by flow cytometry.

Flow cytometry and cell sorting Single cell suspensions were prepared from the spleens, thymi, and lymph nodes and stained with antibodies against TCRβ, CD4, CD8, CD24, CD25, CD44, CD62L, and CD69 (BD Biosciences, San Jose, CA). Annexin-V labeling was performed by surface staining cells with the indicated lineage markers, washing with complete media, and staining for 15 minutes with Annexin-V (BD Biosciences, San Jose, CA). Thymocytes were sorted on a FACS Vantage SE (BD Biosciences, San Jose, CA) by FSC/SSC gating on a live lymphocyte population, followed by gating out CD11b+, CD11c+, and B220+ cells. The remaining cells were then sorted based on expression of CD4 and CD8. Purities were greater than 94% for each population (n = 4 independent experiments). Peripheral CD4+ and CD8+ T cells were isolated using negative selection by MACS magnetic bead sorting according to the manufacturer's instructions (Miltenyi Biotec, Auburn, CA). Peripheral T cells were negatively selected from pooled spleen and lymph node samples, followed by negative selection against either CD4+ or CD8+ cells. Purities averaged 86% for CD4+ cells and 92% for CD8+ cells (n = 4 independent experiments).

Immunoblots Cells were washed with PBS and then lysed in cold NP-40 lysis buffer [0.5% NP-40, 50 mM Tris-Cl, 150 mM NaCl, 1mM EDTA, 1 mM phenylmethylsulfonyl fluoride] or cold lysis buffer B [50mM Tris-HCl pH8.0, 150mM NaCl, 1% Triton X-100, 0.1% SDS, 0.2% deoxycholic acid sodium salt] supplemented with complete pretease inhibitors (Roche, Basel, Switzerland) for 10 minutes at 4°C. Lysates were cleared by centrifugation at 14,000 x g for 10 minutes at 4°C. Samples were analyzed by immunoblotting[21] using antibodies against ATG5 (Novus Biologicals, Littleton, CO and Nanotools, Teningen, Germany), ATG7 (Sigma, St. Louis, MO), LC3 (Novus Biologicals, Littleton, CO) and β-actin (Sigma, St. Louis, MO).

Microarrays and analysis Total thymocyte RNA was harvested from *Atg5*$^{-/-}$ and *Atg5*$^{+/+}$ chimeras by lysing single cell suspensions of thymocytes in Trizol (Invitrogen, Carlsbad, CA). RNA analyses were performed at the microarray core facility at the Harvard Medical School and Partners Healthcare Center for Genetics and Genomics. The quantity, purity and integrity of RNA were evaluated by UV spectrophotometry and RNA-nano Bioanalyzer (Agilent, Santa Clara, CA). Sample processing and hybridization on Mouse Genome 430 2.0 GeneChip microarrays (Affymetrix, Santa Clara, CA) were performed according to manufacturer's instructions. Probe-level normalization of the raw .CEL data files using the GC Robust Multi-array Average (GCRMA) algorithm[51] was implemented in the R programming language. Two-sided t-tests were performed for each probeset, comparing between *Atg5*$^{-/-}$ and *Atg5*$^{+/+}$ chimera samples. Probesets with $p<0.05$

were considered differentially expressed. Hierarchical clustering (pairwise complete-linkage) of probesets corresponding to differentially expressed genes was performed with Cluster 3.0[52] using the Pearson's correlation coefficient as the similarity metric. Z-score transformation was applied to each probeset across all arrays prior to generating 'heatmaps' for visualization implemented in the Python language.

Gene Ontology (GO) analysis Differentially expressed genes were examined in terms of GO cellular component categories[29]. To assess enrichment of these categories within the set of differentially expressed genes against all genes represented by probes on the Affymetrix Mouse Genome 430 2.0 microarray GeneChip, *p*-values were computed using Fisher's exact test implemented in Python and R programming languages. Categories with $p<0.05$ were considered significantly enriched.

Protein interaction network The network was constructed by iteratively connecting interacting proteins, with data extracted from a collection of genome-wide interactome screens and curated literature entries in HPRD[30]. The network uses graph theoretic representations, which abstract components (gene products) as nodes and relationships (e.g. interactions) between components as edges, implemented in the Perl programming language.

Literature co-citation analysis Co-citation analysis was performed using Milano search[32], identifying the number of times a gene was co-cited with a specified term in articles from the PubMed database. Vectors capturing the co-citation profiles for each of these genes were generated for a set of terms and clustered using pairwise complete-linkage hierarchical clustering with the Pearson's correlation coefficient as the similarity measure. The results were displayed as a heatmap implemented in the Python language.

Mitochondria mass/volume assay Cells were loaded with 100nM MitoTracker Green (Invitrogen, Carlsbad, CA) for 30 minutes at 37°C in the presence of flourochome-conjugated antibodies against CD4 and CD8. Cells were washed and then analyzed by flow cytometry. When necessary, Annexin-V was added after washing the cells in complete media.

Statistics All non-gene chip data was analyzed with Prism software (Graphpad; San Diego, CA), using two-tailed unpaired Student's t tests.

References

1. Li, C. *et al.* Autophagy is induced in CD4+ T cells and important for the growth factor-withdrawal cell death. *J. Immunol.* **177**, 5163-5168 (2006).

2. Bell, B.D. *et al.* FADD and caspase-8 control the outcome of autophagic signaling in proliferating T cells. *Proc Natl Acad Sci U. S. A.* **105**, 16677-16682 (2008).

3. Feng, C.G. *et al.* The immunity-related GTPase Irgm1 promotes the expansion of activated CD4+ T cell populations by preventing interferon-gamma-induced cell death. *Nat Immunol.* **9**, 1279-1287 (2008).

4. Espert, L. *et al.* Autophagy is involved in T cell death after binding of HIV-1 envelope proteins to CXCR4. *J. Clin. Invest.* **116**, 2161-2172 (2006).

5. Pua, H.H., Dzhagalov, I., Chuck, M., Mizushima, N. & He, Y.W. A critical role for the autophagy gene Atg5 in T cell survival and proliferation. *J. Exp. Med.* **204**, 25-31 (2007).

6. Zhang, H. *et al.* Mitochondrial autophagy is a HIF-1-dependent adaptive metabolic response to hypoxia. *J. Biol. Chem.* (2008).

7. Papandreou, I., Lim, A.L., Laderoute, K. & Denko, N.C. Hypoxia signals autophagy in tumor cells via AMPK activity, independent of HIF-1, BNIP3, and BNIP3L. *Cell Death Differ.* **15**, 1572-1581 (2008).

8. Scherz-Shouval, R. *et al.* Reactive oxygen species are essential for autophagy and specifically regulate the activity of Atg4. *EMBO J.* **26**, 1749-1760 (2007).

9. Elmore, S.P., Qian, T., Grissom, S.F. & Lemasters, J.J. The mitochondrial permeability transition initiates autophagy in rat hepatocytes. *FASEB J.* **15**, 2286-2287 (2001).

10. Quintana, A. *et al.* T cell activation requires mitochondrial translocation to the immunological synapse. *Proc. Natl. Acad. Sci. U. S. A.* **104**, 14418-14423 (2007).

11. Jones, R.G. & Thompson, C.B. Revving the engine: signal transduction fuels T cell activation. *Immunity.* **27**, 173-178 (2007).

12. Bauer, M.K. *et al.* Role of reactive oxygen intermediates in activation-induced CD95 (APO-1/Fas) ligand expression. *J. Biol. Chem.* **273**, 8048-8055 (1998).

13. Devadas, S., Zaritskaya, L., Rhee, S.G., Oberley, L. & Williams, M.S. Discrete generation of superoxide and hydrogen peroxide by T cell receptor stimulation:

selective regulation of mitogen-activated protein kinase activation and fas ligand expression. *J. Exp. Med.* **195**, 59-70 (2002).

14. Hildeman, D.A. *et al.* Reactive oxygen species regulate activation-induced T cell apoptosis. *Immunity.* **10**, 735-744 (1999).

15. Hildeman, D.A. *et al.* Control of Bcl-2 expression by reactive oxygen species. *Proc Natl Acad Sci U. S. A.* **100**, 15035-15040 (2003).

16. Kaminski, M., Kiessling, M., Suss, D., Krammer, P.H. & Gulow, K. Novel role for mitochondria: protein kinase Ctheta-dependent oxidative signaling organelles in activation-induced T-cell death. *Mol. Cell Biol.* **27**, 3625-3639 (2007).

17. Krammer, P.H., Arnold, R. & Lavrik, I.N. Life and death in peripheral T cells. *Nat. Rev. Immunol.* **7**, 532-542 (2007).

18. Petrovas, C. *et al.* Increased mitochondrial mass characterizes the survival defect of HIV-specific CD8(+) T cells. *Blood.* **109**, 2505-2513 (2007).

19. Shintani, T. & Klionsky, D.J. Autophagy in health and disease: a double-edged sword. *Science.* **306**, 990-995 (2004).

20. Klionsky, D.J. *et al.* Guidelines for the use and interpretation of assays for monitoring autophagy in higher eukaryotes. *Autophagy.* **4**, 151-175 (2008).

21. Miller, B.C. *et al.* The autophagy gene ATG5 plays an essential role in B lymphocyte development. *Autophagy.* **4**, 309-314 (2007).

22. Stephenson, L.M. *et al.* DLGH1 is a negative regulator of T-lymphocyte proliferation. *Mol. Cell Biol.* **27**, 7574-7581 (2007).

23. Kuma, A. *et al.* The role of autophagy during the early neonatal starvation period. *Nature.* **432**, 1032-1036 (2004).

24. Hara, T. *et al.* Suppression of basal autophagy in neural cells causes neurodegenerative disease in mice. *Nature.* **441**, 885-889 (2006).

25. Codogno, P. & Meijer, A.J. Atg5: more than an autophagy factor. *Nat. Cell Biol.* **8**, 1045-1047 (2006).

26. Sanjuan, M.A. *et al.* Toll-like receptor signaling in macrophages links the autophagy pathway to phagocytosis. *Nature.* **450**, 1253-1257 (2007).

27. Zhao, Z. *et al.* Autophagosome-independent essential function for the autophagy protein Atg5 in cellular immunity to intracellular pathogens. *Cell Host Microbe.* **4**, 458-469 (2008).

28. Komatsu, M. *et al.* Impairment of starvation-induced and constitutive autophagy in Atg7-deficient mice. *J. Cell Biol.* **169**, 425-434 (2005).

29. The Gene Ontology project in 2008. *Nucleic Acids Res.* **36**, D440-D444 (2008).

30. Mishra, G.R. *et al.* Human protein reference database--2006 update. *Nucleic Acids Res.* **34**, D411-D414 (2006).

31. Wheeler, D.L. *et al.* Database resources of the National Center for Biotechnology Information. *Nucleic Acids Res.* **36**, D13-D21 (2008).

32. Rubinstein, R. & Simon, I. MILANO--custom annotation of microarray results using automatic literature searches. *BMC Bioinformatics.* **6**, 12 (2005).

33. Calvo, S. *et al.* Systematic identification of human mitochondrial disease genes through integrative genomics. *Nat Genet.* **38**, 576-582 (2006).

34. Levine, B. & Kroemer, G. Autophagy in the Pathogenesis of Disease. *Cell.* **132**, 27-42 (2008).

35. He, C. & Klionsky, D.J. Regulation Mechanisms and Signaling Pathways of Autophagy. *Annu. Rev. Genet.* (2009).

36. Clarke, S.R. & Rudensky, A.Y. Survival and homeostatic proliferation of naive peripheral CD4+ T cells in the absence of self peptide:MHC complexes. *J Immunol.* **165**, 2458-2464 (2000).

37. Ploix, C., Lo, D. & Carson, M.J. A ligand for the chemokine receptor CCR7 can influence the homeostatic proliferation of CD4 T cells and progression of autoimmunity. *J Immunol.* **167**, 6724-6730 (2001).

38. Gudmundsdottir, H. & Turka, L.A. A closer look at homeostatic proliferation of CD4+ T cells: costimulatory requirements and role in memory formation. *J Immunol.* **167**, 3699-3707 (2001).

39. Goldrath, A.W., Bogatzki, L.Y. & Bevan, M.J. Naive T cells transiently acquire a memory-like phenotype during homeostasis-driven proliferation. *J Exp. Med.* **192**, 557-564 (2000).

40. Murali-Krishna, K. & Ahmed, R. Cutting edge: naive T cells masquerading as memory cells. *J Immunol.* **165**, 1733-1737 (2000).

41. Taylor, D.K., Neujahr, D. & Turka, L.A. Heterologous immunity and homeostatic proliferation as barriers to tolerance. *Curr. Opin. Immunol.* **16**, 558-564 (2004).

42. Marrack, P. *et al.* Homeostasis of alpha beta TCR+ T cells. *Nat Immunol.* **1**, 107-111 (2000).

43. Surh, C.D. & Sprent, J. T-cell apoptosis detected in situ during positive and negative selection in the thymus. *Nature.* **372**, 100-103 (1994).

44. Cadwell, K. *et al.* A key role for autophagy and the autophagy gene Atg16l1 in mouse and human intestinal Paneth cells. *Nature.* **456**, 259-263 (2008).

45. Mizushima, N., Ohsumi, Y. & Yoshimori, T. Autophagosome formation in mammalian cells. *Cell Struct. Funct.* **27**, 421-429 (2002).

46. Komatsu, M. *et al.* Loss of autophagy in the central nervous system causes neurodegeneration in mice. *Nature.* **441**, 880-884 (2006).

47. Pua, H.H., Guo, J., Komatsu, M. & He, Y.W. Autophagy is essential for mitochondrial clearance in mature T lymphocytes. *J. Immunol.* **In Press**, (2009).

48. Hildeman, D.A. *et al.* Activated T cell death in vivo mediated by proapoptotic bcl-2 family member bim. *Immunity.* **16**, 759-767 (2002).

49. Marrack, P. & Kappler, J. Control of T cell viability. *Annu. Rev. Immunol.* **22**, 765-787 (2004).

50. Hildeman, D.A., Zhu, Y., Mitchell, T.C., Kappler, J. & Marrack, P. Molecular mechanisms of activated T cell death in vivo. *Curr. Opin. Immunol.* **14**, 354-359 (2002).

51. Wu, Z., Irizarry, R.A., Gentleman, F.M., Martinez-Murillo, F. & Spencer, F. A model-based background adjustment for oligonucleotide expression arrays. *J Am Stat Assoc.* **99**, 909-918 (2004).

52. Eisen, M.B., Spellman, P.T., Brown, P.O. & Botstein, D. Cluster analysis and display of genome-wide expression patterns. *Proc Natl Acad Sci U. S. A.* **95**, 14863-14868 (1998).

CHAPTER 4

The LC3 Conjugation System is Important for Directional Secretion in Osteoclasts

Abstract

Osteoclasts function to degrade bone by regulated secretion of lysosomal enzymes and acid against the bone surface. The mechanisms regulating this secretion are poorly understood. Here we show that the biochemical pathway necessary for autophagy is critical for secretion in osteoclasts. We found that LC3 localizes to the ruffled border in osteoclasts. We hypothesized that this localization may be important for osteoclast function, so we inhibited the LC3 conjugation cascade by deleting the essential autophagy genes *Atg5* or *Atg7* or overexpressing a dominant negative mutant of ATG4B. All of these disruptions inhibited bone resorption and localization of lysosomal markers to the resorptive surface *in vitro*. Expression of dominant negative ATG4B also decreased localization of LC3 to the ruffled border, suggesting that LC3 localization and osteoclast function are connected. Finally, deletion of *Atg5* in osteoclasts and other myeloid-lineage cells *in vivo* protected mice from ovariectomy-induced bone loss, a mouse model of osteoporosis. Our results demonstrate that the LC3 conjugation pathway is important for directional secretion in osteoclasts.

Introduction

Osteoclasts are multinucleated cells of the monocyte lineage that degrade bone by directionally secreting lysosomal enzymes and hydrogen ions against the bone surface (Fig. 1-2, reviewed in [1]). This secretion is targeted through undefined mechanisms to an area of the plasma membrane juxtaposed to the bone and circumscribed by an actin ring, forming a "ruffled border" of convoluted membrane. The goal of this chapter is to determine if autophagy or autophagy genes are important for osteoclast function.

Many of the proteins involved in autophagosome nucleation also regulate vesicle trafficking. There is a growing literature suggesting that autophagy genes downstream of nucleation are important for secretory cell function[2,3,4,5]. In addition, LC3 localizes to the phagosome during phagocytosis and enhances fusion of phagosomes to lysosomes[6], suggesting that the LC3 conjugation system may be involved in vesicular trafficking pathways independent of classical autophagosome formation.

In this chapter we report that LC3 is found concentrated at the ruffled border in osteoclasts, but this localization is reduced in osteoclasts expressing a dominant negative mutant of ATG4B, ATG4B^{C74A}. Deletion of *Atg5* or *Atg7* or overexpression of ATG4B^{C74A} or a mutant of ATG5, ATG5^{K130R}, all inhibit osteoclast function *in vitro*, as measured by bone pit formation and localization of lysosomal proteins to the ruffled border. Deletion of *Atg5* in myeloid-lineage cells *in vivo* protects mice from bone loss induced by ovariectomy. We demonstrate an important role for the LC3 conjugation machinery in osteoclast secretion.

Results

GFP-LC3 localizes to the ruffled border

As a first step to understand the role of autophagy and LC3 conjugation in osteoclasts, we visualized LC3 localization in osteoclasts using GFP-tagged LC3 (GFP-LC3)[7]. LC3 is normally found on the developing autophagosome where it promotes membrane elongation[8,9,10,11,12]. We cultured osteoclasts from GFP-LC3 transgenic mice[13] by growing bone marrow-derived macrophages in the presence of M-CSF-containing conditioned media for 4 days and then replating equal cell numbers on bone in the presence of M-CSF and RANKL, a cytokine necessary for osteoclastogenesis[14]. We stained the cells to visualize actin and GFP-LC3 and identified active osteoclasts as multinucleated cells with an actin ring. Confocal microscopy showed LC3 not only in punctate cytoplasmic structures, which we presume to be autophagosomes, but also concentrated within the actin ring in approximately 25% of osteoclasts (Fig. 4-1). We also stained the cells with an antibody against cathepsin K, a lysosomal protease that is secreted from the cells and localizes to the ruffled border[15]. GFP-LC3 was found in the same region of the cell as cathepsin K, demonstrating that GFP-LC3 localizes to the resorptive microenvironment. Interestingly, we did not observe colocalization of GFP-LC3 and cathepsin K puncta in the cell periphery, suggesting that LC3 does not localize to cathepsin K+ vesicles. Based on these results, we sought to determine the functional significance of the presence of LC3 in the actin ring.

Atg5 is not required for osteoclast differentiation but is important for osteoclast secretion

ATG5 is an essential autophagy protein required for the conjugation and localization of LC3 to autophagosomes and phagosomes[16,6]. To delete *Atg5* in osteoclasts, we bred mice containing two copies of a knock-in *Atg5* gene in which LoxP sites were inserted flanking the third exon [$Atg5^{flox/flox}$][17] to mice expressing the Cre recombinase under control of the LyzM promoter, resulting in expression of the recombinase in cells of the myeloid lineage[17,18,19]. Given the function of *Atg5* in B and T cell development (see Chapters 2 and 3), we first determined if osteoclasts can be differentiated from $Atg5^{flox/flox}$-LyzM-*Cre*+ bone marrow. We counted osteoclasts grown on plastic on days 3, 4, and 5 post addition of RANKL. Osteoclasts were identified as cells with at least 3 nuclei that stained for the osteoclast marker tartrate-resistant acid phosphatase (TRAP)[20,21,22]. $Atg5^{flox/flox}$-LyzM-*Cre*+ cells had a delay in osteoclast formation, but by day 5 we observed equal numbers of mature osteoclasts in $Atg5^{flox/flox}$-LyzM-*Cre*+ and $Atg5^{flox/flox}$-LyzM-*Cre*- cultures (Fig. 4-2). To explore this difference, we performed immunoblots against cathepsin K and c-Src, two proteins that are upregulated during osteoclastogenesis[23,20,24]. Immunoblot analysis revealed similar kinetics of upregulation of both cathepsin K and c-Src, indicating that this aspect of differentiation of macrophages into osteoclasts is not impaired in $Atg5^{flox/flox}$-LyzM-*Cre*+ cells (Fig. 4-3A).

To further assess osteoclast formation in the absence of *Atg5*, we grew cells from $Atg5^{flox/flox}$-LyzM-*Cre*+ and $Atg5^{flox/flox}$-LyzM-*Cre*- mice on bovine cortical bone

fragments and counted the number of nuclei per osteoclast on day 6. We observed no difference in the average number of nuclei per cell between *Atg5*$^{flox/flox}$-LyzM-*Cre*+ and *Atg5*$^{flox/flox}$-LyzM-*Cre*- osteoclasts (Fig. 4-3B). We also stained for actin and confirmed that nearly 100% of both *Atg5*$^{flox/flox}$-LyzM-*Cre*+ and *Atg5*$^{flox/flox}$-LyzM-*Cre*- osteoclasts form actin rings, a hallmark of active osteoclasts grown on bone substrate (data not shown). Finally, to ensure that osteoclasts from *Atg5*$^{flox/flox}$-LyzM-*Cre*+ mice had deleted *Atg5* and that non-recombined cells were not growing out in culture, we analyzed ATG5 protein expression in osteoclasts grown for 6 days *in vitro.* We observed a dramatic reduction in ATG5 protein levels, inhibition of LC3 conjugation, and accumulation of p62, consistent with an inhibition of autophagy in these cells (Fig. 4-4)[25]. From these results we conclude that *Atg5* is not required for osteoclast formation.

We next determined whether *Atg5*-deficient osteoclasts were functionally competent by analyzing their ability to degrade bone *in vitro*. We cultured *Atg5*$^{flox/flox}$-LyzM-*Cre*+ and *Atg5*$^{flox/flox}$-LyzM-*Cre*- osteoclasts on bone for 6 days, removed the osteoclasts from the bone fragments and stained the bones with FITC-conjugated wheat germ agglutinin, a lectin that binds to the organic matrix of bone exposed by degradation[26]. This technique allowed us to measure the depth of bone pits generated by the cells using confocal microscopy. Bone resorption pits formed by *Atg5*$^{flox/flox}$-LyzM-*Cre*- control osteoclasts were approximately twofold deeper than pits formed by *Atg5*$^{flox/flox}$-LyzM-*Cre*+ osteoclasts (Fig. 4-5). This data suggests that *Atg5* is required for normal bone resorption by osteoclasts *in vitro.*

Osteoclast bone degradation requires regulated, directional secretion of lysosomal enzymes against the bone surface (reviewed in [27]). To determine if this process was normal in *Atg5*$^{flox/flox}$-LyzM-*Cre*+ osteoclasts, we examined the intracellular localization of cathepsin K, a lysosomal protease important for bone degradation, and LAMP1, a lysosomal transmembrane protein. Secretion of lysosomes by active osteoclasts localizes both of these markers to the ruffled border, with LAMP1 localized on the plasma membrane[28,15]. We observed a significant reduction in the percentage of *Atg5*$^{flox/flox}$-LyzM-*Cre*+ osteoclasts with cathepsin K localized in the actin ring compared with *Atg5*$^{flox/flox}$-LyzM-*Cre*- osteoclasts (Fig. 4-6; *Atg5*$^{flox/flox}$-LyzM-*Cre*-: 53.1 ± 2.4%; *Atg5*$^{flox/flox}$-LyzM-*Cre*+: 24.3 ± 3.2%; p = 0.002). Similarly, LAMP1 localization was also reduced in *Atg5*$^{flox/flox}$-LyzM-*Cre*+ osteoclasts (Fig. 4-6; *Atg5*$^{flox/flox}$-LyzM-*Cre*-: 59.0 ± 1.4%; *Atg5*$^{flox/flox}$-LyzM-*Cre*+: 23.7 ± 3.7%; p = 0.0009).

Cathepsin K is synthesized as a pro-enzyme that must be cleaved in the lysosome to be active[29]. To confirm that we were measuring lysosome secretion in our immunofluorescence assays and not abnormal cathepsin K expression in *Atg5*$^{flox/flox}$-LyzM-*Cre*+ osteoclasts, we measured levels of pro-form and active cathepsin K. Immunoblotting of lysates from plastic-grown osteoclasts 6 days after addition of RANKL revealed no difference in the levels of the pro-form or processed, active form of cathepsin K (Fig. 4-7), arguing that delivery of cathepsin K to lysosomes is intact in the absence of *Atg5*. Together, this data suggests that secretion of lysosomes at the ruffled border is impaired in the absence of *Atg5*.

Conjugation of ATG5 to ATG12 is important for osteoclast function

To assess if this phenotype may be due to a non-autophagy function of *Atg5*, we deleted *Atg7*, another essential autophagy gene, in osteoclasts. ATG7 is an E1-like enzyme that is required for conjugation of ATG5 to ATG12[30]. We bred *Atg7*$^{flox/flox}$ mice to LyzM-*Cre* mice to generate *Atg7*$^{flox/flox}$-LyzM-*Cre*+ mice[31]. Immunoblotting of osteoclasts grown from these mice revealed that these cells had a significant reduction in ATG7 protein levels and partial inhibition of LC3-I to LC3-II conversion (Fig. 4-8). There was no delay in the formation of *Atg7*$^{flox/flox}$-LyzM-*Cre*+ osteoclasts (data not shown). Similar to our findings with *Atg5*-deficient osteoclasts, we observed a decrease in the depth of bone pits generated by *Atg7*-deficient osteoclasts (Fig. 4-9a). *Atg7*$^{flox/flox}$-LyzM-*Cre*+ osteoclasts also had a significant reduction in cathepsin K localization (Fig. 4-9B; *Atg7*$^{flox/flox}$-LyzM-*Cre*-: 58.6 ± 2.1%; *Atg7*$^{flox/flox}$-LyzM-*Cre*+: 30.2 ± 3.1%; p = 0.017) and LAMP1 localization (Fig. 4-9B; *Atg7*$^{flox/flox}$-LyzM-*Cre*-: 58.6 ± 2.1%; *Atg7*$^{flox/flox}$-LyzM-*Cre*+: 37.8 ± 0.8%; p = 0.0116). These data demonstrate that a second essential autophagy gene is important for osteoclast function. Given the requirement of ATG7 for the conjugation of ATG5 and the concordance of the phenotypes of *Atg5*- and *Atg7*-deficient osteoclasts, we hypothesize that the ATG5-ATG12 conjugate is involved in osteoclast secretion.

To test our hypothesis, we generated retroviruses expressing either mCherry-ATG5^{WT} or mCherry-ATG5^{K130R}, a mutant of ATG5 in which the lysine required for conjugation to ATG12 has been changed to an arginine[32,16,33]. Immunoblotting of transduced osteoclasts demonstrated expression of the wild-type and mutant mCherry-

ATG5 fusion proteins at higher levels than endogenous ATG5. We confirmed that mCherry-ATG5^{K130R} does not form the higher molecular weight band of the expected size for the mCherry-ATG5-ATG12 conjugate, consistent with the published phenotype of this mutant (Fig. 4-10)[32]. Expression of mCherry-ATG5^{WT}, but not mCherry-ATG5^{K130R}, restored the synthesis of LC3-II in *Atg5$^{flox/flox}$*-LyzM-*Cre*+ osteoclasts. Interestingly, expression of the ATG5^{K130R} mutant, but not the wild-type protein, in *Atg5$^{flox/flox}$*-LyzM-*Cre*- osteoclasts reduced LC3-II levels, suggesting that this mutant might function as a dominant negative in the LC3 conjugation pathway in our system.

We measured bone pit depth and cathepsin K localization in ATG5-transduced *Atg5$^{flox/flox}$*-LyzM-*Cre*+ and *Atg5$^{flox/flox}$*-LyzM-*Cre*- osteoclasts. Expression of mCherry-ATG5^{WT} in *Atg5$^{flox/flox}$*-LyzM-*Cre*+ osteoclasts restored bone pit depth to control levels, whereas mCherry-ATG5^{K130R} did not increase bone pit depth (Fig. 4-11A). Similarly, expression of wild-type ATG5, but not ATG5^{K130R}, increased cathepsin K localization in *Atg5$^{flox/flox}$*-LyzM-*Cre*+ osteclasts to levels comparable to *Atg5$^{flox/flox}$*-LyzM-*Cre*- controls (Fig. 4-11B). Interestingly, *Atg5$^{flox/flox}$*-LyzM-*Cre*- osteoclasts expressing mCherry-ATG5^{K130R} had decreased bone pit formation and cathepsin K localization, consistent with our observation that ATG5^{K130R} inhibits the function of endogenous ATG5[33,9,34]. Based on these results and our studies in *Atg7*-deficient osteoclasts, we conclude that the ATG5-ATG12 conjugate is important for osteoclast secretion.

Inhibiting the LC3 conjugation pathway decreases osteoclast secretion

The ATG5-ATG12 conjugate is important for LC3 conjugation, but it may have additional functions in the cell[35]. To determine if LC3 conjugation is required for osteoclast function, we next inhibited the LC3 conjugation pathway without affecting the conjugation of ATG5 to ATG12. ATG4B is a cysteine protease required for processing of the pro-form of LC3 and deconjugation of LC3 from phosphatidylethanolamine (PE) [36]. Mutating the catalytic cysteine residue generates a dominant negative enzyme ($ATG4B^{C74A}$) that sequesters LC3 and inhibits its conjugation to PE, inhibiting autophagy without disrupting formation of the ATG5-ATG12 conjugate[37]. We retrovirally expressed $ATG4B^{C74A}$ fused to mStrawberry in wild-type osteoclasts. As a control, we used either GFP or vector-only retroviruses. Immunoblotting revealed expression of the $ATG4B^{C74A}$ fusion protein (Fig. 4-12). We measured bone pit formation and cathepsin K localization and found that $ATG4B^{C74A}$-expressing osteoclasts had reduced bone pit depth and cathepsin K localization in the actin ring compared with control transduced cells (Fig. 4-13A and 4-13B). Expression of $ATG4B^{C74A}$ in GFP-LC3 osteoclasts also inhibited localization of GFP-LC3 to the actin ring (Fig. 4-14). This data demonstrates that the LC3 conjugation pathway is required for osteoclast function and suggests that LC3 conjugation is an important process in osteoclast secretion. Since inhibition of GFP-LC3 localization correlates with decreased vesicular secretion, one explanation is that osteoclast function requires the proper targeting of LC3 to the actin ring through its conjugation by the autophagy machinery.

Atg5$^{flox/flox}$-LyzM-*Cre*+ mice are protected from ovariectomy-induced bone loss

Estrogen-deficiency osteoporosis is a common disease of the elderly associated with significant morbidity and mortality (reviewed in [38]). This condition can be induced in female lab animals by ovariectomy[39]. To determine if the *Atg5* is important for regulating skeletal mass *in vivo*, we induced osteoclast activity by removing the ovaries from female *Atg5*$^{flox/flox}$-LyzM-*Cre*+ and *Atg5*$^{flox/flox}$-LyzM-*Cre*- mice. We measured bone mass in 8-week old *Atg5*$^{flox/flox}$-LyzM-*Cre*+ and *Atg5*$^{flox/flox}$-LyzM-*Cre*- mice by microcomputed tomography (μCT) before and after ovariectomy or a sham operation. At baseline, we observed a small increase in trabecular bone volume (BV/TV) in *Atg5*$^{flox/flox}$-LyzM-*Cre*+ mice (Fig. 4-15A). One month after the sham operation we observed no difference in the percentage of bone lost between *Atg5*$^{flox/flox}$-LyzM-*Cre*+ and *Atg5*$^{flox/flox}$-LyzM-*Cre*- sham-treated animals. However, *Atg5*$^{flox/flox}$-LyzM-*Cre*+ mice had a 55% reduction ($p = 0.0393$) in ovariectomy-induced bone loss compared with *Atg5*$^{flox/flox}$-LyzM-*Cre*- controls (Fig. 4-15B). This data is consistent with the hypothesis that *Atg5*$^{flox/flox}$-LyzM-*Cre*+ mice have dysfunctional osteoclasts, suggesting that our *in vitro* phenotype is relevant *in vivo*. In addition, the function of *Atg5* in osteoclasts may be important for the pathophysiology of osteoporosis.

Discussion

Here we show that GFP-LC3 localizes to the actin ring in activated osteoclasts. Deletion of two essential autophagy genes (*Atg5*, *Atg7*) in the autophagy pathway or retroviral expression of a dominant negative ATG4B^{C74A} or ATG5^{K130R} inhibit osteoclast function as measured by bone pit depth and cathepsin K localization. We confirmed that the secretion defect in *Atg5$^{flox/flox}$*-LyzM-*Cre*+ osteoclasts is due to deletion of ATG5 in these cells by rescuing this phenotype with retroviral expression of wild-type ATG5. Together, these studies demonstrate that the biochemical pathway required for LC3 conjugation and autophagosome formation is critical for osteoclast secretion. Finally, mice lacking *Atg5* in osteoclasts and other myeloid-lineage cells are protected from ovariectomy-induced bone loss.

Given these findings connecting proteins involved in a cellular degradation pathway and osteoclast secretion, it is useful to compare our results with published phenotypes of osteoclasts deficient in proteins known to be important for bone degradation, osteoclast activation, and secretion. We found a 55% reduction in bone pit depth generated by *Atg5*-deficient osteoclasts, which is comparable with the reduction in pit depth by cathepsin K knockout osteoclasts (44% reduction) and β3 integrin knockout osteoclasts (38% reduction)[40,41]. We observed a twofold reduction in cathepsin K localization in the actin ring, similar to the 3-fold reduction reported in osteoclasts lacking Synaptotagmin VII, an important regulator of lysosome exocytosis[42,43]. Finally, our results demonstrating a 55% reduction in ovariectomy-induced bone loss are comparable with protection offered by bisphosphonate treatment of ovariectomized rats

(74% reduction) or cathepsin K inhibitor treatment of ovariectomized mice (73% reduction)[44,45]. This comparison demonstrates the importance of autophagy genes in osteoclast biology and suggests that the biochemical pathway necessary for autophagy may be a new target to treat bone disease.

The observation that 8-week old *Atg5*$^{flox/flox}$-LyzM-*Cre*+ mice have a minimal increase in basal bone mass but are protected from ovariectomy-induced bone loss suggests that ATG5 is important for osteoclast function after activation *in vivo*. Our *in vitro* results demonstrate that *Atg5*-deficient osteoclasts can be activated, as demonstrated by normal formation of actin rings, but have reduced secretion after activation. Interestingly, β3 integrin-deficient mice are also protected from ovariectomy-induced bone loss, do not have a basal difference in bone density when young (<4 months), but develop severe osteosclerosis by six months of age[41,46]. It will be interesting to determine if *Atg5*$^{flox/flox}$-LyzM-*Cre*+ mice develop osteosclerosis as they age.

We have identified a novel biochemical pathway involved in secretion in osteoclasts. Autophagy genes have been implicated in secretion in other cell types, and the molecular mechanisms connecting autophagy genes and secretion are of great interest[2,3,4,5,47]. In these studies it is unclear how the formation of autophagosomes would be necessary for secretion. In osteoclasts, we favor the working hypothesis that LC3 is conjugated to the plasma membrane at the ruffled border, as suggested by our localization studies with GFP-LC3. In our experiments employing the dominant negative protein ATG4B^{C74A}, localization of GFP-LC3 correlates with osteoclast function, suggesting that LC3 localization might be important for vesicle secretion in osteoclasts (Fig. 4-16). We

hypothesize that LC3 at the ruffled border is important for the trafficking or fusion of lysosomes with the plasma membrane. Indeed, LC3 localization to the phagosome membrane correlates with increased fusion of phagosomes with lysosomes[6]. How the resorptive microenvironment is targeted for LC3 localization remains to be determined.

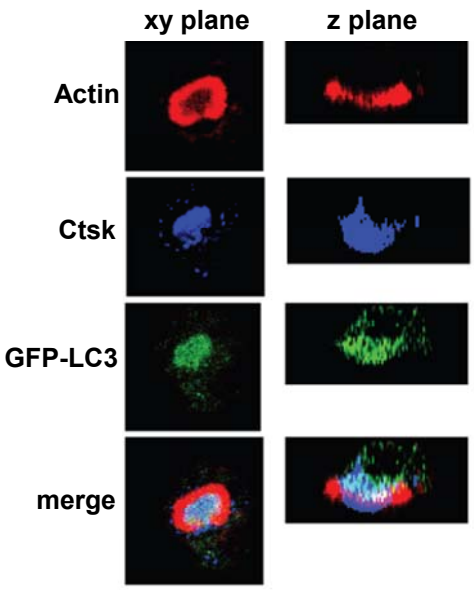

Figure 4-1. GFP-LC3 localizes to the actin ring in active osteoclasts

Confocal image of a GFP-LC3 osteoclast grown on bone stained for actin (red), cathepsin K (ctsk, blue), and GFP (green) showing localization of cathepsin K and GFP-LC3 within the actin ring in both the xy plane and z plane. Representative image from two separate experiments, 3 bones/experiment.

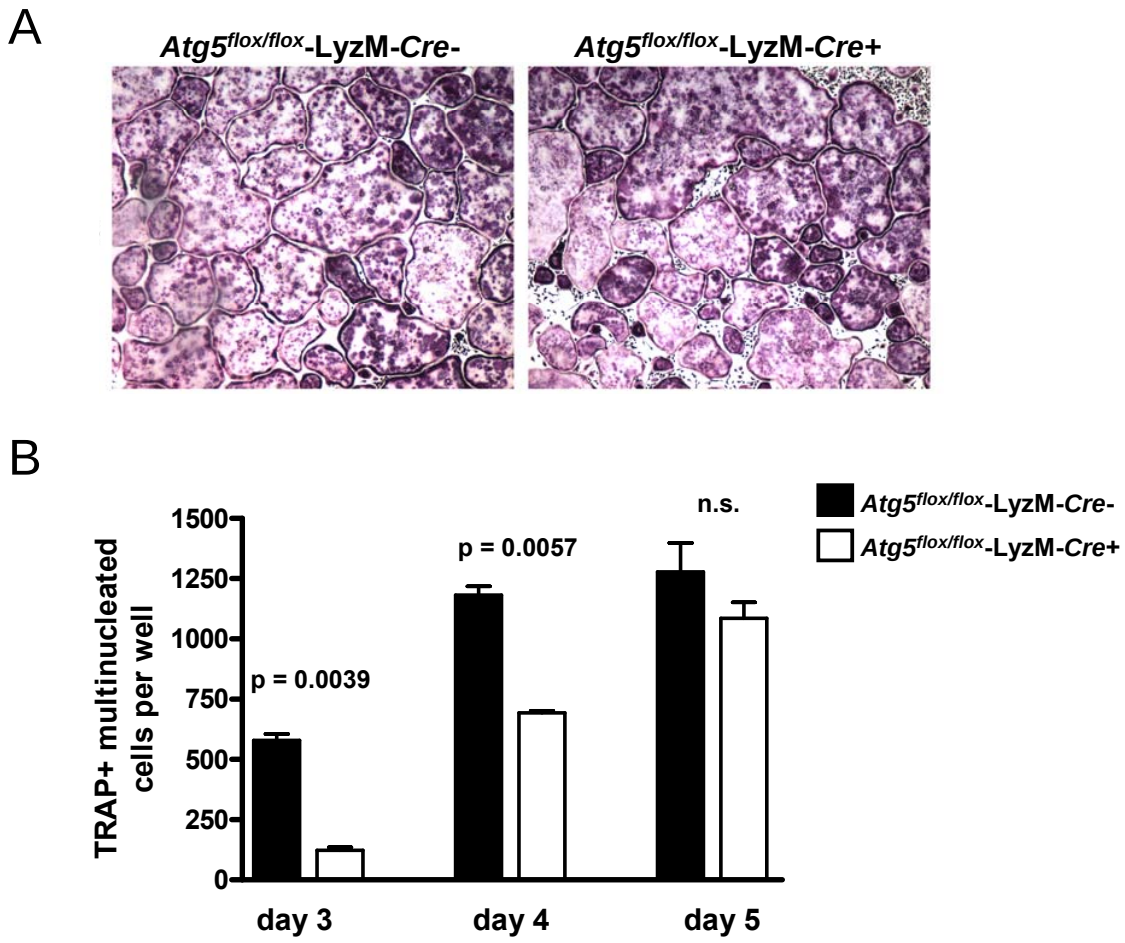

Figure 4-2. *Atg5*$^{flox/flox}$-LyzM-*Cre*+ cells have a slight delay in formation of TRAP+ multinucleated osteoclasts

(A) Representative images of osteoclasts differentiated on plastic for 5 days from *Atg5*$^{flox/flox}$-LyzM-*Cre*- and *Atg5*$^{flox/flox}$-LyzM-*Cre*+ macrophages, stained for the osteoclast marker TRAP (purple). (B) Quantification of the number of TRAP+ multinucleated cells in plastic cultures on day 3-5. Quantification of one representative experiment from 5 independent experiments. P values generated by unpaired Student's t test, n.s. = not statistically significant.

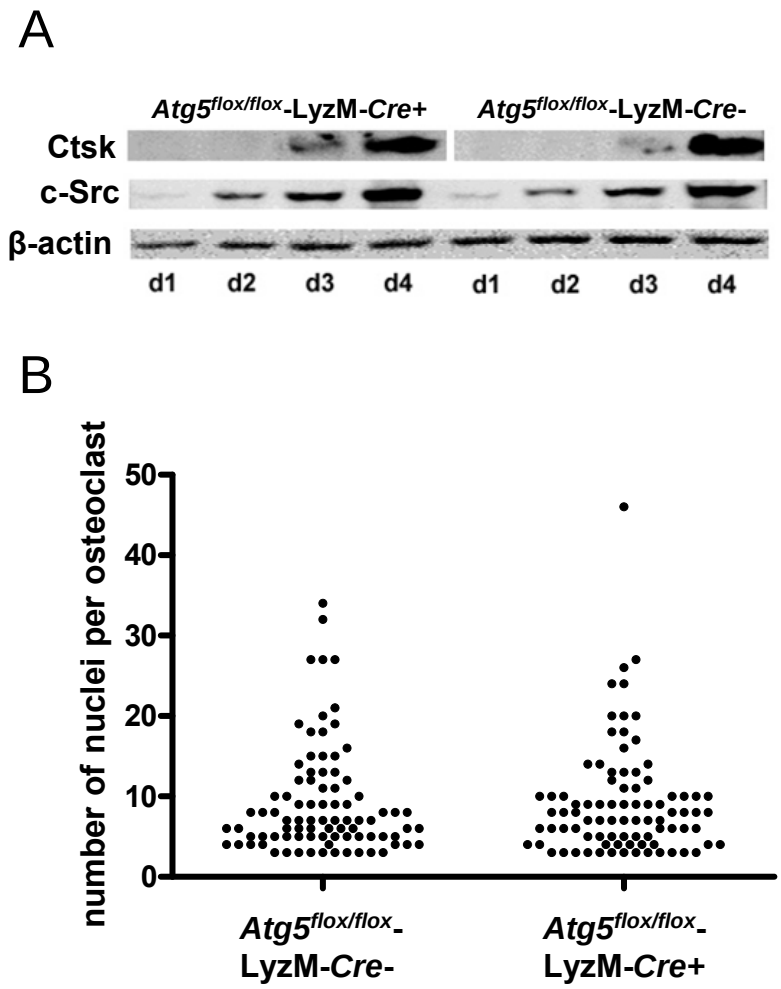

Figure 4-3. *Atg5*$^{flox/flox}$-LyzM-*Cre*+ cells express osteoclast differentiation markers normally during osteoclastogenesis and form osteoclasts with normal numbers of nuclei

(A) Immunoblot analysis of macrophages induced to differentiate into osteoclasts, probed against cathepsin K (Ctsk), c-Src, and β-actin. Lysates were made on the indicated days after addition of osteoclastogenic cytokines. One of four representative blots shown. (B) Quantification of the number of nuclei per osteoclast grown for 6 days on bone.

Individual cells were identified by actin staining and the number of nuclei counted per cell. All cells with 3 or more nuclei were included in this analysis. Data pooled from three independent experiments. There was no statistically significant difference in mean nuclei number in any of the three experiments.

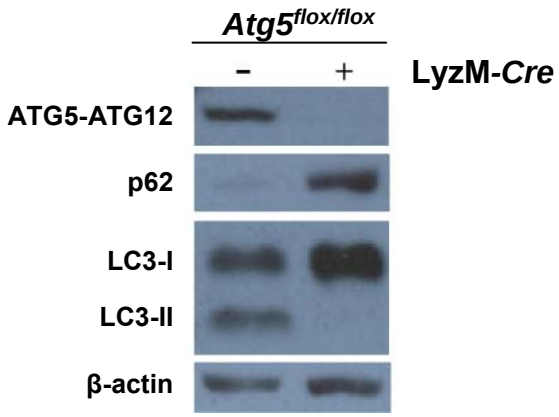

Figure 4-4. *Atg5*$^{flox/flox}$-LyzM-*Cre*+ osteoclasts express reduced levels of ATG5 and LC3-II and increased levels of p62

Immunoblot analysis of lysates from *Atg5*$^{flox/flox}$-LyzM-*Cre*- and *Atg5*$^{flox/flox}$-LyzM-*Cre*+ osteoclasts grown on plastic for 6 days. Lysates were probed with antibodies against ATG5, p62, LC3, and β-actin. Representative blot of 6 independent experiments.

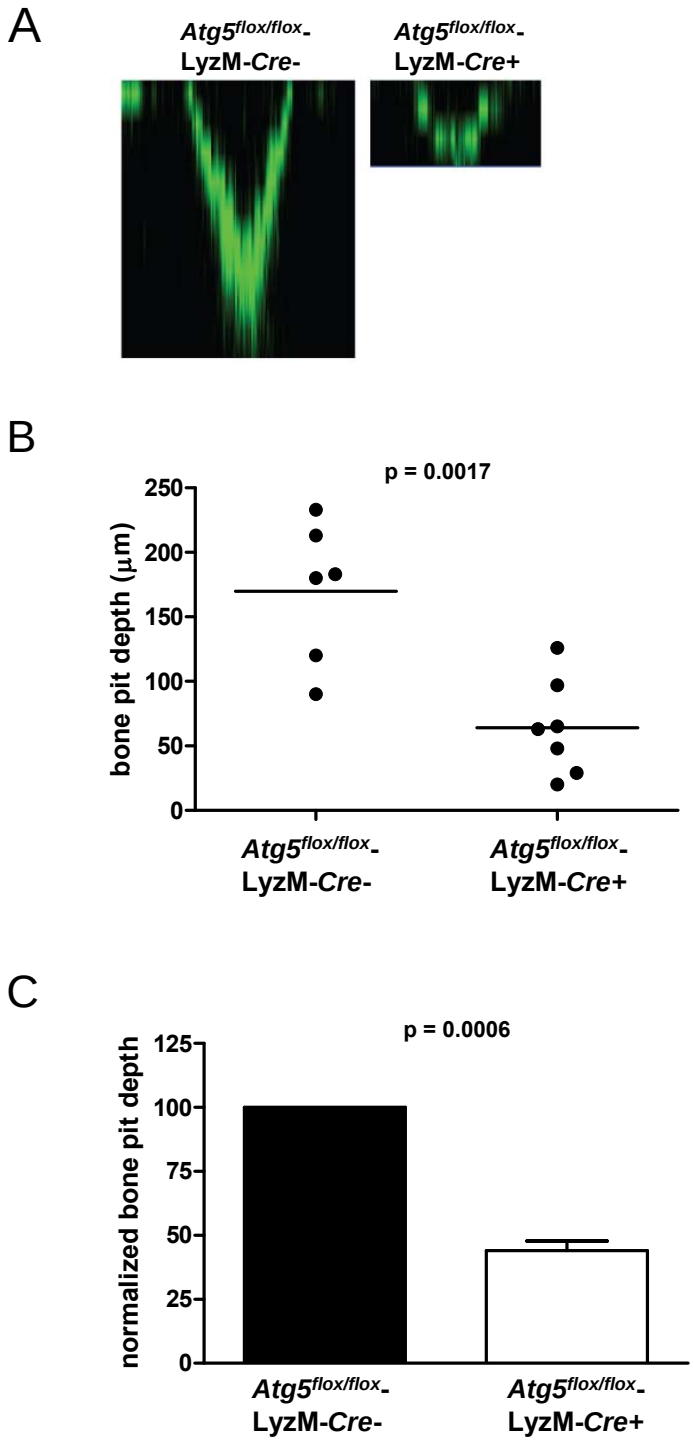

Figure 4-5. *Atg5*$^{flox/flox}$-LyzM-*Cre*+ osteoclasts have a defect in bone pit formation

(A) Bone pits were imaged by removing osteoclasts grown on bone and staining degraded bone with FITC-conjugated wheat germ agglutinin. Representative images of bone pits viewed in the z plane. (B) Quantification of bone pit depth from one of four experiments, analyzed in a blinded fashion. Each point represents an individual bone pit. P value generated by unpaired Student's t test. (C) Pooled analysis of the mean bone pit depths from 4 independent, blindly read experiments. To pool the results, we normalized the mean of the pit depth generated by *Atg5*$^{flox/flox}$-LyzM-*Cre*+ cells to the mean depth generated by *Atg5*$^{flox/flox}$-LyzM-*Cre*- cells, which was set to 100. P value generated by paired Student's t test.

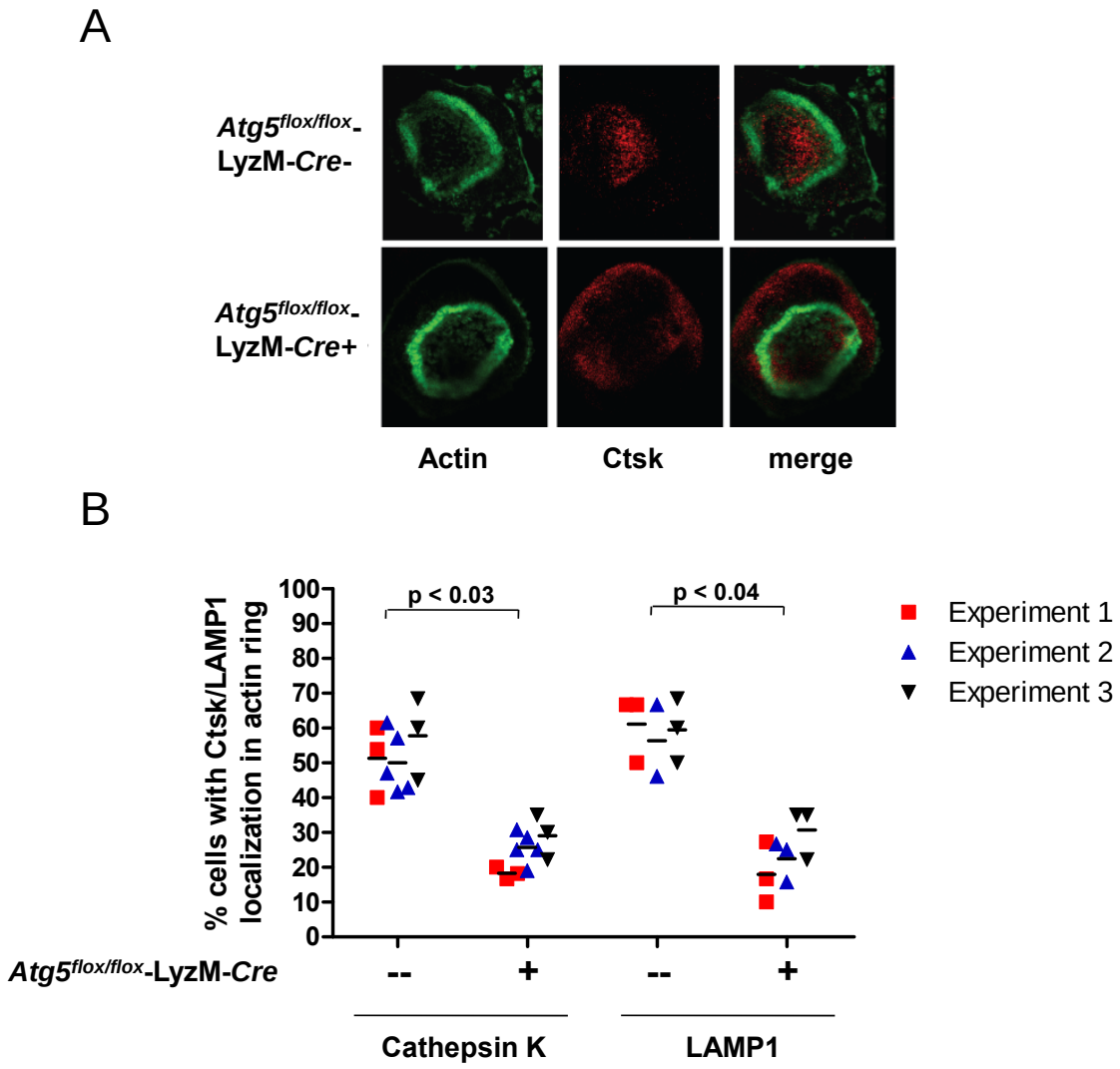

Figure 4-6. *Atg5*$^{flox/flox}$-LyzM-*Cre*+ osteoclasts have reduced localization of cathepsin K and LAMP1 in the actin ring

(A) Representative confocal images of *Atg5*$^{flox/flox}$-LyzM-*Cre*- and *Atg5*$^{flox/flox}$-LyzM-*Cre*+ osteoclasts, grown on bone and stained for actin (green) and cathepsin K (Ctsk, red). (B) Quantification of the percentage of *Atg5*$^{flox/flox}$-LyzM-*Cre*- and *Atg5*$^{flox/flox}$-LyzM-*Cre*+ osteoclasts with cathepsin K or LAMP1 localized in the actin ring. Cells of each

genotype were grown on at least three pieces of bone in separate culture wells. Each point represents the percentage of cells with localization from one bone – a minimum of 10 cells analyzed per bone, with at least three bones analyzed per genotype per experiment. All data was collected by a blinded observer. The largest p value from any of the three experiments is shown, calculated by unpaired Student's t test.

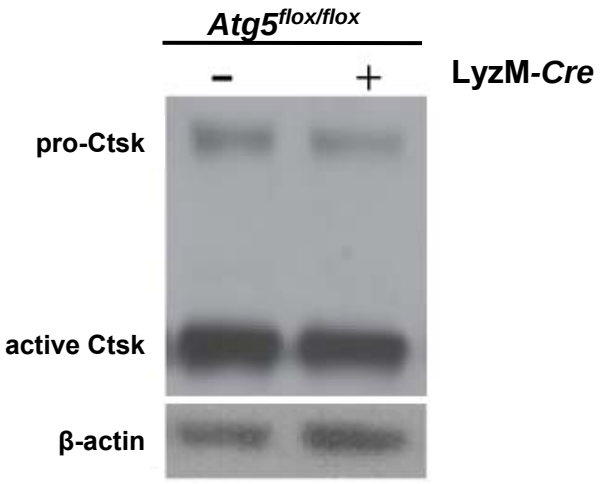

Figure 4-7. No difference in cathepsin K processing in *Atg5*$^{flox/flox}$-LyzM-*Cre*- and *Atg5*$^{flox/flox}$-LyzM-*Cre*+ osteoclasts

Immunoblot of lysates from *Atg5*$^{flox/flox}$-LyzM-*Cre*- and *Atg5*$^{flox/flox}$-LyzM-*Cre*+ osteoclasts grown on plastic for 6 days and probed for cathepsin K (Ctsk) and β-actin. One representative of four independent experiments shown.

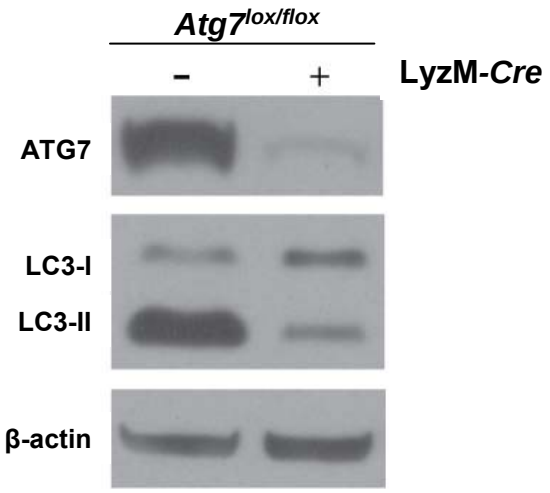

Figure 4-8. *Atg7*$^{flox/flox}$-LyzM-*Cre*+ osteoclasts have reduced expression of ATG7 and LC3-II

Immunoblot analysis of lysates from day 6 *Atg7*$^{flox/flox}$-LyzM-*Cre*- and *Atg7*$^{flox/flox}$-LyzM-*Cre*+ osteoclasts grown on plastic. Lysates were probed for ATG7, LC3, and β-actin. One representative of three independent experiments shown.

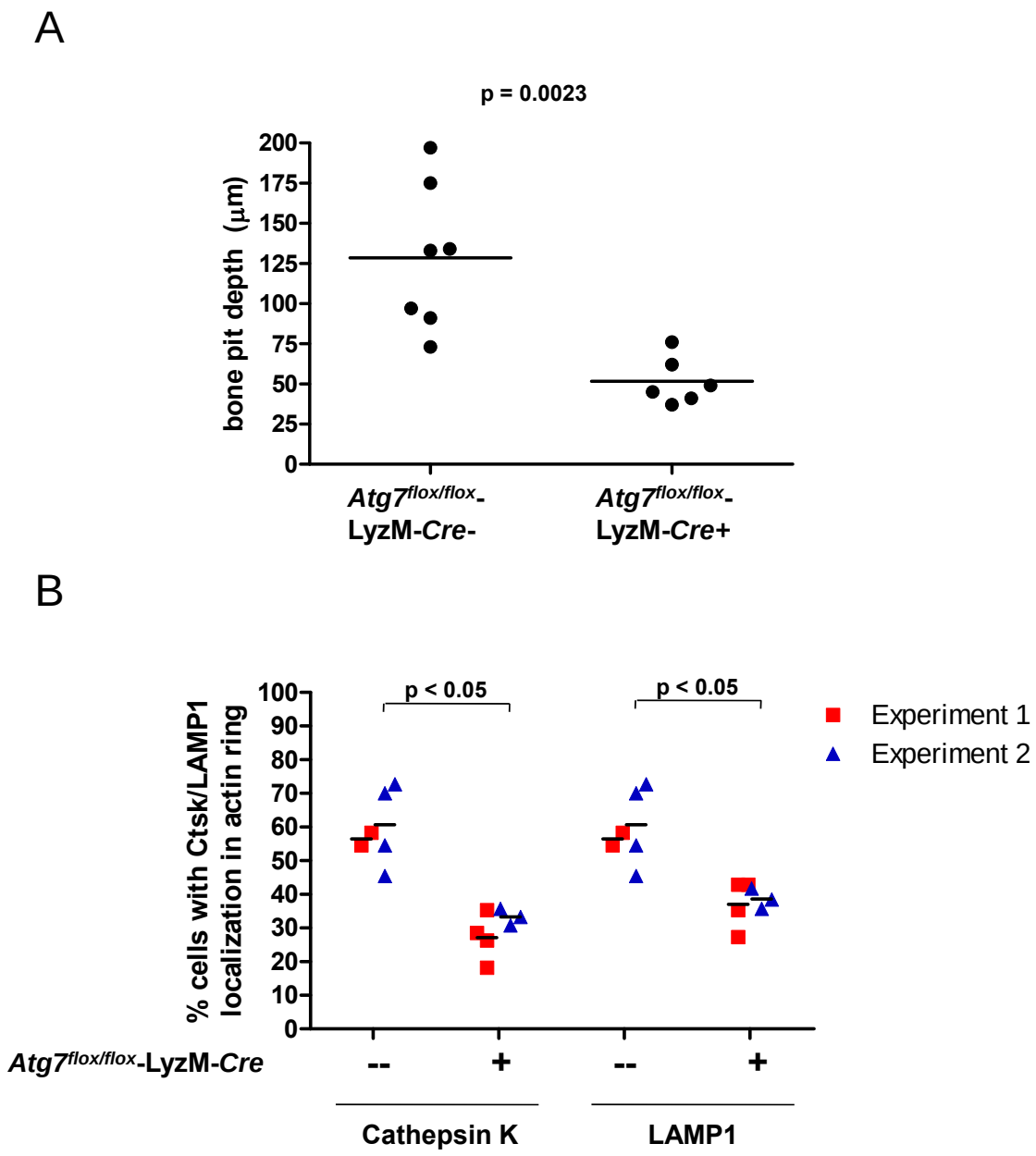

Figure 4-9. *Atg7*$^{flox/flox}$-LyzM-*Cre*+ osteoclasts have a defect in bone pit formation and cathepsin K and LAMP1 localization

(A) Quantification of bone pit depth from one of two experiments. Each point represents an individual bone pit. All data was collected by a blinded observer. P value generated

by unpaired Student's t test. (B) Quantification of the percentage of *Atg7*$^{flox/flox}$-LyzM-*Cre*- and *Atg7*$^{flox/flox}$-LyzM-*Cre*+ osteoclasts with cathepsin K (Ctsk) or LAMP1 localized in the actin ring. Each point represents the percentage of cells with localization from one bone – a minimum of 10 cells analyzed per bone, with at least two bones analyzed per genotype per experiment. All data was collected by a blinded observer. The largest p value from any of the two experiments is shown, generated by unpaired Student's t test.

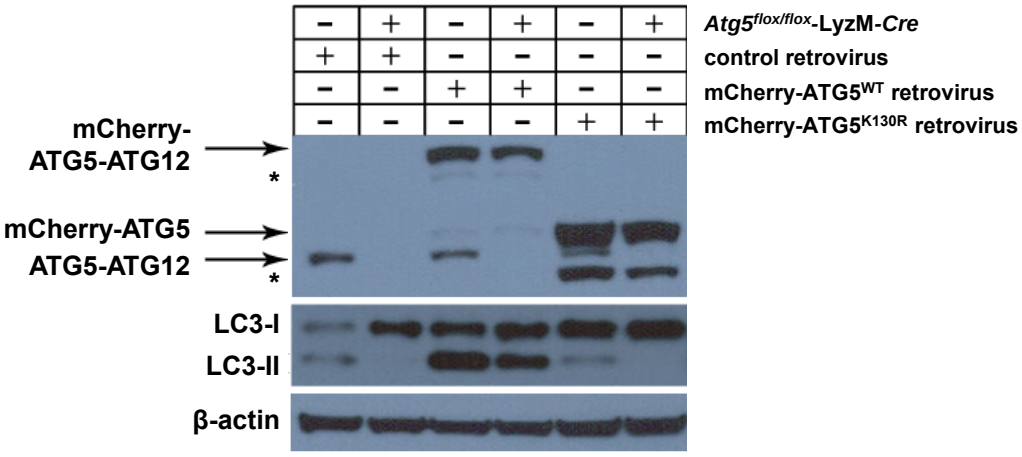

Figure 4-10. Expression of ATG5^{WT}, but not ATG5^{K130R}, rescues LC3 conjugation in *Atg5*$^{flox/flox}$-LyzM-*Cre*+ osteoclasts

Immunoblot analysis of *Atg5*$^{flox/flox}$-LyzM-*Cre*- and *Atg5*$^{flox/flox}$-LyzM-*Cre*+ osteoclasts transduced with control retrovirus or retroviruses expressing mCherry-Atg5^{WT} or mCherry-ATG5K^{130R} fusion proteins. Lysates were probed for ATG5, LC3, and β-actin. Asterisks (*) indicate unpredicted bands that we hypothesize are degradation products of the fusion protein. One of three experiments shown.

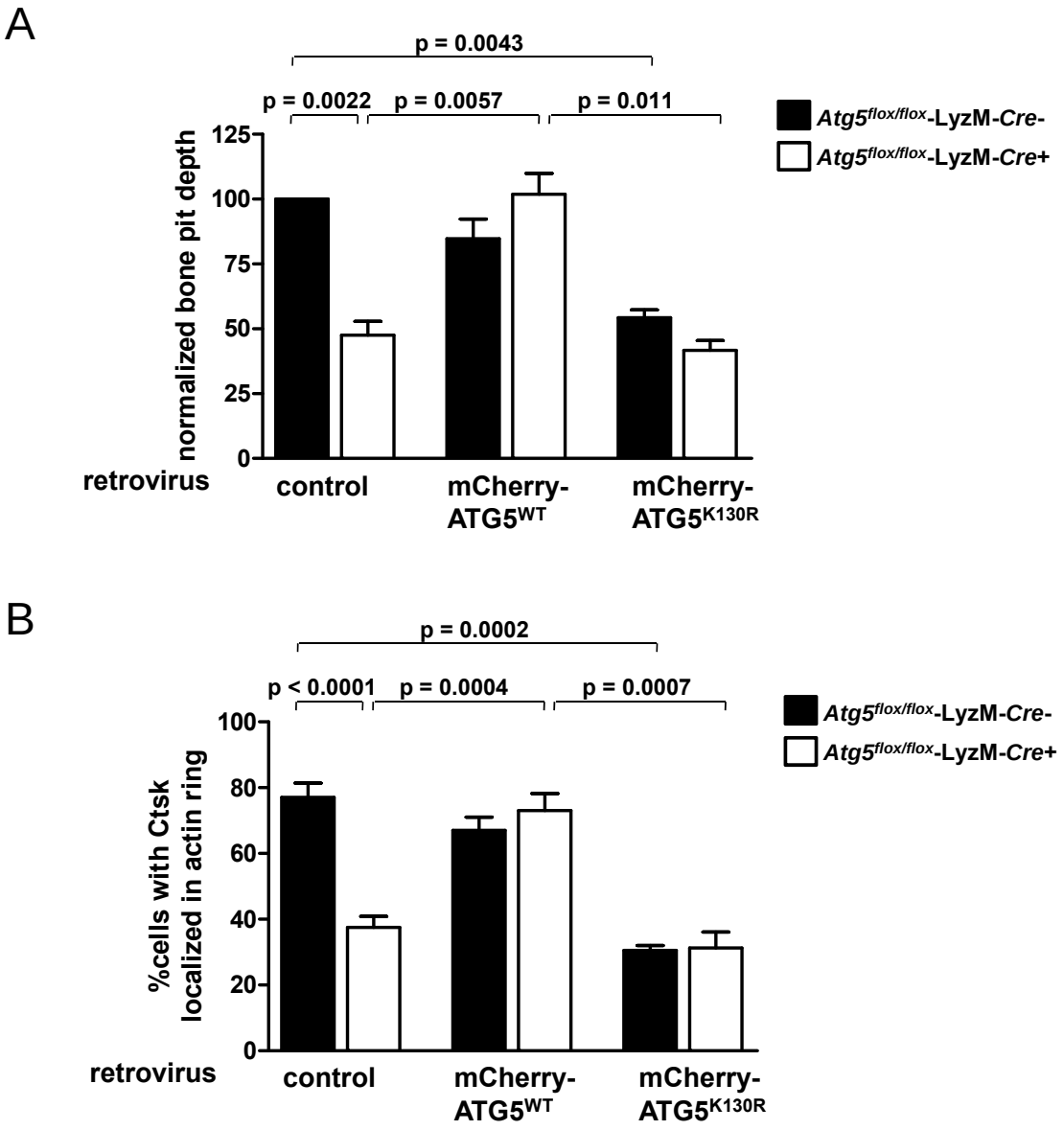

Figure 4-11. Expression of ATG5^{WT}, but not ATG5^{K130R}, rescues bone pit depth and cathepsin K localization in *Atg5$^{flox/flox}$*-LyzM-*Cre*+ osteoclasts

(A) *Atg5*$^{flox/flox}$-LyzM-*Cre*- and *Atg5*$^{flox/flox}$-LyzM-*Cre*+ osteoclasts were transduced with control retroviruses or retroviruses expressing mCherry-ATG5^{WT} or mCherry-ATG5^{K130R}. Pooled analysis of the mean bone pit depths from 2-3 independent, blindly read experiments. Data normalized as described in Figure 4-5. P values calculated by paired Student's t test. (B) Quantification of cathepsin K localization in actin rings in transduced *Atg5*$^{flox/flox}$-LyzM-*Cre*- and *Atg5*$^{flox/flox}$-LyzM-*Cre*+ osteoclasts. Average localization from 2-3 independent experiments was pooled. All data was collected by a blinded observer. P values generated by unpaired Student's t test.

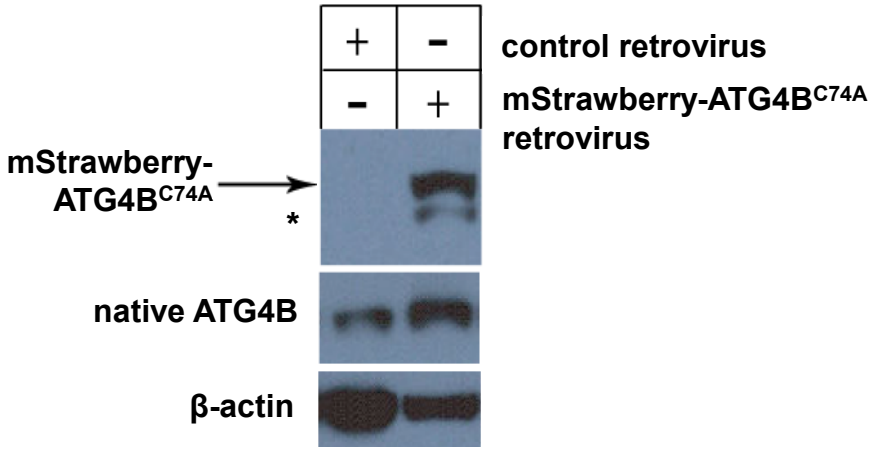

Figure 4-12. mStrawberry-ATG4B^{C74A} is expressed in wild-type osteoclasts after retroviral transduction

Immunoblot analysis of lysates from wild-type osteoclasts transduced with mStawberry-ATG4B^{C74A}-expressing or control retrovirus, probed with antibodies against ATG4B and β-actin. The asterisk (*) indicates an unpredicted band that we hypothesize is a degradation product of the fusion protein. One representative blot of three independent experiments shown.

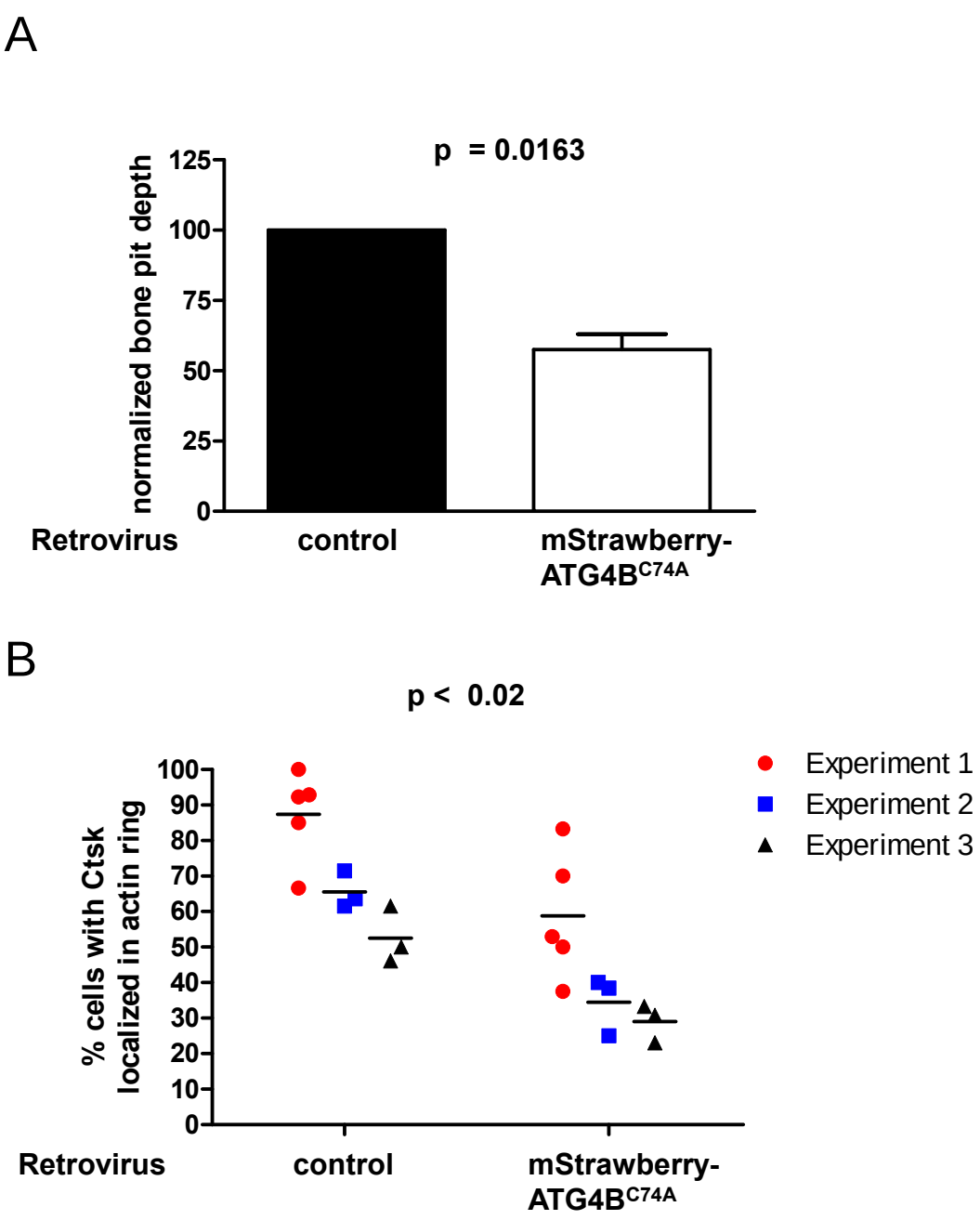

Figure 4-13. Transduction of wild-type osteoclasts with retrovirus expressing mStrawberry-ATG4B^{C74A} causes a reduction in bone pit depth and cathepsin K localization

(A) Wild-type osteoclasts were transduced with control retrovirus or retrovirus expressing mStrawberry-ATG4B^{C74A}. Pooled analysis of the mean bone pit depths from 3 independent, blindly read experiments. Data normalized as described above in Figure 4-5. P values generated by paired Student's t test. (B) Quantification of the percentage of mStrawberry-ATG4B^{C74A} or control transduced osteoclasts with cathepsin K (Ctsk) localized in the actin ring. Each point represents the percentage of cells with localization from one bone – a minimum of 10 cells analyzed per bone, with at least three bones analyzed per genotype per experiment. All data was collected by a blinded observer. The largest p value from any of the three experiments is shown, generated by unpaired Student's t test.

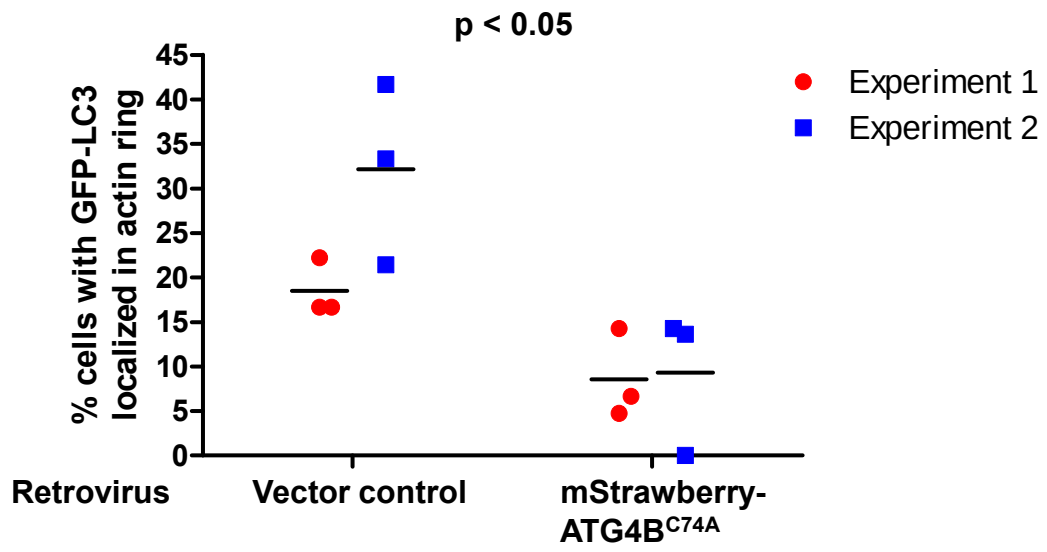

Figure 4-14. Expression of mStrawberry-ATG4B^{C74A} in GFP-LC3 osteoclasts decreases GFP-LC3 localization in the actin ring

Quantification of the percentage of mStrawberry-ATG4B^{C74A} or control transduced osteoclasts with GFP-LC3 localized in the actin ring. Each point represents the percentage of cells with localization from one bone – a minimum of 10 cells analyzed per bone, with at least three bones analyzed per genotype per experiment. All data was collected by a blinded observer. The largest p value from either experiment is shown, generated by unpaired Student's t test.

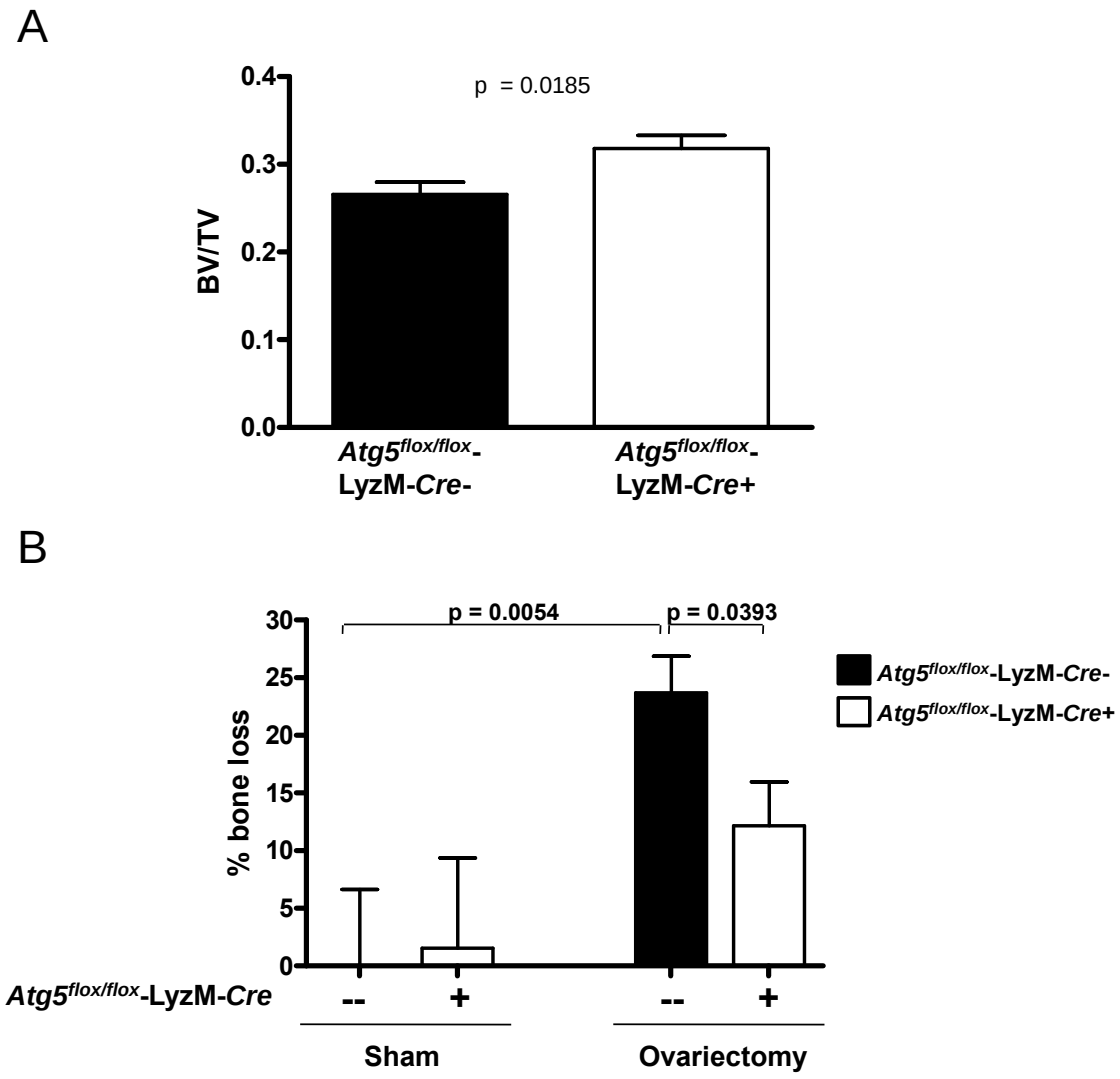

Figure 4-15. *Atg5*$^{flox/flox}$-LyzM-*Cre*+ mice are protected from ovariectomy-induced bone loss

(A) Trabecular bone volume over total volume of the marrow space (BV/TV) of 8-week old female *Atg5*$^{flox/flox}$-LyzM-*Cre*- and *Atg5*$^{flox/flox}$-LyzM-*Cre*+ mice, as measured by microcomputed tomography. Pooled data from 3 independent experiments, n = 12 mice per genotype. P value generated by unpaired Student's t test. (B) Quantification of

ovariectomy-induced bone loss. BV/TV was measured at day 0, mice were ovariectomized or sham operated on day 1, and BV/TV was reanalyzed at day 29. The average bone loss in sham-operated *Atg5*$^{flox/flox}$-LyzM-*Cre*- control animals was subtracted from all measurements. Pooled data from 2 (sham) or 3 (ovariectomy) independent experiments, n = 4-5 mice for the sham treatment and 7-8 mice for the ovariectomy treatment groups.

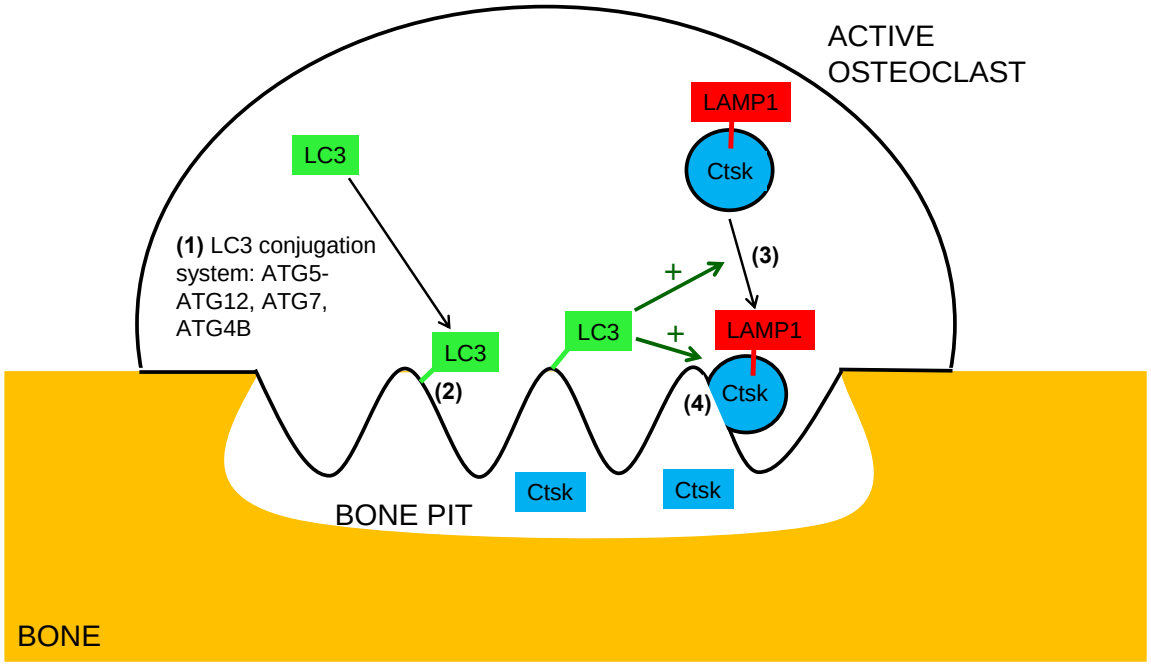

Figure 4-16. Working hypothesis for the role of LC3 and the LC3 conjugation pathway in osteoclast function

We propose the following model to explain the function of the LC3 conjugation pathway in osteoclast secretion. **(1)** We speculate that the LC3 conjugation cascade (see Fig. 1-1), employing ATG7, the ATG5-ATG12 conjugate, and ATG4B, is involved in localization of LC3 to the ruffled border, suggesting that LC3 is directly conjugated to the ruffled border **(2)**. We did not observe colocalization of LC3 and cathepsin K puncta in the cell periphery, arguing that LC3 is not conjugated to the membranes of secretory lysosomes. At the ruffled border, LC3 may function either to promote (green arrows) trafficking of cathepsin K-containing, LAMP1 positive vesicles to the ruffled border **(3)** or the fusion of these vesicles with the plasma membrane **(4)**. Key: cathepsin K (Ctsk) – blue; LAMP1 – red; conjugated LC3 – green box with green line; bone – orange box

Materials and Methods

Mice The generation of *Atg5*$^{flox/flox}$, *Atg7*$^{flox/flox}$, *Atg5*$^{flox/flox}$-LyzM-*Cre*+, and GFP-LC3 mice has been previously reported[17,31,18,13]. To generate *Atg7*$^{flox/flox}$-LyzM-*Cre*+ mice, we bred mice *Atg7*$^{flox/flox}$ mice to mice expressing the Cre recombinase from the Lysozyme M locus (strain #004781, Jackson Laboratory, Bar Harbor, ME). *Atg5*$^{flox/flox}$, *Atg7*$^{flox/flox}$, *Atg5*$^{flox/flox}$-LyzM-*Cre*+ mice were genotyped as described[48]. GFP-LC3 mice were genotyped with primers GFP-1: 5′-TCCTGCTGGAGTTCGTGACCG-3′ and LC3: 5′-TTGCGAATTCTCAGCCGTCTTCA

TCTCTCTCGC-3′ using PCR [94°C(4 min); 35 cycles of 94°C (30 sec), 57°C (30 sec), 72°C (1 min); 72°C (5 min)]. Mice were maintained at Washington University School of Medicine in accordance with institutional policies for animal care and usage.

Cell culture Osteoclasts were grown in alpha10 media, containing alpha-MEM (Sigma Aldrich, St. Louis, MO), 10% fetal calf serum (Hyclone, Waltham, MA), 100U/mL penicillin and 100ug/mL streptomycin. Plat-E retrovirus packaging cells were purchased from Cell Biolabs, Inc. (San Diego, CA) and maintained in DMEM media (Cellgro, Manassas, VA) containing 10% fetal calf serum (Hyclone, Waltham, MA), and 2mM L-glutamine (Gibco, Carlsbad, CA). Osteoclasts were differentiated from bone marrow as described, with minor modifications[42]. Briefly, bone marrow was extracted from mice and cultured in the presence of 10% CMG 14-12 supernatant[49], an M-CSF-

containing cell supernatant, on day -4. After 4 days (day 0), cells were lifted and replated on plastic or bovine bone fragments in alpha10 media supplemented with 2% CMG and 100ng/mL recombinant RANKL. Bone grown cells were fixed in 4% paraformaldehyde 6 or 7 days after plating for immunofluorescence and bone pit measurements. Plastic-grown cells were fixed on days 3, 4, and 5 in 4% paraformaldehyde/PBS for osteoclastogenesis or lysed on various days for immunoblot analysis. TRAP staining on fixed cells was performed using a commercially available kit according to the manufacturer's instructions (Sigma, St. Louis, MO).

Retroviral DNA constructs mCherry-ATG5^{WT} and mCherry-ATG5^{K130R} were generated in the laboratory of Dr. A. B. Gustafsson[33]. mStrawberry-ATG4B^{C74A} was kindly provided by Dr. T. Yoshimori[37]. The eGFP construct was purchased from Clontech (Mountain View, CA). All constructs were cloned into the pMXs-IRES-Puro retroviral vector (Cell Biolabs, Inc., San Diego, CA). eGFP-IRES-Puro retrovirus and vector only retrovirus were used as controls.

Retroviral transduction Retroviral transduction of bone marrow macrophages was done as previously described, with slight modifications[42]. Briefly, 8ug of retroviral DNA was transfected into Plat-E cells using the Fugene HD transfection reagent (Roche, Basel, Switzerland) the same day as bone marrow isolation. Plat-E media was replaced 24

hours later and virus harvested 48 and 72 hours after for transduction of plated bone marrow cells. To transduce the bone marrow cells, culture media was replaced at 48 and 72 hours with alpha10 containing 25% Plat-E viral media, 10% CMG 14-12 supernatant, and 4ug/mL polybrene. At 96 hours the transduction media was replaced with alpha10 with 10% CMG 14-12 supernatant and 2ug/mL puromycin. Cells were allowed to grow for 3 days before being harvested and plated to form osteoclasts. Control, untransduced cells were killed by the puromycin.

Immunofluorescence Osteoclasts grown on bone fragments were fixed in 4% paraformaldehyde for 10 minutes and washed in PBS. Cells were permeabilized in 0.1% Triton-X for 10 minutes at room temperature and blocked for 1 hour in PBS containing 0.2% BSA, 10% normal goat serum, and 10% normal rabbit serum. The following antibodies and detection reagents were used: anti-cathepsin K (Millipore, Billerica, MA) (1:500 dilution), mouse IgG1 isotype control (Southern Biotech, Birmingham, AL), anti-GFP conjugated to Alexa 488 (Molecular Probes, Carlsbad, CA), polyclonal rabbit antibody conjugated to Alexa 488 isotype control (anti-fluorescein, Molecular Probes, Carlsbad, CA), anti-CD107a (eBioscience, San Diego, CA), rat anti-mouse IgG2a isotype control (anti-mouse CD8a, BD Biosciences, San Jose, CA), phalloidin-Alexa 555 and phalloidin-Alexa 488 (Molecular Probes, Carlsbad, CA), goat anti-rat-Alexa 488 (Molecular Probes, Carlsbad, CA), goat anti-mouse Cy5 (Jackson Immunoresearch, West Grove, PA), and donkey anti-mouse-Alexa 555 (Jackson Immunoresearch, West Grove,

PA). All antibodies were diluted in blocking buffer. Primary antibodies were applied overnight. After washing in PBS, secondary antibodies were applied for 1 hour at room temperature. Bones were then mounted in 30% glycerol or VECTASHIELD Mounting Media with DAPI (Vector labs, Burlingame, CA) and imaged on a Nikon Eclipse epifluorescent microscope (Nikon, Melville, NY), Olympus BX51 epifluorescent microscope (Olympus, Center Valley, PA), or Axiovert 100M confocal microscope (Zeiss, Thornwood, NY). Confocal images were analyzed using LSM 510 software (Zeiss, Thornwood, NY). For localization of GFP-LC3, cathepsin K, and LAMP1, confocal microscopy was used to identify cells with complete actin rings. If the area outlined by the actin ring was completely occupied by CatK in any z-plane containing the actin ring, and CatK was not visualized outside the ring in those z-planes, the cell was said to have positive CatK localization. The same procedure was followed for LAMP1 and GFP-LC3 localization. All data was collected by a blinded observer.

Bone pit depth measurements Osteoclast-generated bone pits were stained by removing the cells from bone fragments with a soft brush and incubating with 20ug/mL FITC conjugated wheat germ agglutinin (Sigma, St. Louis, MO) for 30 minutes at room temperature. After washing the bones, pits were imaged by confocal microscopy. The pit depth was measured from the surface of the bone down to the deepest point in the pit. All data was collected by a blinded observer.

Nuclei and actin ring measurements Osteoclasts were grown on bone for 6 days and fixed and permeabilized as described above. Cells were stained with Alexa 555-conjugated phalloidin and mounted with VECTASHIELD Mounting Media with DAPI to visualize actin rings and nuclei. Actin rings were quantified in any cell with at least three nuclei. Nuclei per cell were quantified counting any cell with at least three nuclei.

Immunoblots Cells were lysed in RIPA buffer + protease inhibitors for 10 minutes on ice, the lysates were clarified, 5x Laemmli sample buffer added, and the samples boiled. Immunoblotting was performed using antibodies against ATG5 (Nanotools, Teningen Germany) (1:200 dilution), LC3 (Cosmo Bio Co, LTD, Tokyo, Japan) (1:500 dilution), ATG7 (Sigma-Aldrich, St. Louis MO) (1:2,000 dilution), B-actin (Sigma-Aldrich, St. Louis MO) (1:40,000 dilution), p62 (Progen Biotechnik, Heidelberg, Germany) (1:1,000 dilution), ATG4B (MBL, Woburn, MA) (1:1,000 dilution), c-Src (monoclonal antibody directed against c-Src was a gift from A. Shaw) (final concentration: 2ug/mL), and cathepsin K (Millipore, Billerica, MA) (1:500 dilution).

Microcomputed tomography and ovariectomy Trabecular volume in the distal femoral metaphysis (right leg) was measured using *in vivo* microcomputed tomography (vivaCT 40, Scanco Medical, Brüttisellen, Switzerland) while the mice were anesthetized with isofluorane. A threshold linear attenuation coefficient of 1.2 cm^{-1} was used to

differentiate bone from non-bone. A threshold of 120 was used for evaluation of all scans. 30 slices were analyzed, starting with the first slice in which condyles and primary spongiosa were no longer visible. Trabecular volume was measured one day before ovariectomy or sham operation (basal bone volume) and 28 days after surgery (post-ovx). For ovariectomies, mice were anesthetized with ketamine/xylene delivered by intraperitoneal injection, and ovaries were removed through two small dorsal incisions. Sham operated mice were anesthetized and opened equivalently, but ovaries were not removed.

Statistics All data was analyzed with Prism software (Graphpad, San Diego, CA), using two-tailed unpaired or paired Student's t tests, as indicated. Error bars represent standard error of the mean (SEM).

References

1. Teitelbaum, S.L. & Ross, F.P. Genetic regulation of osteoclast development and function. *Nat. Rev. Genet.* **4**, 638-649 (2003).

2. Cadwell, K., Patel, K.K., Komatsu, M., Virgin, H.W. & Stappenbeck, T.S. A common role for Atg16L1, Atg5, and Atg7 in small intestinal Paneth cells and Crohn's disease. *Autophagy.* **5**, 250-252 (2008).

3. Cadwell, K. *et al.* A key role for autophagy and the autophagy gene Atg16l1 in mouse and human intestinal Paneth cells. *Nature.* **456**, 259-263 (2008).

4. Ebato, C. *et al.* Autophagy is important in islet homeostasis and compensatory increase of Beta cell mass in response to high-fat diet. *Cell Metab.* **8**, 325-332 (2008).

5. Jung, H.S. *et al.* Loss of autophagy diminishes pancreatic Beta cell mass and function with resultant hyperglycemia. *Cell Metab.* **8**, 318-324 (2008).

6. Sanjuan, M.A. *et al.* Toll-like receptor signaling in macrophages links the autophagy pathway to phagocytosis. *Nature.* **450**, 1253-1257 (2007).

7. Kabeya, Y. *et al.* LC3, a mammalian homologue of yeast Apg8p, is localized in autophagosome membranes after processing. *EMBO J.* **19**, 5720-5728 (2000).

8. Yousefi, S. *et al.* Calpain-mediated cleavage of Atg5 switches autophagy to apoptosis. *Nat. Cell Biol.* **8**, 1124-1132 (2006).

9. Pyo, J.O. *et al.* Essential roles of Atg5 and FADD in autophagic cell death: dissection of autophagic cell death into vacuole formation and cell death. *J. Biol. Chem.* **280**, 20722-20729 (2005).

10. Xie, Z., Nair, U. & Klionsky, D.J. Atg8 controls phagophore expansion during autophagosome formation. *Mol. Biol. Cell.* **19**, 3290-3298 (2008).

11. Sou, Y.S. *et al.* The Atg8 conjugation system is indispensable for proper development of autophagic isolation membranes in mice. *Mol. Biol. Cell.* **19**, 4762-4775 (2008).

12. Nakatogawa, H., Ichimura, Y. & Ohsumi, Y. Atg8, a ubiquitin-like protein required for autophagosome formation, mediates membrane tethering and hemifusion 4. *Cell.* **130**, 165-178 (2007).

13. Mizushima, N., Yamamoto, A., Matsui, M., Yoshimori, T. & Ohsumi, Y. In vivo analysis of autophagy in response to nutrient starvation using transgenic mice

expressing a fluorescent autophagosome marker. *Mol Biol Cell.* **15**, 1101-1111 (2004).

14. Yasuda, H. *et al.* Osteoclast differentiation factor is a ligand for osteoprotegerin/osteoclastogenesis-inhibitory factor and is identical to TRANCE/RANKL. *Proc. Natl. Acad. Sci. U. S. A.* **95**, 3597-3602 (1998).

15. Yamaza, T. *et al.* Study of immunoelectron microscopic localization of cathepsin K in osteoclasts and other bone cells in the mouse femur. *Bone.* **23**, 499-509 (1998).

16. Mizushima, N. *et al.* Dissection of autophagosome formation using Apg5-deficient mouse embryonic stem cells. *J Cell Biol.* **152**, 657-668 (2001).

17. Hara, T. *et al.* Suppression of basal autophagy in neural cells causes neurodegenerative disease in mice. *Nature.* **441**, 885-889 (2006).

18. Zhao, Z. *et al.* Autophagosome-independent essential function for the autophagy protein Atg5 in cellular immunity to intracellular pathogens. *Cell Host Microbe.* **4**, 458-469 (2008).

19. Clausen, B.E., Burkhardt, C., Reith, W., Renkawitz, R. & Forster, I. Conditional gene targeting in macrophages and granulocytes using LysMcre mice. *Transgenic Research.* **8**, 265-277 (1999).

20. Takayanagi, H. *et al.* Induction and activation of the transcription factor NFATc1 (NFAT2) integrate RANKL signaling in terminal differentiation of osteoclasts. *Dev. Cell.* **3**, 889-901 (2002).

21. Minkin, C. Bone acid phosphatase: tartrate-resistant acid phosphatase as a marker of osteoclast function. *Calcif. Tissue. Int.* **34**, 285-290 (1982).

22. Ballanti, P. *et al.* Tartrate-resistant acid phosphate activity as osteoclastic marker: sensitivity of cytochemical assessment and serum assay in comparison with standardized osteoclast histomorphometry. *Osteoporos. Int.* **7**, 39-43 (1997).

23. Horne, W.C. *et al.* Osteoclasts express high levels of pp60c-src in association with intracellular membranes. *J Cell Biol.* **119**, 1003-1013 (1992).

24. Faust, J. *et al.* Osteoclast markers accumulate on cells developing from human peripheral blood mononuclear precursors. *J Cell Biochem.* **72**, 67-80 (1999).

25. Klionsky, D.J. *et al.* Guidelines for the use and interpretation of assays for monitoring autophagy in higher eukaryotes. *Autophagy.* **4**, 151-175 (2008).

26. Salo, J., Lehenkari, P., Mulari, M., Metsikko, K. & Vaananen, H.K. Removal of osteoclast bone resorption products by transcytosis. *Science.* **276**, 270-273 (1997).

27. Coxon, F.P. & Taylor, A. Vesicular trafficking in osteoclasts. *Semin. Cell Dev. Biol.* **19**, 424-433 (2008).

28. Akamine, A. *et al.* Increased synthesis and specific localization of a major lysosomal membrane sialoglycoprotein (LGP107) at the ruffled border membrane of active osteoclasts. *Histochemistry.* **100**, 101-108 (1993).

29. Claveau, D. & Riendeau, D. Mutations of the C-terminal end of cathepsin K affect proenzyme secretion and intracellular maturation. *Biochem. Biophys. Res. Commun.* **281**, 551-557 (2001).

30. Mizushima, N. *et al.* A protein conjugation system essential for autophagy. *Nature.* **395**, 395-398 (1998).

31. Komatsu, M. *et al.* Impairment of starvation-induced and constitutive autophagy in Atg7-deficient mice. *J. Cell Biol.* **169**, 425-434 (2005).

32. Mizushima, N., Sugita, H., Yoshimori, T. & Ohsumi, Y. A new protein conjugation system in human. The counterpart of the yeast Apg12p conjugation system essential for autophagy. *J Biol. Chem.* **273**, 33889-33892 (1998).

33. Hamacher-Brady, A. *et al.* Response to myocardial ischemia/reperfusion injury involves Bnip3 and autophagy. *Cell Death Differ.* **14**, 146-157 (2007).

34. Hamacher-Brady, A., Brady, N.R. & Gottlieb, R.A. Enhancing macroautophagy protects against ischemia/reperfusion injury in cardiac myocytes. *J Biol. Chem.* **281**, 29776-29787 (2006).

35. Jounai, N. *et al.* The Atg5 Atg12 conjugate associates with innate antiviral immune responses. *Proc Natl Acad Sci U. S. A.* **104**, 14050-14055 (2007).

36. Kabeya, Y. *et al.* LC3, GABARAP and GATE16 localize to autophagosomal membrane depending on form-II formation. *J. Cell Sci.* **117**, 2805-2812 (2004).

37. Fujita, N. *et al.* An Atg4B mutant hampers the lipidation of LC3 paralogues and causes defects in autophagosome closure. *Mol. Biol. Cell.* **19**, 4651-4659 (2008).

38. Teitelbaum, S.L. Osteoclasts: what do they do and how do they do it? *Am. J Pathol.* **170**, 427-435 (2007).

39. Weitzmann, M.N. & Pacifici, R. Estrogen deficiency and bone loss: an inflammatory tale. *J Clin Invest.* **116**, 1186-1194 (2006).

40. Saftig, P. *et al.* Impaired osteoclastic bone resorption leads to osteopetrosis in cathepsin-K-deficient mice. *Proc. Natl. Acad. Sci. U. S. A.* **95**, 13453-13458 (1998).

41. McHugh, K.P. *et al.* Mice lacking beta3 integrins are osteosclerotic because of dysfunctional osteoclasts. *J Clin Invest.* **105**, 433-440 (2000).

42. Zhao, H. *et al.* Synaptotagmin VII regulates bone remodeling by modulating osteoclast and osteoblast secretion. *Dev. Cell.* **14**, 914-925 (2008).

43. Martinez, I. *et al.* Synaptotagmin VII regulates Ca(2+)-dependent exocytosis of lysosomes in fibroblasts. *J Cell Biol.* **148**, 1141-1149 (2000).

44. Itoh, F. *et al.* Treatment effects of bisphosphonates on ovariectomy-induced osteopenia in rats: comparison between clodronate and etidronate. *J Bone. Miner. Metab.* **17**, 252-258 (1999).

45. Xiang, A. *et al.* Changes in micro-CT 3D bone parameters reflect effects of a potent cathepsin K inhibitor (SB-553484) on bone resorption and cortical bone formation in ovariectomized mice. *Bone.* **40**, 1231-1237 (2007).

46. Zhao, H. *et al.* Critical role of beta3 integrin in experimental postmenopausal osteoporosis. *J Bone. Miner. Res.* **20**, 2116-2123 (2005).

47. Ganesan, A.K. *et al.* Genome-wide siRNA-based functional genomics of pigmentation identifies novel genes and pathways that impact melanogenesis in human cells. *PLoS Genet.* **4**, e1000298 (2008).

48. Stephenson, L.M. *et al.* Identification of Atg5-dependent transcriptional changes and increases in mitochondrial mass in Atg5-deficient T lymphocytes. *Autophagy.* **5**, 1-11 (2009).

49. Takeshita, S., Kaji, K. & Kudo, A. Identification and characterization of the new osteoclast progenitor with macrophage phenotypes being able to differentiate into mature osteoclasts. *J Bone. Miner. Res.* **15**, 1477-1488 (2000).

CHAPTER 5

Conclusions and Future Directions

Summary of Results

The canonical functions of autophagy are to degrade unwanted cytoplasmic constituents and provide recycled material back to the cell. As groups have identified and studied the molecular mechanisms of autophagy in a variety of model organisms and cell types, it has become clear that autophagy and autophagy genes have a plethora of additional functions. The goal of this thesis is to better understand the functions of autophagy genes in primary mammalian cells with important physiologic functions. We chose to study B cells, T cells, and osteoclasts because much is known about the development, homeostasis, and functions of these cell types.

Our studies in lymphocytes revealed a role for autophagy genes in cellular development and homeostasis. B cells lacking *Atg5* had an increase in cell death during the late stages of development in the bone marrow and decreased numbers of B-1a B cells. In contrast, T cells deficient in either *Atg5* or *Atg7* had a profound defect in peripheral homeostasis, associated with an increase in markers of cell death and decreased ability to proliferate. Transcriptional studies suggested abnormalities in mitochondria, which we corroborated by demonstrating an increase in mitochondrial mass. High mitochondrial mass correlated with the increased markers of cell death in *Atg5*-deficient T cells.

In contrast to lymphocytes, *Atg5*-deficient osteoclasts did not have gross abnormalities in cellular development. Instead, these cells had a reduction in their capacity to degrade bone. Delivery of the lysosomal markers cathepsin K and LAMP1 to

the bone surface was impaired in the absence of *Atg5*, suggesting a role for *Atg5* in cell secretion. To further explore the mechanism behind this observation, we showed that osteoclasts lacking *Atg5* or *Atg7* or overexpressing ATG5^{K130R} or ATG4B^{C74A} all shared the same phenotype. Together, this data identifies the biochemical pathway necessary for LC3 conjugation as important for osteoclast secretion. Interestingly, LC3 is found at the ruffled border in activated osteoclasts. This localization is inhibited by ATG4B^{C74A} expression, suggesting a connection between LC3 localization and osteoclast function.

Conclusions and Future Directions: Lymphocytes

Cell type specificity

Our studies reveal that *Atg5* has very dramatic cell-type specific functions. B and T lymphocytes are closely-related lineages that differentiate from a common progenitor, yet *Atg5* is required for peripheral T cell, but not B-2 B cell, homeostasis. Also, T cells accumulate mitochondria in the absence of *Atg5*, whereas peripheral B-2 B cells do not[1]. Even more striking is the discrepancy within B cells – B-1a B cell numbers are dramatically reduced in *Atg5*$^{flox/flox}$-CD19-*Cre*+ mice, but B-1b and B-2 B cells are not. These results demonstrate that one must be cautious when taking lessons learned about the function of autophagy genes in one biological system or cell type and trying to apply them to another, and support our bias that it is necessary to study the function of autophagy genes in primary cells with physiologically important roles.

Autophagy in lymphocyte survival and death

There are many reports in the literature that autophagy can accelerate or induce cell death in different cell types[2,3,4]. Even within the T cell literature, autophagy is suggested to be an important death pathway after nutrient withdrawal, exposure to HIV, or in a variety of genetic deletion models[5,6,7,8]. In contrast to these results, we observed either no effect or an increase in cell death when we deleted autophagy genes in primary T cells. If autophagy were a physiologically important cell death pathway in lymphocytes, one would have predicted an accumulation of B and T cells, possibly resulting in autoimmunity. We have followed both *Atg5*$^{flox/flox}$-CD19-*Cre*+ and *Atg5*$^{flox/flox}$-Lck-*Cre*+ mice and their *Cre*- controls as they age and have not seen abnormalities in long-term survival. We hypothesize that in physiologic circumstances autophagy functions as a pro-survival mechanism in lymphocytes, and that this process is only important for inducing cell death in conditions of genetic abnormalities or when excessively induced.

One of the major questions raised by our studies in T lymphocytes is why the lack of *Atg5* or *Atg7* resulted in decreased T cell survival. Both our work and the work of Pua *et al.*[1] demonstrate that mitochondria are abnormal in the absence of essential autophagy genes, suggesting that autophagy is important in T cells for degradation of excess or damaged mitochondria. While it is known that damaged mitochondria can produce toxic byproducts, such as reactive oxygen species, that can result in cell death, we were unable to rescue T cell survival with pharmacologic inhibitors of reactive oxygen species (data not shown). Until *Atg5*-deficient T cells can be rescued from cell death, the downstream

cause of death from deletion of essential autophagy genes will be unknown. Given the important role of Bcl-2 family members in T cell survival and the misregulation of these proteins in *Atg7*-deficient T cells[1], one hypothesis is that disruption in the balance of pro- and anti-apoptotic Bcl-2 family members contributes to T cell death in the absence of autophagy genes. One could breed *Atg5*$^{flox/flox}$-Lck-*Cre* mice to mice expressing Bcl-2 in T cells[9] to determine if overexpression of this anti-apoptotic molecule protects *Atg5*-deficient T cells from death and restores peripheral T cell numbers. Rescue of *Atg5*-deficient T cell death by Bcl-2 overexpression would suggest that the T cells are dying in a Bax/Bad-dependent fashion, prompting further studies of the regulation of these family members in *Atg5*-deficient T cells.

B cell secretion

Given the role of autophagy genes in osteoclast secretion, it would be interesting to determine if B lymphocytes lacking *Atg5* are able to secrete antibody. *Atg5*$^{flox/flox}$-CD19-*Cre* mice provide a good model system in which to study B cell antibody production, both *in vivo* and *in vitro*. Antibody titers in serum from naïve *Atg5*$^{flox/flox}$-CD19-*Cre*+ mice should be measured to determine if *Atg5* is important for the homeostasis of antibody levels. Given that antibody levels are tightly regulated,[10] a deficiency in B cell secretion may not be observable until the mice are challenged to produce an antibody response. Injection of mice with standard, well-characterized antigens that elicit robust immunoglobulin production (i.e. TNP-KLH) would allow

measurement of specific antibody responses. Also, B cell antibody production can be measured *in vitro* by stimulating cells with LPS and measuring total IgM levels in the supernatant. Given that our anti-phosphocholine titer experiments in these mice suggest that *Atg5*-deficient B cells are able to secrete antibody, we hypothesize that antibody secretion will be unaffected in *Atg5*$^{flox/flox}$-CD19-*Cre*+ B cells. It is likely that autophagy genes are not involved in secretion in every cell type, as mice lacking *Atg5* or *Atg7* in neurons are able to survive for weeks, proving that neuronal secretion is not dramatically inhibited[11,12].

Conclusions and Future Directions: Osteoclasts

The function of autophagy genes in cell secretion is an area of active interest in our lab, given the importance of these genes in Paneth cell secretion and the work described in Chapter 4 in osteoclasts. Osteoclasts provide a manipulable *in vitro* system for pursuing mechanistic questions. Using this system we have identified that the LC3 conjugation pathway is important for osteoclast secretion, and our data suggest that LC3 localization to the ruffled border may be involved. Based on this data we have developed a working model summarized in Figure 4-16.

Exploring the role of LC3 in osteoclasts

To test our working model, one must first confirm that LC3 localization to the ruffled border requires LC3 conjugation. Second, identification of the membrane(s) onto

which LC3 is conjugated would guide our hypotheses about the function of LC3. Finally, direct assessment of LC3 function would be important to determine the mechanism of its action at the ruffled border. Each of these three lines of inquiry is discussed in more detail below.

The first hypothesis predicted from our model is that LC3 conjugation is required for localization of GFP-LC3 to the ruffled border. Our studies with the ATG4B^{C74A} mutant suggest this conclusion, but given that this mutant binds to and sequesters LC3[13], it is possible that the inhibition in GFP-LC3 localization is simply due to sequestering of LC3 in the cytoplasm. To test if conjugation is required for localization, one could transduce GFP-LC3 into cells lacking ATG5. We predict that GFP-LC3 will localize to the ruffled border in *Atg5*$^{flox/flox}$-LyzM-*Cre*- but not *Atg5*$^{flox/flox}$-LyzM-*Cre*+ osteoclasts, indicating that *Atg5* is required for LC3 localization. This hypothesis could be further assessed by transducing control osteoclasts with a mutant of LC3 that cannot be conjugated to phosphatidylethanolamine (LC3^{G120A})[14]. If our hypothesis is correct, then GFP-LC3^{WT}, but not GFP-LC3^{G120A}, will localize to the ruffled border. If LC3 conjugation is not required for localization, then one would study the functions of the LC3 conjugation pathway outside of the context of LC3. For example, this pathway is required for conjugation of additional mammalian ATG8 homologues, including GABARAP, GATE16, and ATG8L[15,16,17], that may be responsible for the observed osteoclast phenotype.

If LC3 conjugation is required for its localization, it will be important to know what structure(s) LC3 is conjugated to within the actin ring. Immunoelectron microscopy of active GFP-LC3 osteoclasts on bone should allow us to determine if the LC3 is located on the plasma membrane or on vesicles or autophagosomes near the ruffled border. Electron microscopy would also be useful to determine if there are any double-membrane bound vesicles in the vicinity of the ruffled border in control cells which might suggest a role for autophagosomes in cell secretion.

Finally, the function of LC3 in mediating directional secretion needs to be determined. As a first step towards addressing this question, it would be useful to understand the kinetics of LC3 localization using live cell imaging of osteoclasts on bone substrate[18]. Luckily, live imaging of both the dynamics of actin ring formation in osteoclasts and GFP-LC3 localization in macrophages has already been reported,[19,18] suggesting that it might be possible to visualize both of these processes in live osteoclasts. Trafficking of lysosomes can also be visualized in live cells[20].

Kinetic analysis experiments might explain two puzzling observations from our studies: first, why we observe GFP-LC3 localization in only 25% of osteoclasts, despite localization of cathepsin K in 50% of osteoclasts; second, why nearly 100% of cells with localization of GFP-LC3 in the actin ring also had localization of cathepsin K in the actin ring. Three non-mutually exclusive hypotheses may explain these results. First, LC3 localization may function to enhance secretion (through some of potential mechanisms discussed below), but may not required for initial secretion. Visualizing the kinetics of

lysosome and GFP-LC3 trafficking to the actin ring could address this hypothesis. Second, targeting of LC3 to the ruffled border may be a transient signal that rapidly initiates secretion. Kinetic studies would also address this hypothesis. Third, cathepsin K and LAMP1 may be targeted to the ruffled border via two distinct secretory pathways (i.e. secretory lysosomes and directly from the Golgi apparatus, see Chapter 1), only one of which requires the LC3 conjugation machinery. To study this hypothesis, one would need to do a detailed analysis of cathepsin K secretion in osteoclasts. Luckily, such an analysis is currently underway in the laboratory of one of our collaborators, Dr. Judith Klumperman. Understanding which, if any, of these hypotheses is correct may also explain why *Atg5*- and *Atg7*-deficient osteoclasts still are able to form shallow bone pits and localize cathepsin K in a fraction of cells.

LC3 is a multifunctional protein that could mediate directional secretion in osteoclasts through several potential mechanisms. First, LC3 interacts with many different proteins in the cell[21,22,23,24] including p62, an important molecule in osteoclast biology. Second, LC3 promotes the tethering and hemifusion of membranes[25], suggesting it may be part of the machinery necessary for vesicle fusion with the plasma membrane at the ruffled border. Third, LC3 binds to microtubules[26], suggesting that it might be important for vesicle trafficking on the cytoskeleton. As we do not observe colocalization of GFP-LC3 and cathepsin K puncta in the cell periphery in osteoclasts, we do not believe that LC3 is localized to secretory lysosomes in osteoclasts and will not discuss this hypothesis further.

P62 is an attractive target for study because mutations in p62 have been associated with Paget's disease of bone (PDB), a human disease characterized by focal areas of bone degradation and hyperactive osteoclasts (reviewed in [27]). Understanding the role of p62 in PDB has been very complicated because of the multiple roles of this scaffolding protein, including interacting with many signaling molecules necessary for osteoclast formation[28]. There is little known about the functions of p62 in osteoclasts outside of these osteoclastogenic signaling pathways. LC3 targeted to the ruffled border may function by binding p62, localizing this important scaffold molecule to the resorptive microenvironment. As a first step to understand if LC3 binding to p62 is potentially important for the function of LC3 at the ruffled border, one could determine if p62 localizes within the actin ring and colocalizes with LC3. It would also be useful to determine if the interaction of these proteins is important by studying mutants of p62 that abolish LC3 binding[29,23]. Transducing these mutants into *p62*$^{-/-}$ macrophages before inducing osteoclastogenesis may rescue the defect in osteoclast formation in these cells[28] and allow analysis of the function of the p62-LC3 interaction in osteoclasts.

LC3 is also involved in membrane tethering and hemifusion, an important function for autophagosome formation[25]. The fusion machinery required for secretion of vesicles at the ruffled border in osteoclasts is unknown. The ability of LC3 to facilitate membrane tethering and fusion may be important at the ruffled border for either bringing the vesicular membrane in proximity with the plasma membrane or for directly fusing these two membranes to allow release of vesicular contents. To test this hypothesis, one could generate mutants of LC3 that cannot participate in membrane fusion. These

mutants have already been generated and characterized in ATG8, the yeast homologue of LC3[25]. Overexpression of these mutants in osteoclasts may inhibit secretion.

Differentiating the functions of autophagy from the functions of autophagy genes

As discussed briefly throughout this thesis, one of the major challenges that the field of autophagy is now facing is to understand the difference between the functions of autophagy genes and the autophagy pathway. The gold standard for defining that a phenotype is dependent on autophagy requires demonstration that the mechanism involves a function of autophagosomes, such as degradation of long-lived proteins or organelles. Alternatively, inhibiting the autophagy pathway at multiple points, from induction to autophagosome-lysosome fusion, and demonstrating that each has the same phenotype is highly suggestive that autophagosome formation is involved. Unfortunately, even processes that require proteins from multiple steps in autophagosome formation may not involve classical autophagy. For example, both Beclin-1 and LC3 localize to single-membrane bound phagosomes before phagosome-lysosome fusion[19], suggesting co-opting of the autophagy machinery from the class III PI3K to LC3 conjugation for phagosome maturation.

Our studies in osteoclasts have identified that the LC3 conjugation pathway is important for secretion, but we do not know if this pathway is working in the context of autophagosome formation or in an alternative role. To address this question, one could knock down or knock out proteins in the autophagy pathway outside of the LC3

conjugation pathway and determine if osteoclast secretion is inhibited. Since many of the upstream signaling molecules have separate functions in vesicular trafficking[30,31] (reviewed in [32]), targets for knockdown must be carefully selected. mATG9 is a homologue of the yeast protein ATG9 that is hypothesized to transport membrane to the forming autophagosome (reviewed in [33]). ATG14L is a binding partner in the Vps34-beclin complex necessary for autophagosome induction[30,31]. Knocking down these proteins in mammalian cells inhibits autophagosome formation[34,30,31] but is not known to affect vesicular trafficking. If knocking down expression of these proteins does not affect osteoclast secretion but still inhibits autophagosome formation in osteoclasts, this would demonstrate that autophagosomes are not required for osteoclast secretion. ATG14L, and possibly mATG9, is important for LC3 conjugation[34,30,31]. If these knockdowns do inhibit osteoclast secretion but also inhibit LC3 conjugation, it does not prove that autophagosomes are required for secretion. The best approach is to inhibit multiple proteins both upstream and downstream of LC3 conjugation and demonstrate that they all result in defects in osteoclast secretion. This result would be highly suggestive that formation of autophagosomes is important for osteoclast secretion. The alternative hypothesis is that the biochemical pathway required for autophagy has an entirely separate and currently undefined function in secretion. Immunoelectron microscopy studies to localize LC3 and electron microscopy to visualize double-membrane bound vesicles in osteoclasts would help distinguish between these two hypotheses.

Autophagy genes in cell secretion

Cell secretion in osteoclasts is not well understood, but a number of lines of evidence suggest that the vesicles involved in secretion are secretory lysosomes (see Chapter 1). It is interesting to note that of the three cell types in which autophagy genes have been shown to be important for secretion – Paneth cells, melanocytes, and now osteoclasts – both melanocytes and osteoclasts utilize secretory lysosomes (reviewed in [35]). This suggests that there may be a common mechanism employing autophagy machinery for the secretion of lysosomes. Also, this may explain why some cells require autophagy genes for secretion, whereas other cells do not. It would be interesting to determine if the role of autophagy genes in cell secretion is specific for secretory lysosomes, and if this role is applicable across multiple cell types.

Related to the hypothesis that there may be a common mechanism for the secretion of lysosomes that involves the autophagy machinery, a small GTPase, Rab7, is known to be important both for autophagosome fusion to lysosomes[36,20,37] and osteoclast localization of vacuolar H+ ATPase to the actin ring[38]. These results suggest that molecular machinery may be shared between autophagosome maturation and vesicular secretion in osteoclasts. This may be due to a role for autophagosomes in secretion or a function of the LC3 conjugation pathway in recruiting shared mechanisms. It would be interesting to determine if additional molecules involved in autophagosome maturation, such as the vesicular snare VAMP7[39], are also involved in vesicular secretion in osteoclasts and other cell types with secretory lysosomes.

In conclusion, we have shown that autophagy genes have important functions in survival, development, mitochondrial maintenance, and secretion in primary mammalian cells. We have also demonstrated that these functions are highly cell-type specific. Together, these results suggest that autophagy or autophagy genes have been co-opted for multiple functions during evolution.

References

1. Pua, H.H., Guo, J., Komatsu, M. & He, Y.W. Autophagy is essential for mitochondrial clearance in mature T lymphocytes. *J. Immunol.* **In Press**, (2009).

2. Berry, D.L. & Baehrecke, E.H. Growth arrest and autophagy are required for salivary gland cell degradation in Drosophila. *Cell.* **131**, 1137-1148 (2007).

3. Koike, M. *et al.* Inhibition of autophagy prevents hippocampal pyramidal neuron death after hypoxic-ischemic injury. *Am. J Pathol.* **172**, 454-469 (2008).

4. Wang, Y. *et al.* Loss of macroautophagy promotes or prevents fibroblast apoptosis depending on the death stimulus. *J. Biol. Chem.* **283**, 4766-4777 (2008).

5. Li, C. *et al.* Autophagy is induced in CD4+ T cells and important for the growth factor-withdrawal cell death. *J. Immunol.* **177**, 5163-5168 (2006).

6. Bell, B.D. *et al.* FADD and caspase-8 control the outcome of autophagic signaling in proliferating T cells. *Proc Natl Acad Sci U. S. A.* **105**, 16677-16682 (2008).

7. Feng, C.G. *et al.* The immunity-related GTPase Irgm1 promotes the expansion of activated CD4+ T cell populations by preventing interferon-gamma-induced cell death. *Nat Immunol.* **9**, 1279-1287 (2008).

8. Espert, L. *et al.* Autophagy is involved in T cell death after binding of HIV-1 envelope proteins to CXCR4. *J. Clin. Invest.* **116**, 2161-2172 (2006).

9. Sentman, C.L., Shutter, J.R., Hockenbery, D., Kanagawa, O. & Korsmeyer, S.J. bcl-2 inhibits multiple forms of apoptosis but not negative selection in thymocytes. *Cell.* **67**, 879-888 (1991).

10. Roopenian, D.C. *et al.* The MHC class I-like IgG receptor controls perinatal IgG transport, IgG homeostasis, and fate of IgG-Fc-coupled drugs. *J Immunol.* **170**, 3528-3533 (2003).

11. Komatsu, M. *et al.* Loss of autophagy in the central nervous system causes neurodegeneration in mice. *Nature.* **441**, 880-884 (2006).

12. Hara, T. *et al.* Suppression of basal autophagy in neural cells causes neurodegenerative disease in mice. *Nature.* **441**, 885-889 (2006).

13. Fujita, N. *et al.* An Atg4B mutant hampers the lipidation of LC3 paralogues and causes defects in autophagosome closure. *Mol. Biol. Cell.* **19**, 4651-4659 (2008).

14. Kabeya, Y. *et al.* LC3, a mammalian homologue of yeast Apg8p, is localized in autophagosome membranes after processing. *EMBO J.* **19**, 5720-5728 (2000).

15. Hemelaar, J., Lelyveld, V.S., Kessler, B.M. & Ploegh, H.L. A single protease, Apg4B, is specific for the autophagy-related ubiquitin-like proteins GATE-16, MAP1-LC3, GABARAP, and Apg8L. *J Biol Chem.* **278**, 51841-51850 (2003).

16. Tanida, I., Komatsu, M., Ueno, T. & Kominami, E. GATE-16 and GABARAP are authentic modifiers mediated by Apg7 and Apg3. *Biochem. Biophys. Res. Commun.* **300**, 637-644 (2003).

17. Tanida, I., Sou, Y.S., Minematsu-Ikeguchi, N., Ueno, T. & Kominami, E. Atg8L/Apg8L is the fourth mammalian modifier of mammalian Atg8 conjugation mediated by human Atg4B, Atg7 and Atg3. *FEBS. J.* **273**, 2553-2562 (2006).

18. Saltel, F., Destaing, O., Bard, F., Eichert, D. & Jurdic, P. Apatite-mediated actin dynamics in resorbing osteoclasts. *Mol. Biol. Cell.* **15**, 5231-5241 (2004).

19. Sanjuan, M.A. *et al.* Toll-like receptor signaling in macrophages links the autophagy pathway to phagocytosis. *Nature.* **450**, 1253-1257 (2007).

20. Kimura, S., Noda, T. & Yoshimori, T. Dissection of the autophagosome maturation process by a novel reporter protein, tandem fluorescent-tagged LC3. *Autophagy.* **3**, 452-460 (2007).

21. Kirkin, V. *et al.* A role for NBR1 in autophagosomal degradation of ubiquitinated substrates. *Mol. Cell.* **33**, 505-516 (2009).

22. Pankiv, S. *et al.* p62/SQSTM1 binds directly to Atg8/LC3 to facilitate degradation of Ubiquitinated protein aggregates by autophagy. *J. Biol. Chem.* (2007).

23. Zheng, Y.T. *et al.* The adaptor protein p62/SQSTM1 targets invading bacteria to the autophagy pathway. *J Immunol.* **183**, 5909-5916 (2009).

24. Furuta, S. *et al.* Light Chain 3 associates with a Sos1 guanine nucleotide exchange factor: its significance in the Sos1-mediated Rac1 signaling leading to membrane ruffling. *Oncogene.* **21**, 7060-7066 (2002).

25. Nakatogawa, H., Ichimura, Y. & Ohsumi, Y. Atg8, a ubiquitin-like protein required for autophagosome formation, mediates membrane tethering and hemifusion 4. *Cell.* **130**, 165-178 (2007).

26. Mann, S.S. & Hammarback, J.A. Molecular characterization of light chain 3. A microtubule binding subunit of MAP1A and MAP1B. *J. Biol. Chem.* **269**, 11492-11497 (1994).

27. Helfrich, M.H. & Hocking, L.J. Genetics and aetiology of Pagetic disorders of bone. *Arch. Biochem. Biophys.* **473**, 172-182 (2008).

28. Duran, A. *et al.* The atypical PKC-interacting protein p62 is an important mediator of RANK-activated osteoclastogenesis. *Dev. Cell.* **6**, 303-309 (2004).

29. Ichimura, Y. *et al.* Structural basis for sorting mechanism of p62 in selective autophagy. *J Biol. Chem.* **283**, 22847-22857 (2008).

30. Matsunaga, K. *et al.* Two Beclin 1-binding proteins, Atg14L and Rubicon, reciprocally regulate autophagy at different stages. *Nature Cell Biology*. Epub ahead of print (2009).

31. Zhong, Y. *et al.* Distinct regulation of autophagic activity by Atg14L and Rubicon associated with Beclin 1-phosphatidylinositol-3-kinase complex. *Nat. Cell Biol.* **11**, 468-476 (2009).

32. Longatti, A. & Tooze, S.A. Vesicular trafficking and autophagosome formation. *Cell Death. Differ.* **16**, 956-965 (2009).

33. He, C. & Klionsky, D.J. Regulation Mechanisms and Signaling Pathways of Autophagy. *Annu. Rev. Genet.* (2009).

34. Yamada, T. *et al.* Endothelial nitric-oxide synthase antisense (NOS3AS) gene encodes an autophagy-related protein (APG9-like2) highly expressed in trophoblast. *J Biol. Chem.* **280**, 18283-18290 (2005).

35. Blott, E.J. & Griffiths, G.M. Secretory lysosomes. *Nat. Rev. Mol. Cell Biol.* **3**, 122-131 (2002).

36. Jager, S. *et al.* Role for Rab7 in maturation of late autophagic vacuoles. *J. Cell Sci.* **117**, 4837-4848 (2004).

37. Gutierrez, M.G., Munafo, D.B., Beron, W. & Colombo, M.I. Rab7 is required for the normal progression of the autophagic pathway in mammalian cells. *J Cell Sci.* **117**, 2687-2697 (2004).

38. Zhao, H., Laitala-Leinonen, T., Parikka, V. & Vaananen, H.K. Downregulation of small GTPase Rab7 impairs osteoclast polarization and bone resorption. *J Biol. Chem.* **276**, 39295-39302 (2001).

39. Fader, C.M., Sanchez, D.G., Mestre, M.B. & Colombo, M.I. TI-VAMP/VAMP7 and VAMP3/cellubrevin: two v-SNARE proteins involved in specific steps of the autophagy/multivesicular body pathways. *Biochim. Biophys. Acta.* (2009).